Effects of Operational Parameters on Microgranular Adsorptive Filtration (μGAF)

James C.W. Liu

A dissertation submitted in partial fulfillment of the requirements for the degree of

Doctor of Philosophy

University of Washington

2015

Reading Committee:

Mark M. Benjamin, Chair

Yujung Chang

Michael C. Dodd

Gregory V. Korshin

Program Authorized to Offer Degree:

Department of Civil and Environmental Engineering

University of Washington

Abstract

Effect of Operational Parameters on Microgranular Adsorptive Filtration (μGAF)

James C.W. Liu

Chair of Supervisory Committee:
Professor Mark M. Benjamin
Department of Civil and Environmental Engineering

Low-pressure membrane filtration has been used as a separation technique in water treatment applications for decades and is effective at removing particulates from water. However, it has limited ability to reject soluble materials such as natural organic matter (NOM). NOM can not only cause fouling by clogging the membrane pores or by accumulating on the membrane surface, but can also react with disinfectants to form harmful disinfection by-products (DBPs) and can interfere with other water treatment processes.

This study investigated microgranular adsorptive filtration (μGAF), a process that integrates granular media filtration and packed bed adsorption by passing water through a layer of pre-deposited adsorbent on a filter media. With proper choice of adsorbent, μGAF can serve as a pre-treatment process prior to membrane filtration, as the pre-deposited adsorbent layer captures the contaminants on or within the layer and

thereby prevents contaminants from reaching membrane.

Heated aluminum oxide particles (HAOPs) were used as the main adsorbent in this study. Operational factors affecting the process performance, including flux, applied pressure and solution chemistry (pH, ionic strength and concentration of divalent cations) were investigated. The μGAF process achieved better NOM removal and fouling control with increasing flux, and applied pressure had no effect on the μGAF process. Low pH promotes NOM adsorption onto HAOPs, resulting in better fouling control. Ionic strength had a limited effect on the ability of HAOPs to collect foulants. Adding extra divalent cations to the feed solution reduced fouling slightly, possibly due to the agglomeration of polysaccharide macromolecules promoted by the divalent cations.

Particulate and colloidal materials were the key foulants in the μGAF units, and soluble materials such as NOM dominated membrane fouling. Fouling of the μGAF unit could be modeled by the classic blocking models developed by Hermia, with the intermediate fouling scenario having the best fit to the experimental data ($R^2 \geqq 0.95$).

Lastly, larger bench scale μGAF/membrane processes were carried out with various types of meshes, membrane materials and feed water quality. In these tests, μGAF achieved good NOM removal and fouling control in all experiments, thereby supporting its potential in full-scale water treatment systems.

TABLE OF CONTENTS

LIST OF FIGURES

Figure numbers **Page**

LIST OF TABLES

Table numbers **Page**

ACKNOWLEDGEMENTS

It has been four years for me to finish this dissertation and complete this degree. I have received enormous help and support from many people along with this sometimes bumpy, but mostly amazing journey. I would like to express my gratitude here.

First, I would like to show my greatest appreciation to my advisor, Dr. Mark Benjamin, for his guidance and mentoring. Mark is not only a good teacher and researcher to me, but also a generous and warm mentor. During my Ph.D. program at University of Washington, Mark also showed his conscientious scholarship and virtuous personality, which I learned as a person and respect very much.

Next, I want to acknowledge Dr. Yujung Chang, Dr. Michael Dodd, Dr. Gregory Korshin and Dr. Lilo Pozzo, for all the valuable discussions and advices which helped me to improve and to complete my research.

I would also like to thank all the staffs of the Department of Civil and Environmental Engineering for all the work they have done during this four years. Particularly, I would like to show my appreciation to the lab managers, Sean Yeung and Songling Wang, for all the help on lab related issues.

Many thanks to my dear colleagues and friends in the department, Zhenxiao Cai, Beata Malczewska, Siamak Modarresi, Davide Scannapieco, Henry Moen, Ryan Hale, Annie Alsheimer, Sam Landsman, Longfei Wang, Libing Chu, Bing Tang, Chuhui Zhang, Ao Xie, Peiran Zhou, Niccolette Zhou, Bo Li and Stephany Wei for all the friendship and support.

Yuan Gao, who gives me love, happiness and understanding. I feel very fortunate to meet Yuan during my graduate study, and to have her standing beside me and support me every single day.

Lastly, my deepest appreciation goes to my family: my parents, Chao Kai Liu and Bau Dau Shen, my sister and her husband, Cheng Ying Liu and Shih Chia Cheng. They have helped and supported me in every stage in my life. I would not have been able to finish this without them, and I would like to have them share any honor I received by completing this degree.

DEDICATION

To my family

Chao Kai Liu and Bau Dau Shen
Cheng Ying Liu and Shih Chia Cheng

Effect of Operational Parameters on Microgranular Adsorptive Filtration (μGAF)

1. Introduction

Both low- and high-pressure membrane filtrations have been used as separation techniques in water treatment in the past few decades. Low-pressure filtration includes microfiltration (MF) and ultrafiltration (UF) and is widely applied in drinking water treatment to remove suspended solids, bacteria and (to a lesser extent) viruses. High-pressure filtration includes nanofiltration (NF) and reverse osmosis (RO), which are used in more sophisticated water purification that requires higher permeate quality and, in particular, removal of dissolved contaminants and ions.

Although membrane filtration is an effective water treatment procedure, it is limited by membrane fouling. Membrane fouling is caused by contaminants in the feed that accumulate on the membrane surface or within membrane pores during filtration, blocking or clogging the membranes and lowering their permeability. Membrane fouling leads to declined flux and/or increased transmembrane pressure (TMP), resulting in decreased efficiency of filtration and increased energy cost.

Low-pressure membrane processes are effective at rejecting solid contaminants, but have limited removal efficiency for soluble contaminants, some of which cause significant and irreversible membrane fouling. Natural organic matter (NOM), a complex combination of soluble organic compounds mainly derived from plant/vegetation debris and metabolic products, is ubiquitous in natural waters and is a major membrane foulant. Numerous studies regarding NOM – including NOM characteristics, fractionations and interactions among different NOM fractions – have helped shed light on the effect of NOM on membrane fouling [1–10]. NOM

molecules can cause fouling through adsorption onto membrane pore walls and/or by forming a cake/gel layer on the membrane surface. Further, the layer formed by NOM can trap particulates or colloids that are in the feed water, exacerbating the fouling. Besides causing the fouling, NOM can also react with disinfectants to form disinfection by-products (DBPs) and can interfere with other water treatment processes.

Much effort has been devoted to mitigating membrane fouling and enhancing membrane process performance. Historically, most attempts to reduce membrane fouling have focused on process operational parameters and membrane cleaning. Reducing filtration flux and applying cross-flow filtration are the most common operational approaches, with cross-flow filtration especially effective at mitigating fouling caused by particles. Hydraulic backwashing is invariably performed periodically to maintain acceptable long-term performance. By applying these approaches, membrane fouling can be controlled to some extent, but limited improvement can be achieved once a gel layer containing NOM has formed, leading to irreversible fouling. Once irreversible fouling exceeds a certain level, the operation needs to be halted so that a chemical cleaning step ("clean in place" or CIP) can be carried out to recover the filtration efficiency.

Another approach to control membrane fouling is pretreatment to remove potential foulants before they reach the membrane. Conventional pretreatment processes include: 1. Pre-filtration through granular media or coarser membranes prior to the primary membrane modules; 2. Coagulation or adsorption, by applying metal based coagulants (aluminum sulfate or ferric chloride) or powdered activated carbon (PAC) to pre-treat feed water, and 3. Pre-oxidation, by dosing oxidant into the feed to suppress microbial growth and enhance coagulation [11]. Again, these approaches can reduce membrane fouling, but frequent backwashing is still required

to maintain process performance.

A novel pretreatment process, referred to as microgranular adsorptive filtration (μGAF), has been developed by our research group. μGAF combines adsorption, granular media filtration and membrane filtration by pre-depositing a layer of adsorbent directly onto the membrane surface or other support [12–17] through which the feed must pass prior to reaching the membrane. With the proper choice of adsorbent, μGAF is able to achieve substantial NOM removal and membrane fouling reduction simultaneously. In μGAF, most foulants are collected within the adsorbent layer. As a result, when the adsorbent layer is rinsed off the support surface at the end of a filtration cycle, the surface is almost as clean as when it was new [15,16].

There are several advantages to use of μGAF as a pretreatment. First, μGAF substantially reduces cleaning efforts required for the membrane (less membrane fouling). Although it inserts an additional step prior to membrane filtration, the maintenance effort for a μGAF system is likely to be easier and more efficient compared to a membrane system, because one can use a cheap and resilient material in μGAF unit, so a more aggressive cleaning approach can be applied without interfering with or damaging the material. From a research perspective, another advantage is that separating the μGAF and membrane units allows one to identify where the fouling actually occurs. If the adsorbent were deposited onto membrane surface directly, it would not be possible to tell whether the increase in pressure across the whole system was caused by fouling of the adsorbent layer or the membrane. On the other hand, if μGAF and membrane unit are separated, one can monitor the pressure increase for each unit and thereby distinguish which unit is actually getting fouled.

The potential value of μGAF as a pretreatment process in water treatment is huge. The process integrates adsorption and granular media filtration and thus can save

space used for coagulation in conventional treatment processes. μGAF is also capable of removing soluble NOM and mitigating membrane fouling substantially, and therefore can greatly reduce maintenance effort and energy cost.

The research described here provides a deeper understanding of the μGAF process and further explores the potential application of the process. As a relatively new technology, the operational parameters that can potentially impact μGAF performance have not been thoroughly investigated. Therefore, the main goal of this research is to evaluate the effect of operational parameters on μGAF performance and to exploit the potential of μGAF in water treatment applications. Physical/chemical operational parameters investigated in this study include applied flux, applied pressure, solution pH and solution ionic environment. Also, attempts were made to identify the fouling mechanism in μGAF. Clarifying those aspects can help in evaluating the potential of μGAF from both fundamental and application perspectives and is ultimately beneficial for developing a better pretreatment process for the water treatment industry. Lastly, large bench-scale tests were conducted to exploit the potential of μGAF as a pretreatment for membrane filtration.

This dissertation is divided into five chapters. The current chapter provides a brief introduction of the whole study; Chapter 2 summarizes background literature of related research; Materials and experimental methodology are described in Chapter 3; Chapter 4 presents experimental results and discussion. Lastly, Chapter 5 summarizes the entire dissertation.

2. Literature Review

This chapter begins with a discussion of NOM characteristics and analysis. Then, the relationship between major natural water contaminants (NOM and colloids) and membrane fouling is reviewed, followed by a summary of approaches for reducing membrane fouling.

2.1. NOM analysis

Much research on NOM properties has been published in the past few decades [18–28]. Natural water NOM is a mixture of complex organic compounds derived from aquatic plant debris and/or microbiological reaction products, with molecular weight (MW) ranging from several hundred to 100 kDa. Typical aquatic NOM consists of aromatic and aliphatic hydrocarbons with attached ketone, amide, carboxyl and hydroxyl functional groups.

Since NOM comprises a continuous spectrum of organic components, it is difficult to identify specific NOM components. Many approaches have been used to classify NOM fractions, but typically only about 10% of the NOM has been identified as specific compounds [28]. Nevertheless, many methods have been developed to characterize composite NOM properties, including measurement of total organic carbon, spectrometric methods (such as UV-vis absorbance and fluorescence), chromatographic methods (HP-SEC) and resin fractionation [18,28].

Total organic carbon (TOC) and dissolved organic carbon (DOC) are probably the most commonly used bulk parameters to represent the NOM content in water. The analysis is achieved by mineralizing all the organic carbon in the sample and measuring the CO_2 that is generated. DOC is defined as the organic carbon in the filtrate after the sample is filtered through a 0.45 μm filter, while TOC is the

corresponding value for an unfiltered sample.

UV-vis absorbance is a quantitative measure of all components that absorb UV and/or visible light; wavelengths between 220 and 280 nm are in general considered appropriate for NOM analysis. Absorbance at 254 nm is thought to reflect the aromatic groups in a water sample and is considered a surrogate for humic-like substances. Absorbance at 254 nm is strongly correlated with the DOC concentration and is widely used in natural water NOM analysis [18]. The main advantage of using UV-vis absorbance is that it is a simple and fast analysis, and it does not require sophisticated instrumentation. The specific UV-absorbance (SUVA) is defined as the UV absorbance divided by DOC concentration. SUVA at 254 nm ($SUVA_{254}$) is often used as an indicator of the hydrophobicity of the sample. In general, if a sample has a $SUVA_{254}$ value >4 L/mg-m, the NOM of the sample is considered mainly composed of hydrophobic and aromatic materials.

Not all NOM compounds absorb ultraviolet or visible light. Recently, fluorescence spectroscopy has received more attention in natural water analysis. In this method, molecules in the sample are excited by irradiation, and the emitted radiation at different wavelengths is measured. Different fluorophores yield signals at different excitation and emission wavelengths, so the method is helpful for determining the structural composition of NOM, especially humic materials. Fluorescence spectroscopy also has the advantage of simple and fast detection like UV-vis absorbance, but it has better sensitivity and selectivity. Chen et al. [29] reported that, in typical natural water samples, the major fluorophores of NOM can be grouped into humic-like molecules, fulvic-like molecules, aromatic proteins and soluble microbial by-product materials.

Size exclusion chromatography (SEC) fractionates NOM based on molecular size. Samples are injected into a column filled with a porous gel. Smaller NOM

molecules are more capable of traveling through internal void space of the porous gel and thus experience longer travel distances, leading to higher retention time. The method has been used since the 1960s and has been coupled with high-performance liquid chromatography (referred as HP-SEC) since the 1970s. Chin et al. [30] combined HP-SEC analysis with UV-vis and/or DOC detection for both quantitative and qualitative determination of NOM.

NOM can also be fractionated based on hydrophobicity. The International Humic Substance Society (IHSS) has adopted a method for separating NOM based on hydrophobicity, in which the hydrophobic and aromatic fraction of NOM is collected with Amberlite XAD-8 resins, weakly hydrophobic acid fractions (commonly defined as transphilic NOM fraction) are captured with XAD-4 resins, and NOM that does not adsorb onto either XAD-8 or XAD-4 resins is defined as hydrophilic. However, extreme pH levels and changes during the fractionation process may affect the chemical or physical properties of the NOM, and irreversible NOM adsorption to the resins can influence the results. Nevertheless, resin fractionation is a useful approach for understanding NOM in natural water and has been widely used and accepted for NOM analysis.

2.2. NOM and membrane fouling

Historically, it was widely believed that humic substances are the fraction of aquatic NOM primarily responsible for membrane fouling. Yuan and Zydney [6,7] evaluated fouling caused by humic acid in MF and UF systems, and reported that fouling occurs mainly at the membrane surface. Jucker and Clark [31] also investigated the fouling potential of humic substances, but they found that fouling was mainly caused by adsorption to membrane pore walls rather than aggregation of humics on the membrane surface. Impacts of different fractions of humic acids

contributing to fouling have also been studied. Yuan and Zydney [6,7] reported that macromolecules caused more rapid fouling that smaller molecules did, and Lin and co-workers [32,33] also found that the high molecular weight fraction of humic substances is responsible for major flux decline.

Non-humic, hydrophilic fractions in NOM, especially polysaccharides and proteins, can also be responsible for membrane fouling. Many research studies have focused on the relationship between polysaccharides and membrane fouling. For instance, Nataraj et al. [34] examined polysaccharide (xanthan) fouling in a cross-flow membrane system and reported that cake formation is the predominant mechanism; Jermann et al. [3] investigated UF membrane fouling caused by humic acid and polysaccharide (using alginate as surrogate) and reported more rapid flux decline during filtration of alginate in comparison to humic acid. The authors also proposed that humic acid tends to adsorb onto membrane surfaces and in the pores, whereas alginate fouls membranes mainly via cake formation on the membrane surface.

A group of polysaccharides called transparent exopolymer particles (TEP) have received increased attention in membrane research in recent years [35–43]. TEP comprises sticky gel-like particles that are mainly acidic polysaccharides. In natural systems, TEP is mainly generated from polysaccharides released by algae and is ubiquitous in natural waters [44,45]. TEP can cause membrane fouling not just by forming a sticky gel layer on the membrane surface, but also by initiating membrane biofouling [35,36]. Torre and co-workers [37–39] reported a significant relationship between TEP concentration and membrane fouling in an MBR system, and Wu et al. [46] reported that higher levels of soluble TEP lead to more rapid membrane fouling in MBRs. Studies of TEP fouling potential in surface waters have also been reported. Berman et al. [36] investigated UF membrane fouling using lake water, reported that

the TEP concentration is significantly correlated with membrane fouling rate, and suggested that TEP is responsible for biofilm forming on the membrane surface. Villacorte et al. [40] investigated RO filtration of sea water and fresh surface waters. They correlated TEP with RO membrane fouling and found TEP deposition on the RO membrane surface via membrane autopsy. Kennedy et al. [41] found TEP to be responsible for UF membrane fouling in both surface water and secondary wastewater effluent. The authors also reported that coagulation with alum effectively reduced TEP fouling in the UF system.

Unlike humic substances, polysaccharides have relatively low UV absorbance and fluorescence sensitivity, so they cannot easily be measured using these analytical approaches. Colormetric methods were developed for polysaccharide measurement in the 1940s. In these methods, anthrone or phenol reagents bind to the polysaccharide under acidic conditions and promote solution discoloration, so that samples can be analyzed using spectroscopic methods [47–50]. A specific analysis for TEP measurement was originally developed by Passow and Alldredge [51] and then modified by other researchers [40,41,52]. In short, dye is used to bind with and stain TEP in a water sample, and the stained TEP can be analyzed spectroscopically.

The relationship between NOM hydrophobicity and membrane fouling also has been investigated. Fan et al. [9] fractionated NOM into four different fractions and reported the fouling potential decreased in the following order: hydrophilic neutral compounds > hydrophobic acids > transphilic acids > hydrophilic charged compounds. Carroll et al. [53] found that small hydrophilic neutral compounds caused more rapid flux decline and were more resistant to coagulation. Lastly, Lee et al. [25] reported that, in natural waters, hydrophilic macromolecules with apparent molecular weight (AMW) between 10 kDa to 100 kDa (most likely natural polysaccharides) caused significant flux decline in low-pressure membrane filtration.

Different solution chemistry (for instance, solution pH, ionic strength or presence of specific cations) can impact NOM properties, interactions between NOM and membranes and/or interaction among NOM molecules. Yuan and Zydney [7] reported that humic acid caused more rapid fouling at low pH, higher ionic strength or in the presence of Ca^{2+}. Elimelech and co-workers [54,55] examined NF membrane fouling by humic acids at different ionic strengths and found higher NOM deposition onto the membrane in the presence of Ca^{2+}. The authors suggested that the interaction between Ca^{2+} and humic carboxyl functional groups reduced the repulsion between humic macromolecules and resulted in enhanced NOM deposition onto the membrane surface. Humic acids also caused more rapid flux decline at low pH. The authors suggested that protonation of the carboxylic groups reduced the charge on NOM macromolecules and the electrostatic repulsion between NOM and the membrane, resulting in more extensive NOM deposition. Lee et al. [5] observed faster fouling by NOM and colloids in NF processes at higher ionic strength and in the presence of Ca^{2+}. Similar to Elimelech's [54,55] interpretation, the authors suggested that NOM-Ca^{2+} complexation and better colloid destabilization at higher ionic strength were responsible for more severe fouling. Ahn et al. [56] also reported that Ca^{2+} promotes NOM aggregation and leads to enhanced membrane fouling. Kim and Dempsey [57] tested several commercial NOM sources (alginate, SMP, EfOM, humic acid and NOM) and reported that Ca^{2+}, increased the colloid concentration in all sources of NOM tested and led to more severe membrane fouling by most of them except for alginate. Lastly, Tian et al. [58] investigated the effects of Na^{+} and Ca^{2+} on UF membrane fouling and reported that both sodium and calcium ions enhanced fouling by humic acids and proteins, but they had only a small effect on fouling by polysaccharides.

2.3. Colloidal membrane fouling

Historically, a main goal of membrane processes was to eliminate particulates in feed water. A large amount of research has been conducted investigating fouling by particulates and colloids [59–73]. These studies have investigated the effects of hydrodynamics (flow pattern, applied flux, applied pressure) and particle and membrane properties (size, material, surface charge, etc.), in an attempt to predict the fouling pattern and process efficiency. In general, colloid stability is an important factor in membrane fouling, with destabilized particles having a tendency to deposit onto membranes. In a review paper, Tang et al. [68] concluded that applying cross-flow can help reduce colloidal fouling, and this operational option is applied in many water treatment plants. Yiantsios and Karabelas [64] evaluated the effect of ionic strength on colloid stability and fouling and suggested that destabilization of colloids leads to significant deposition on the membrane surface and membrane fouling. Boussu et al. [61] drew a similar conclusion for an NF process. The authors also suggested that solution pH plays an important role in affecting fouling by altering the interaction forces among colloids and/or between colloids and membranes. Lastly, the authors suggested that colloids form dense cakes on hydrophobic membranes, leading to more severe fouling.

Research on fouling by colloids and particles led to the concept of a *critical flux*. The general idea is that under given experimental conditions (such as particulate sizes, membrane material and water chemistry), membrane fouling can be avoided by operating at a flux less than a specific value [69–71]. This concept is further discussed in a later section.

Studies like those cited above provide useful information for understanding particulate membrane fouling; however, most of those studies investigated idealized scenarios where particulates were the only foulant in the feed solution. In real

membrane applications, the feed water contains a mixture of particulates, organic and inorganic colloids, and soluble contaminants such as NOM, leading to "synergistic" effects of different constituents on membrane fouling. Elimelech [5,74] reported that when the feed solution contained both colloids and soluble NOM, membranes were fouled more rapidly than the expectation based on the sum of the individual foulants.

2.4. Membrane fouling model and cake layer

A classic membrane fouling model was published by Hermia [75], in which he identified four fouling scenarios and developed equations to predict the permeate flux decline in each, for constant-pressure, dead-end membrane filtration. In the first scenario, referred to as complete blocking, foulants are assumed to reside only on the surface of the membrane and to block a portion of the open area (pore mouth) where they deposit. In this scenario, the amount of the membrane opening blocked is proportional to the amount of water filtered. In the second scenario, referred to as intermediate blocking, the foulants are assumed to deposit either directly on the membrane surface or on previously rejected particles. The third scenario is referred to as standard blocking, in which foulants are assumed to deposit on internal pore walls and narrow the effective pore diameter. Lastly, in the cake filtration scenario, foulants are assumed to form a uniform and steadily growing cake layer on the membrane surface, increasing the permeation resistance. Conceptual images of these mechanisms are illustrated in Figure 2.1 [76].

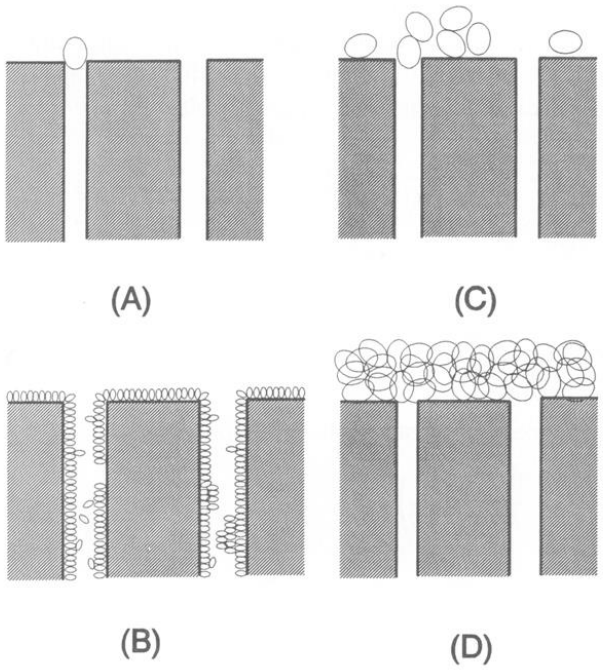

Figure 2.1 Conceptual graphs of the four membrane fouling mechanisms: (A) complete blocking, (B) standard blocking, (C) intermediate blocking and (D) cake filtration [76]

Since the equations developed by Hermia apply only for constant-pressure filtration system with incompressible foulants, Hlavacek and Bouchet [77] further developed equations for constant flowrate filtration, and Chellam and Xu [78] extended these models to compressible cakes.

Cake layer formation during membrane filtration can play an important role in membrane fouling. Modeling efforts have mostly represented cake layers as idealized structures (e.g., made of uniform, spherical particles), but in truth cakes or gel layers are composed of a complex mix of contaminants including both soluble and insoluble foulants. Many researchers have monitored the formation of foulant layers and reported on the dramatic increase of permeation resistance that they can cause, especially in MBR systems [53,54,65–72]. In general, cake layer compressibility and porosity are strongly related to permeation resistance and can be affected by factors such as permeation flux, flow pattern, foulant type and solution chemistry. Several

models and cake layer monitoring methods have also been developed. These attempts have mostly been empirical and have been conducted under different conditions, and no consensus has been reached.

2.5. Membrane fouling reduction attempts

Numerous approaches have been tested to reduce membrane fouling and to enhance process performance. As mentioned previously, adjusting operational parameters and applying pretreatment processes are the most common approaches. The following sections provide information about those approaches.

2.5.1. Effect of operation flux and the concept of critical/sustainable flux

Operation flux can be a critical impact factor for membrane fouling. It has been observed and reported by many researchers that higher permeation rates lead to more rapid membrane fouling. Chudacek and Fane [86] studied the effect of permeation flux on membrane fouling with three different types of deposit (colloid, protein and chain polymer) and found that specific resistance of the deposit layer increased with increasing initial permeation rate. Similar patterns were observed by other researchers, especially for research using proteins or polysaccharides as the main foulant. Opong and Zydney [87] observed lower permeability of the protein deposit layer on membranes with higher initial operation flux and suggested that the porosity of the deposited layer could be affected by the compressive pressure introduced by the permeate flow. Siotopoulos and Karabelas [88] used commercial sodium alginate as the foulant in a dead-end, constant flux UF process and reported higher initial pressure causes more severe compression on the deposited alginate layer and leads to a more rapid increase in the specific resistance. Based on theoretical modeling, Song and Elimelech [89] suggested that the deposition of foulant could be affected by the

interaction between the drag force (induced by permeate flow) and the electrostatic repulsion. At high permeate flux, the drag effect overwhelms electrostatic repulsion and leads to more efficient foulant deposition onto the membrane.

The concept of a limiting flux when filtering water that contains colloidal particles was first introduced in 1986 by Cohen and Probstein [60]. Subsequently, Belfort et al. [38] investigated the effects of ionic strength and surface interaction on colloidal fouling. The term "critical flux" is defined differently in different publications, but in all cases the general idea is that it is a flux at which a significant change in fouling occurs [69–71]. For instance, Bacchin et al. [69] defined critical flux as "the flux below which no fouling occurs". They hypothesized that, at fluxes below the critical value, particle repulsion was too strong to allow deposition of colloids onto the membrane surface. Field et al. [70] defined the critical flux as the flux at which the flux-TMP relationship becomes non-linear. Lastly, Howell et al. [71] defined critical flux as the "flux below which there is no fouling by colloidal particles", thereby excluding fouling caused by macromolecules or other soluble foulants. Chen et al. [90] reported that, when the flux is sub-critical, the dependence of TMP on flux is stable, whereas significant hysteresis occurs in the TMP-flux relationship under super-critical flux conditions.

The studies on critical flux cited above provide useful information, but they were conducted under idealized conditions, considering only colloids and excluding macromolecules. In any practical membrane application, the feed water contains a mixture of foulants, and interactions among foulants and the membrane can affect the critical flux. Numerous papers have been published reporting on experimental approaches for evaluating the critical flux in practical applications [55,91–97]. These studies provide information about the effects of different feed water quality, membrane materials, and operational conditions (different fluxes or foulants) on the

critical flux.

As a practical matter, a goal of minimizing or eliminating irreversible fouling (i.e., achieving *sustainable flux*) is probably more achievable and more important than eliminating fouling altogether. Early water treatment membrane systems were mostly operated in dead-end filtration mode, primarily for simplicity. However, in dead-end filtration, the permeate flux forces all foulants to move towards the membrane surface, which can lead to severe concentration polarization and more rapid intrusion/adsorption of foulants onto the membrane surface or into membrane pores [65]. Cross-flow filtration, in which the flow is tangential to the membrane surface, was introduced to mitigate this drawback. However, applying cross-flow filtration requires more energy than applying periodic backwashing in full-scale applications. Therefore, at present, cross-flow filtration is the mostly used in laboratory-scale experiments. On the other hand, dead-end filtration is commonly used for full-scale scenarios as well as laboratory-scale experiments.

2.5.2. Pretreatment processes

Besides adjusting operational parameters, another strategy often used for membrane fouling mitigation is pretreatment. Traditional pretreatment processes include coagulation, adsorption, pre-filtration and pre-oxidation [11].

Conventionally, in coagulation and/or adsorption, a coagulant and/or adsorbent is added to the feed water in a well-mixed reactor, where it binds the contaminant. After a period of mixing, the majority of the solids are removed by sedimentation or granular media filtration. Coagulation using Fe or Al salts is usually effective at reducing membrane fouling. Upon addition to a solution, these salts react with water and form monomeric or polymeric ions or insoluble hydroxides. The ions can lead to flocculation by charge neutralization, and the insoluble hydroxides are gelatinous

particles with large surface area which can promote sweep-flocculation. The solids are also good adsorbents for many polar, weakly ionic species. Fe and Al cations can also form precipitates and complexes with NOM. Organic coagulants are also often employed in water pre-treatment process. These soluble polymers are usually charged (and are therefore called polyelectrolytes) and have a random coil configuration. Through electrostatic interaction, bridging flocculation and charge neutralization, organic polymers promote formation of tighter flocs and thereby enhance flocculation [98]. Cationic polyelectrolytes and alum often have a beneficial synergistic effect on removal of humic substances through coagulation [98–101]. Kam and Gregory [102] reported that the performance of cationic polymers improved with increasing charge density.

Underdosing of coagulant can lead to formation of fine flocs that are hard to settle, and, if they are of similar size to MF membrane pores, can cause membrane fouling. On the other hand, overdosing of coagulant can lead to re-stabilization of particles, resulting in lower settling efficiency and eventually more severe membrane fouling. In comparison, in an optimal dose scenario, larger, settable flocs are formed, and, with the floc size larger than typical MF membrane pore size, membrane fouling can be reduced. Typically, laboratory or pilot scale experiments are required to determine the optimal dose for removing contaminants and reducing fouling.

Powdered activated carbon (PAC) is the most studied and applied adsorbent in pretreatment processes. PAC invariably removes some NOM from water, but it does not necessarily reduce membrane fouling. In several studies, applying PAC adsorption in conjunction with a UF process led to more rapid fouling [32,33,103,104]. Instead of feeding the PAC-treated solution containing suspended adsorbent particles directly to a membrane, Li and Chen [105] removed the adsorbent particles prior to membrane filtration. The authors used Aldrich humic acid as the NOM source. PAC removed a

portion of the humic acids but was not effective at reducing membrane fouling. Lastly, Cai [17] used alginate as a surrogate for polysaccharide and reported that PAC removed very little alginate, and the alginate caused significant fouling.

Besides adsorption with PAC, metal (especially Fe and Al) salts are also capable of adsorbing soluble contaminants in water and are commonly used in water treatment applications. Vilge-Ritter et al. [106] reported the selectivity of various adsorbents for different fractions of NOM. They reported that polysaccharides bind preferentially to aluminum polychlorosulfate (PACS) over aluminum sulfate and ferric chloride. Besides traditional application of iron or aluminum salts, Benjamin and co-workers [15] used heated aluminum oxide particles (HAOPs) and heated iron oxide particles (HIOPs) as adsorbents and achieved substantial NOM removal efficiency and membrane fouling reduction.

Researchers have also tried to remove NOM by ion exchange processes. Originated and developed by Australian researchers, magnetic anion exchange resin (MIEX) has been applied to water treatment and received more attention in recent years. MIEX has a positively charged polyacrylic structure which is good at attracting anionic substances in natural water, and has a magnetized iron oxide component which helps in the agglomeration and separation steps during and after the ion exchange process. Efficient and rapid removal of negatively charged NOM from natural water, especially humic and fulvic substances, has been reported [107–110]. Over 80% removal of DOC and UV_{254} was achieved using MIEX alone, and even higher removals were achieved when MIEX was combined with a conventional coagulation process. MIEX can also adsorb bromide from the raw water, leading to a reduction in DBP formation. However, the effects of MIEX pretreatment on membrane fouling are not entirely consistent. In several studies, MIEX treatment reduced membrane fouling [90,91], but others found that MIEX was effective at

removing DOC but had a negligible effect on membrane fouling reduction [113]. Allpike et al. [114] tested MIEX treatment with different DOC fractions and found that the high MW fraction was not effectively adsorbed by MIEX. Humbert et al. [113] suggested that this high MW fraction was responsible for the majority of membrane fouling. Additional studies are required to explore the relationship between MIEX, NOM and membrane fouling.

Adding oxidant into the feed solution can suppress microbial growth and increase contaminant removal, mainly via particle destabilization and/or oxidation of soluble metal species, resulting in contaminant precipitation [115–117]. In a study of ozonation of secondary effluent, Wang et al. [118] found that low doses of ozone can improve the bio-degradability of NOM, altering the size distribution of the molecules and their contribution to membrane fouling. Heng et al. [119] also reported that chlorination enhanced algae inactivation and adsorption by manganese dioxide, leading to better UF membrane fouling control. In several other studies, less NOM fouling was observed when ozone was applied as a preoxidant [99,100]. Inorganic species, however, may have an adverse impact on membrane fouling when pre-oxidation is applied. Schlichter et al. [122] reported ozonation had negligible effect on membrane fouling by clay minerals, and Chae et al. [123] found that chlorination promoted precipitation of Mn and Fe species and eventually led to more severe fouling of a PVDF membrane.

Physical pretreatment approaches, such as pre-filtration, are also used for membrane fouling reduction. Granular media pre-filtration is widely used in conventional water treatment plants to remove particles. It is also sometimes used prior to membrane filtration to reduce membrane fouling [124]. However, granular media filtration removes little soluble material, and that material might cause fouling. Another disadvantage of granular media filtration is that it requires a large amount of

land.

2.5.3. Pretreatment by micro-granular adsorptive filtration (μGAF) process

Instead of dosing adsorbent directly into solution, some researchers have combined adsorption and membrane filtration by pre-depositing a thin layer of adsorbent directly onto the membrane surface. Chang and Benjamin [12] first proposed this method, using heated iron oxide particles (HIOPs) as the pre-deposited absorbents, and achieved both high NOM removal and substantial reduction of fouling. Later, Chang et al. [13] applied the HIOP-UF process to 16 different natural water sources and reported enhanced reduction of permeate TOC concentration and DBP formation potential, as well as substantial UF membrane fouling reduction.

The choice of adsorbent used in pre-deposition can have a critical effect on the process performance. Chang and Benjamin [12] found that unheated iorn oxide particles (UHIOPs) block membrane pores (based on SEM images) and caused membrane fouling while HIOPs do not. Similar results have been reported by Lee and Choo [125,126], who found that although pre-depositing iron oxide particles (IOPs) reduced irreversible membrane fouling, it also caused significant initial flux decline. The authors suggested that the IOPs were poorly crystalized ferric hydroxide particles with gluey structures, which exacerbated membrane fouling by blocking membrane pores. Zhang et al. [127] used PAC as a pre-deposited adsorbent on UF membranes and reported that although PAC removed a portion of the NOM from the feed solution, membrane fouling became more severe with increasing adsorbent dose. Based on SEM images, the authors suggested that the NOM enhanced the binding among the NOM, PAC and the membrane, forming a foulant cake layer with low permeability.

Since the pre-deposited adsorbent layer can be thought of as a miniature granular media bed, the research group led by Benjamin referred to this method as

microgranular adsorptive filtration (μGAF), because the process integrates granular media filtration and adsorption. The μGAF process was further investigated and explored by Benjamin and co-workers [14–17]. In these studies, the performance of the μGAF process (depositing HIOPs or HAOPs onto the membrane surface) and conventional coagulation/adsorption processes were compared, and better NOM removal and substantial membrane fouling control (extended filtration cycle by several fold) were achieved with the μGAF process. At the end of a filtration cycle, the pre-deposited adsorbent layer in the μGAF process can be washed off the membrane surface hydraulically and, based on SEM images, the membrane beneath adsorbent layer was virtually identical (clean) to a virgin membrane. The permeability of the membrane was almost fully recovered, implying that foulants were collected within the adsorbent layer.

The research group also compared the μGAF process performance using either unheated $Al(OH)_3$ particles or HAOPs and found that the unheated $Al(OH)_3$ particles formed a more compact layer which caused high initial hydraulic resistance and more rapid pressure buildup during filtration. They suggested that the characteristics of metal oxide particles were changed and the particles were partially dehydrated during the heating process, leading to the formation of less amorphous particles. When pre-deposited onto a membrane, the adsorbent layer had much lower hydraulic resistance than unheated metal oxide particles and stayed permeable with or without NOM accumulation.

In the studies noted above, the performance of μGAF with PAC and HAOPs was also compared. Although PAC removed more NOM than HAOPs or HIOPs, membrane fouling was more severe with the μGAF process using PAC. Analysis of SEM images was consistent with the previous study of Zhang et al. [127], which indicated that PAC, foulants and membrane surface all adhered together, so fouling

was exacerbated. By contrast, as mentioned above, the HAOPs or HIOPs layer and accumulated foulants can be easily removed from the membrane surface. An alternative explanation proposed by the researchers was that PAC selectively adsorbed non-foulant NOM, while HAOPs selectively adsorbed foulant NOM.

2.6. Summary

Membrane processes are widely used for water treatment. The biggest limitation of these processes is membrane fouling, which lowers process efficiency and increases the effort and cost of maintaining the membranes. Membrane fouling is caused by contaminants in the feed water, mainly colloids and NOM. Major fouling mechanisms include cake layer formation and membrane pore clogging; in most cases, fouling is caused by both mechanisms.

Factors impacting membrane process performance include the concentration and nature of the contaminants, operational conditions and pretreatment processes. Colloids and NOM are the major foulants in feed water. Colloidal stability, which can be affected by pH and ionic environment, is strongly related to colloid deposition mechanisms and membrane fouling. Fractionation of NOM, based mainly on molecular weight and hydrophobicity, has been used to identify the most problematic NOM fractions in membrane processes. In general, NOM with high molecular weight causes more severe fouling in low pressure membrane systems. Hydrophilic neutral compounds are currently thought to have the highest fouling potential, followed by hydrophobic acids, transphilic acids and hydrophilic charged compounds. The ionic environment also impacts NOM fouling, with higher ionic strength and divalent cations (especially Ca^{2+}) enhancing membrane fouling by promoting interactions among NOM molecules or between NOM molecules and membrane surfaces. Flow-patterns (dead end or cross-flow filtration) and applied fluxes can be modified

to reduce foulant accumulation on membrane surfaces. In addition, pretreatment processes can remove contaminants prior to the membrane and thus mitigate membrane fouling. Correlations between operational parameters (including contaminant types, applied flux, applied pressure, and solution chemistry such as pH or ionic environment) and membrane fouling have been investigated in many studies. These studies provide a great deal of information, but most of those studies focused on direct membrane filtration and were carried out under idealized conditions.

The μGAF process, a novel pretreatment process developed in recent years, integrates granular media filtration and adsorption and has been shown to be more efficient than conventional approaches at removing NOM and mitigating membrane fouling substantially.

3. Materials and methodology

In this chapter, materials used in this study are described, followed by detailed experimental methodology.

3.1. Experimental materials

3.1.1. Natural water samples and synthetic water

In cartridge filtration tests, water collected from Lake Pleasant (LP, located at Bothell, WA, USA) was used as the primary source of natural water. Water samples were filtered through a 5-μm cartridge filter (Harmsco, Inc., USA) right after collection to eliminate large particles. They were then stored at 4 ℃ and brought to room temperature before being used in experiments. In most cases, the LP water was diluted 1:1 with dionized (DI) water for experiments. For some experiments, reagent grade 1 M or 0.1 M NaOH or HCl was added to adjust the feed pH to within 0.05 units of the desired value. Solution pH was measured with a pH meter (Thermo Scientific, Orion Star A211).

LP water with 50% dilution had a pH of 7.2-7.6, TOC concentration of 7.5-10.0 mg/L, and UV_{254} of 0.360-0.475 cm^{-1}, yielding $SUVA_{254}$ values of 3.60~4.75 L/mg-m. Figure 3.1 shows the excitation-emission matrix (EEM) fluorescence spectrum of 50% LP water. The spectrum has peaks at Ex/Em of 220-240/330-350 nm (peak A), Ex/Em of 330-340/425-430 nm (B) and Ex/Em of 380-390/450-470 nm (C), representing aromatic proteins, fulvic-like substances and humic-like substances, respectively, according to the characterization guideline reported by Chen et al. [29]. Figure 3.2 illustrates a typical SEC chromatogram of LP water, in which five fractions of NOM can be identified.

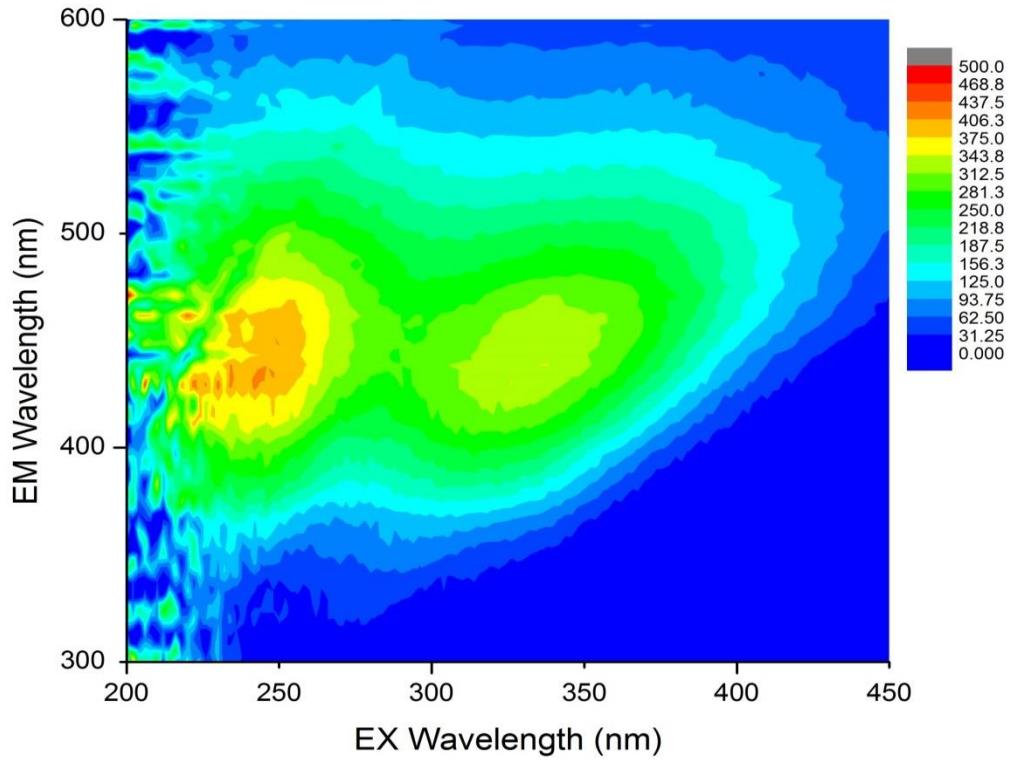

Figure 3.1 Fluorescence spectrum of 50% LP water

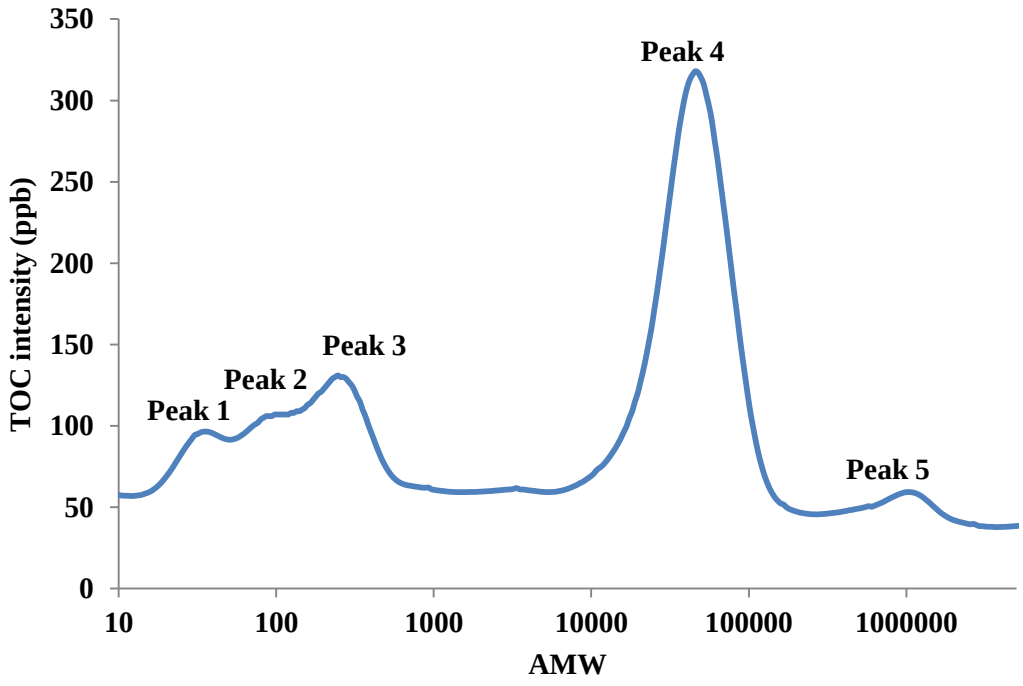

Figure 3.2 SEC eluent profile of LP water

Water collected from Lake Union (LU, located at Portage Bay near the University of Washington, Seattle, WA, USA) was used for tubular filtration tests. LU water was pumped and filtered through a 70-μm mesh filter (to eliminate coarse particulates) into a holding tank. The water was then fed directly to the filtration systems. LU water had a typical pH range of 6.8-7.1, DOC concentration of 2.0-3.8 mg/L, UV_{254} of 0.04-0.07 cm^{-1}, and $SUVA_{254}$ of 1.05-3.5 L/mg-m.

Table 3.1 summarizes the basic properties of LP (50% dilution) and LU water.

Table 3.1 Basic properties of feed water used in this study

Water	pH	DOC concentration (mg/L)	UV_{254} absorbance (cm^{-1})	$SUVA_{254}$ (L/mg-m)
50% LP	7.2-7.6	7.5-10.0	0.360-0.475	3.60-4.75
LU	6.8-7.1	2.0-3.8	0.04-0.07	1.05-3.50

3.1.2. Adsorbents

Heated aluminum oxide particles (HAOPs) were the main adsorbent used in this research. HAOPs were prepared by neutralizing aluminum sulfate (Arcos Organics, USA) solution with NaOH (4M) to pH 7.0 to precipitate $Al(OH)_{3(s)}$. The suspension was then heated in a closed glass jar at 110℃ for 24 hours. After heating, the HAOPs solution was cooled to room temperature prior to being used in experiments. The stock solution concentration was 10 g/L as aluminum.

Besides HAOPs, two commercial PACs – Norit SA Super (Cabot Corp., Alpharetta, GA) and WPH (Calgon Carbon Corp., Moon Township, PA) – were used in this study. Basic adsorbent properties are summarized in Table 3.2.

Table 3.2 Basic properties of adsorbents used in this study

Parameters	HAOPs	PAC – Norit SA Super	PAC - WPH
Volume-based d_{50}, μm[a]	29.5	15	10
BET surface area, m^2/g	35.6	1150	903
Micropore surface area, m^2/g	NA	NA	888
Mesopore surface area, m^2/g	NA	NA	15

[a]Volume-based d_{50} for HAOPs was determined by the method described in Section 3.3.5. d_{50} for two commercial PACs were based on product information provided from the manufacturers

3.1.3. Mesh filters, cartridge filters and membranes

Nylon mesh was used in most experiments to support the adsorbent in the μGAF pretreatment step. The nylon mesh had a 677 x 470 twilled Dutch weave pattern and nominal 5-μm openings (Product 03-5/1, SEFAR Inc., USA). In some experiments, #316 stainless steel mesh was used as the adsorbent support media. The stainless steel mesh had a 200 x 1400 twilled Dutch weave pattern with nominal 10-μm openings (Howard Wire Cloth Corp., Hayward, CA).

In some experiments, cartridge filters of nominal pore openings of 1 or 0.35 μm (Harmsco Inc., USA) were used to pre-filter the feed solution prior experiments. The cartridge filters were made from polypropylene. A cartridge filter had a length and outer diameter of 24.8 and 6.35 cm, respectively.

Flat-sheet polyethersulfone (PES) UF membranes (Mirodyn-Nadir, Netherlands) with nominal 0.05-μm pores were used as the downstream membranes in most μGAF tests. SEM images for the nylon mesh, stainless steel mesh and a PES membrane are shown in Figure 3.3.

In some experiments, tubular ceramic membranes were used. The ceramic membranes were manufactured by Cascade Designs, Inc. (Seattle, WA). The tubes

had a nominal pore size of 0.2 μm and were 21.2 cm long, with an internal diameter (ID) of 1.2 cm and wall thickness of 0.4 cm. Lastly, polymeric UF membrane modules containing PES hollow fibers (Seccua GmbH, Germany) with nominal 8-nm pores were used in some experiments as downstream membranes. Characteristics of the meshes and membranes used in the experiments are summarized in Table 3.3 and Table 3.4, respectively.

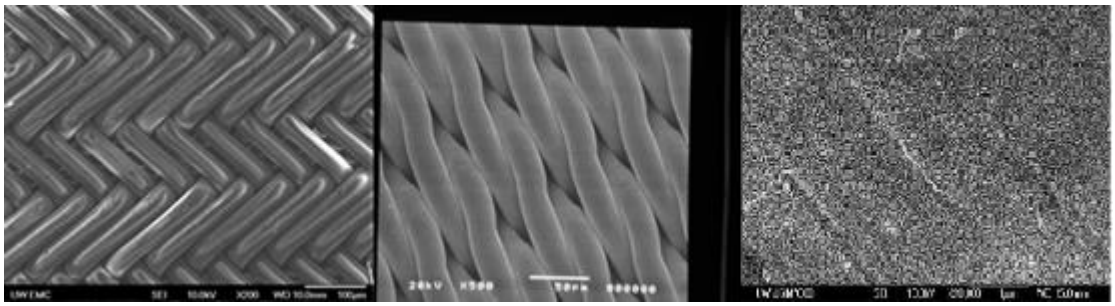

Figure 3.3 SEM images for clean nylon mesh (left), stainless steel mesh (middle) and PES membrane (right)

Table 3.3 Characteristics of meshes used in μGAF experiments

Material	Pore Size (μm)	Weaving Pattern	Manufacturer
Nylon	5	Twilled Dutch, 677x470	SEFAR
#316 Stainless steel	10	Twilled Dutch, 200x1400	Howard Wire Cloth, Co.

Table 3.4 Characteristics of membranes used in µGAF experiments

Material	Pore size, µm	Geometry	Surface area, m^2	Manufacturer
PES	0.05	Flat sheet disk D = 47 mm	0.001	Microdyn Nadir
Ceramic	0.2	Tubular ID = 1.2 cm L = 21.2 cm	0.008	Cascade Design, Inc.
PES	0.008	Hollow fibers ID = 0.7 mm L = 230 mm	0.076	Seccua

3.1.4. Fluorescence polystyrene beads

Fluorescence polystyrene particles (Thermo Scientific, Fluro-Max Dyed series) were used in some experiments. Particle sizes used in this study are 1-µm, 0.31-µm and 0.1-µm.

3.2. Experimental methods

3.2.1. Batch adsorption tests

Batch adsorption tests were conducted with different adsorbents and coagulants at room temperature. After the desired dose of adsorbent was added to the water, the pH of the samples was adjusted to 7.0 ± 0.2 with 0.1 M NaOH or HCl. Sample flasks then were placed on a shaker and shaken at 200 rpm. After 2 hours of contact, samples were filtered with a 0.45-μm syringe filter and analyzed.

3.2.2. Cartridge system: sequential μGAF-membrane filtration

The schematic setup for cartridge filtration tests is illustrated as Figure 3.4. All cartridge filtration tests were operated in dead-end mode. Sheets of mesh or membrane material were cut into 47 mm disks (effective area 9.62 cm^2), fit into filter cartridge holders (Pall Co., USA) and sealed with rubber O-rings. In all cartridge filtration tests, nylon mesh was used in the upstream cartridge to hold the adsorbent, and flat sheet PES membranes were used in the downstream cartridge.

HAOPs were deposited onto the surface of the nylon mesh by injecting a small amount of stock solution into the cartridge with a syringe. During injection, the cartridge was gently swirled to ensure an even distribution of deposited adsorbent. The injection volume was adjusted to achieve the desired surface loading (mass of adsorbent per unit area, g/m^2). After adsorbent deposition, DI water was fed through the cartridge for at least 30 minutes. A PES membrane disk was installed into the downstream cartridge, and the same pre-conditioning procedure was applied.

After pre-conditioning of the system, feed solution was directed through the μGAF unit at the desired flux. The permeate line passed through a three-way pinch valve, with one outlet channel connected to an auto-sampler for sampling and another to the permeate reservoir. In some experiments, composite μGAF permeate was

collected in the reservoir and was fed immediately to the downstream membrane unit. The reservoir had a volume of 20 cm^3, and the hydraulic retention time was 10 minutes. In other experiments, permeate from the µGAF unit was collected in a 2-liter beaker during the entire filtration period, and the composite permeate was then fed to the downstream membrane unit.

The pressure at the entrance to each cartridge (µGAF and membrane units) was monitored with pressure transducers (Omega Engineering, USA) connected to a data logger (34970A, Agilent, USA).

Control membrane tests were conducted by filtering feed water directly through a membrane without pretreatment via µGAF unit.

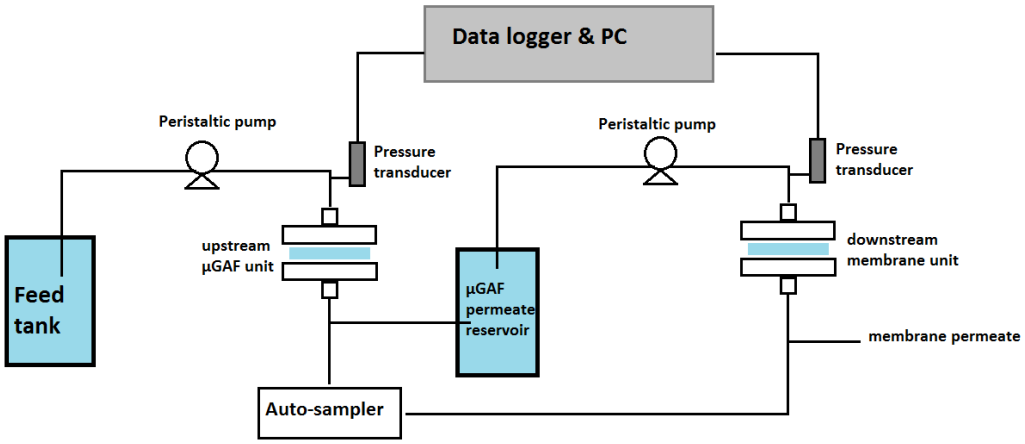

Figure 3.4 Schematic setup of cartridge sequential µGAF-membrane filtration system

3.2.3. Tubular system: sequential μGAF-membrane filtration

A similar sequential filtration setup was employed in tubular filtration tests, as shown in Figure 3.5. An upstream mesh tube with deposited adsorbent (μGAF unit) served as the pretreatment unit for the downstream membrane unit. Filter tubes were set vertically and operated with dead-end, inside-out filtration. A typical filtration cycle started with HAOPs deposition by circulating the adsorbent stock solution axially through the upstream mesh tubes while a constant permeate flux was passed across the wall. HAOPs were carried by this permeate flow and captured by the filter, and were thereby deposited on the tube wall in a thin layer. Raw feed water was then fed directly to the filtration system at the desired, fixed flux. Permeate from the μGAF unit was collected in a temporary reservoir and used as feed solution for the downstream membrane unit, and sample collection and TMP monitoring setups were similar to those used in the cartridge filtration tests. At the end of a filtration cycle, the filter was cleaned hydraulically. A cleaning cycle consisted of four 15-second pulses of a combination of crossflow/backflow washing and air injection, with a 10-second relaxation period between pulses. The entire cleaning procedure took one minute, and a new filtration cycle started right after the cleaning period.

In tubular μGAF tests, a tube constructed of either nylon mesh or #316 stainless steel mesh tube was used as the adsorbent support in the μGAF unit. Either a ceramic membrane or the Seccua PES hollow fiber module was used as the downstream membrane unit. In a few experiments, μGAF was employed in a single unit by depositing the adsorbent directly onto the ceramic membrane. Control membrane tests were conducted by filtering feed water directly through a membrane without pretreatment via μGAF unit.

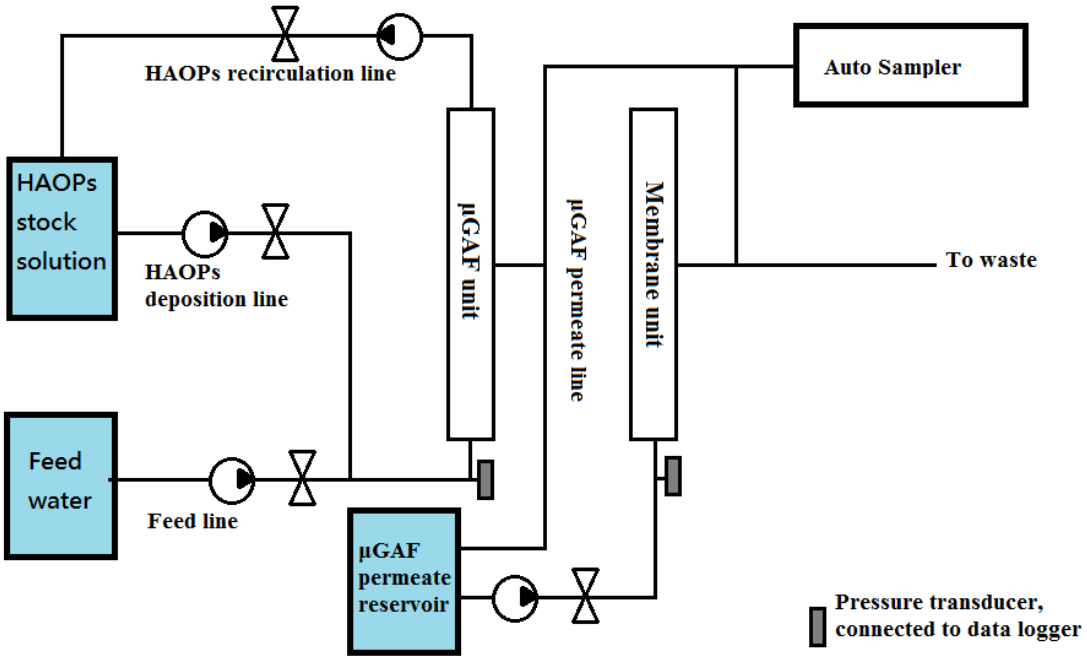

Figure 3.5 Schematic setup of tubular sequential µGAF-membrane filtration system

3.3. Analytical methods

3.3.1. UV absorbance and TOC

UV absorbance at 254 nm (UV_{254}) was measured with a dual-beam spectrophotometer (Lambda-18, Perkin-Elmer, USA) with a 1-cm quartz cell. Spectral data were recorded at wavelengths of 200-400 nm with 0.5-nm resolution. TOC was measured with a TOC analyzer (TOC-V_{CSH}, Shimadzu, Japan).

3.3.2. Fluorescence Spectroscopy

Fluorescence EEMs were acquired using a benchtop fluorometer (Horiba Scientific, Aqualog) with a 1-cm quartz cell. The spectrometer used a xenon excitation source with excitation and emission slits set at a 5-nm band pass. Spectral data were recorded between excitation and emission wavelengths of 200-450 nm and 300-600 nm, respectively, with 1-nm resolution.

3.3.3. TEP

TEP was measured based on a modified spectrophotometric method reported by Arruda Fatobello et al. [52]. The method involves the use of alcian blue (Arco Organics Fisher Scientific, Pittsburgh, PA), a cationic dye which binds to acidic polysaccharides. A 0.06% (m/v) alcian blue stock solution was prepared by dissolving the solids in 0.2 mol/L acetate buffer solution (pH 4). The solution was stored for no more than one month, since alcian blue may aggregate over time, affecting its ability to bind polysaccharides.

To analyze sample TEP, 9 ml of sample was added into a centrifuge tube. One-half ml of 0.06% (m/v) alcian blue stock solution was added into the tube, followed by 0.5 ml of 0.2 mol/L acetate buffer solution (pH 4) to make up the solution volume to 10 ml. The sample was then stirred with a vortex mixer for 30 seconds and

centrifuged at 2160 g for 30 minutes. After centrifugation, the absorbance of the supernatant was measured at 602 nm with a dual-beam spectrophotometer (Lambda-18, Perkin-Elmer, Waltham, MA).

A calibration curve is required to quantify the TEP concentration in water samples. Xanthan gum (MP biomedicals, USA) was used as a standard surrogate for calibrating TEP concentration. A new calibration curve was prepared for each batch of alcian blue solution used. One such calibration curve is illustrated in Figure 3.6.

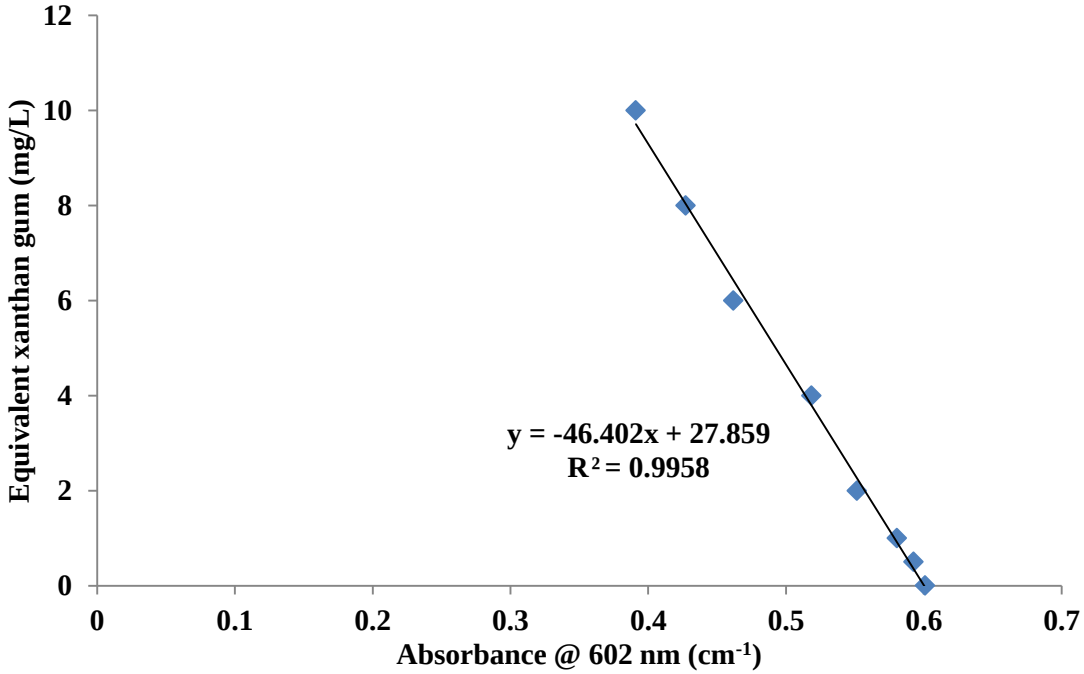

Figure 3.6 An example calibration curve for TEP analysis (xanthan gum used as standard)

3.3.4. Size Exclusion Chromatography (SEC)

For SEC analysis, isocratic flow of 0.01 M NH_4HCO_3 was used as eluent and pumped through a Torso TSKgel G3000PWxl column (with ID of 7.8-mm, length of 30-cm and particle size of 7-µm) at 0.5 ml/min with a DIONEX Ultimate 3000 HPLC system. A TOC analyzer (Siever 900 Portable TOC Analyzer, GE, USA) was employed after the column to collect TOC data.

A calibration curve for AMW was established by using polyethylene glycol (PEG) standards (Alfa Aesar, USA). A good linear relationship was obtained, as illustrated in Figure 3.7.

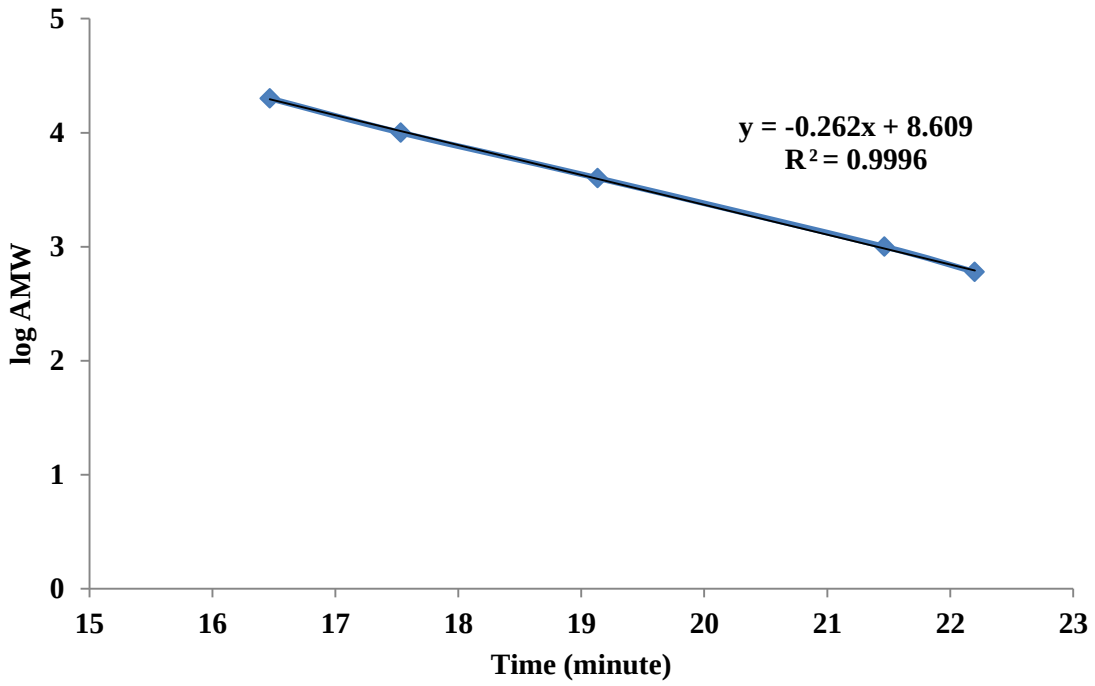

Figure 3.7 HPLC-SEC calibration curve for apparent molecular weight (AMW) distribution analysis, using polyethylene glycol (PES) as standard

3.3.5. Particle size distribution and zeta potential analysis

Adsorbent particles were rinsed with DI several times and sonicated for 15 minutes to avoid aggregation and then analyzed with a particle size distribution analyzer (SALD-3101 Laser Diffraction Particle Size Distribution Analyzer, Shimadzu).

For zeta potential determination, adsorbent particles were rinsed with DI and then diluted and sonicated for 15 minutes in 1 mM KCl solution. The sample was then analyzed with a zeta potential analyzer (ZetaPlus, Brookhaven Instruments Co., NY).

3.3.6. Scanning electron microscope (SEM) images

Images of mesh or membrane surfaces were obtained with a field emission SEM (JEOL JSM-7000, Japan). The instrument was operated in SEI mode at an accelerating voltage of 10 kV.

For sample preparation, each sample was cut into appropriate sizes and attached to an aluminum specimen mount with conductive tape and silver paste solution, and then air-dried in a vacuumed desiccator for 24 hr. The sample was then coated with 10 nm of platinum (Gatan Model 682 Precision Etching Coating System, Gatan Inc., Japan) and analyzed with the SEM.

4. Results and Discussion

In this chapter, experimental results are presented and discussed. Basic properties of HAOPs (the primary adsorbent used throughout the study) are presented first. Second, batch adsorption tests to evaluate the NOM removal efficiency by PAC and HAOPs are discussed. Next, an evaluation of the potential of μGAF as a pretreatment for membrane filtration is presented.

The effects of operational parameters on μGAF process are presented in the following sections. Physical operational parameters, including the applied μGAF flux and pressure, were investigated. Next, the effects of chemical operational parameters on the μGAF process, including feed solution pH, ionic strength and the concentration of divalent cations are described.

In the subsequent section, the fouling mechanism in μGAF is explored, based on experimental results and mathematical modeling. Lastly, to further exploit the potential of μGAF application in water treatment, a set of larger bench-scale experiments with different system geometries and materials is presented.

4.1. HAOPs properties

Some basic properties of HAOPs are presented in Figure 4.1 through Figure 4.3. The volume-based particle size distribution of HAOPs is illustrated in Figure 4.1. The volume-based mean diameter of HAOPs is about 25 μm. Figure 4.2 shows that HAOPs have a zeta potential of about +17 mV at pH 7.0 and a point of zero charge at pH 7.6. Cai [17] reported the solubility of HAOPs under different pH conditions, as shown in Figure 4.3. HAOPs have a solubility similar to aluminum hydroxide ($Al(OH_3)$); the solubility is very low (< 1 μg/L) from pH 4.5 to 9.3.

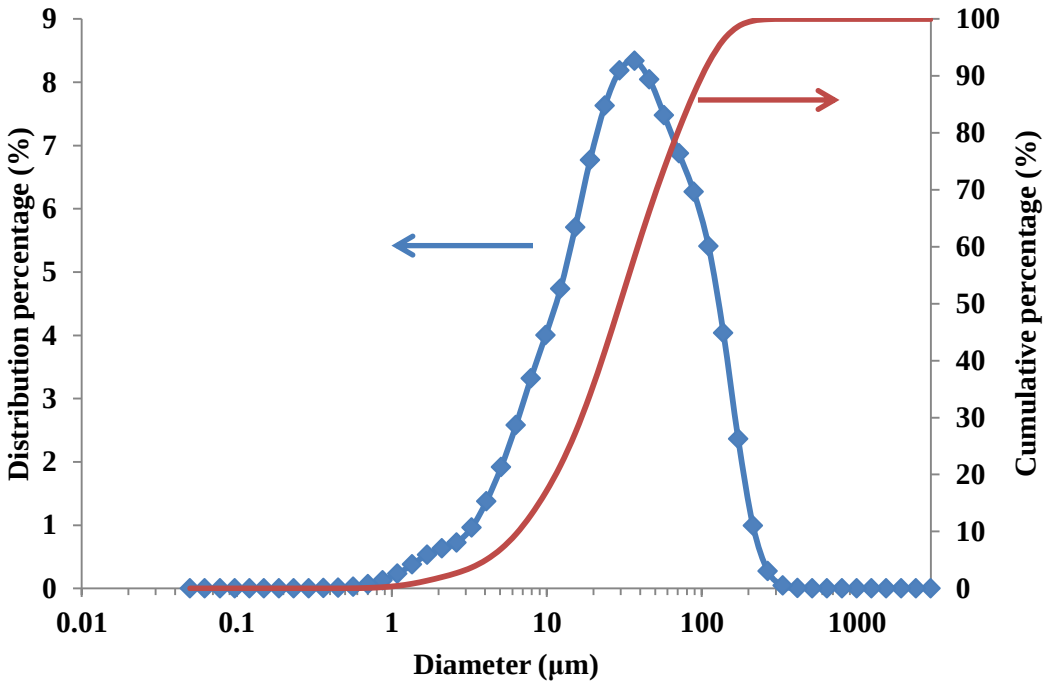

Figure 4.1 HAOPs volume-based particle size distribution diagram

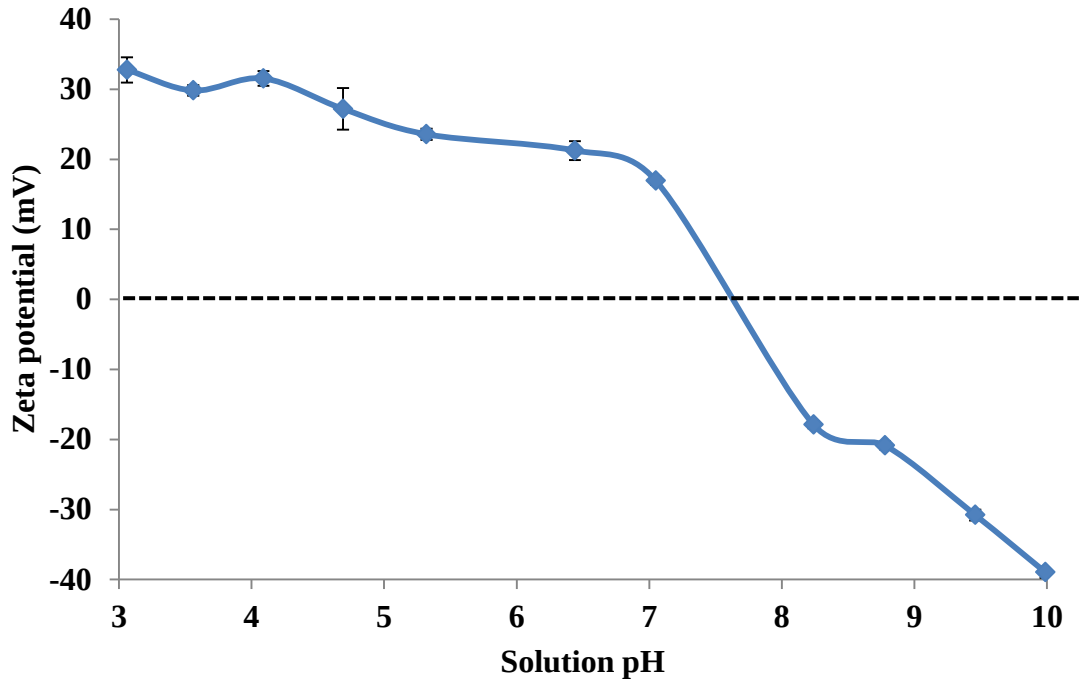

Figure 4.2 Zeta potential of HAOPs as function of pH

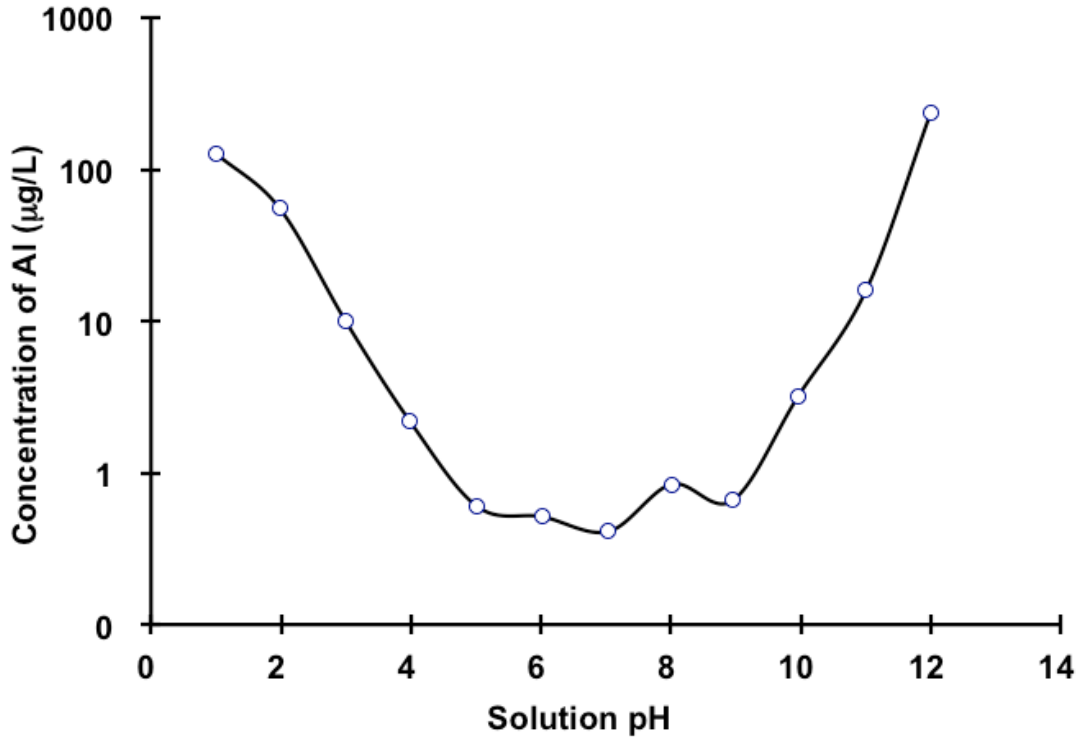

Figure 4.3 Solubility of HAOPs as function of pH [17]

When preparing HAOPs, the pH is adjusted to 7.0 during the neutralization step, but it drops to around 5 after the heating step. A possible explanation for this change is discussed next.

4.2. Determine the molecular formula of HAOPs

To prepare HAOPs, aluminum sulfate is dissolved in water, and NaOH is used for solution neutralization. In an ideal situation, one mole of aluminum sulfate requires six moles of NaOH to neutralize, yielding an Al/OH^- ratio of 3. However, in practice, during solution neutralization the observed Al/OH^- ratio was around 2.4, suggesting that the actual reaction might be:

$$\mathbf{Al_2(SO_4)_3 + 4.8NaOH \rightarrow}$$

$$\mathbf{2Al(OH)_{2.4}(SO_4)_{0.3} \cdot nH_2O_{(s)} + 4.8Na^+ + 2.4SO_4^{2-}} \quad (\mathbf{1})$$

As noted previously, the solution pH decreased to ~5.0 during the heating step, indicating that some protons were released during heating. This process can be explained by release of sulfate during the heating step, as follows:

$$\mathbf{Al(OH)_{2.4}(SO_4)_{0.3} \cdot nH_2O \xrightarrow{\Delta}}$$

$$\mathbf{Al(OH)_{2.4+m}(SO4)_{0.3-0.5m} \cdot (n-m)H_2O + 0.5mSO_4^{2-} + mH^+} \quad (\mathbf{2})$$

To investigate the molecular formula of HAOPs, a batch of 250 ml HAOPs was prepared. The solution pH was 4.94 after the heating step. The HAOPs slurry was then titrated with NaOH to adjust the pH back to 7.0 to determine the amount of acid released during the heating step. In this step, 770 µL of 4.01 M NaOH was used to offset the acid released, corresponding to a molar ratio of Al to H (i.e., a value of m) equal to 0.03. Equation (2) then becomes:

$$\mathbf{Al(OH)_{2.4}(SO_4)_{0.3} \cdot nH_2O \xrightarrow{\Delta}}$$

$$\mathbf{Al(OH)_{2.43}(SO_4)_{0.285} \cdot (n-0.03)H_2O + 0.015SO_4^{2-} + 0.03H^+} \quad (\mathbf{3})$$

To determine the value of n, two 10-ml samples of HAOPs stock solution (10 g Al/L) were filtered and rinsed with DI water several times. The filter papers containing HAOPs were air-dried in a vacuum desiccator for 24 h, and the mass of the dried solids was then determined. Since the concentration of stock solution was known, the mass fraction of aluminum in the dried solids could be calculated, allowing n and the complete HAOPs formula to be determined.

The experimental results are summarized in the Table 4.1. On average, the mass fraction of Al in HAOPs was 0.26, which is consistent with previous study by Cai [17]. This ratio was then used to calculate n:

$$\mathbf{0.26} = \frac{\mathbf{27}}{\mathbf{27 \times 1 + 17 \times 2.43 + 96 \times 0.285 + (18n - 18 \times 0.03)}},$$

$$\mathbf{n = 0.48}$$

And equation (3) becomes:

$$\mathbf{Al(OH)_{2.4}(SO_4)_{0.3} \cdot 0.48H_2O} \xrightarrow{\Delta}$$

$$\mathbf{Al(OH)_{2.43}(SO_4)_{0.285} \cdot (0.45)H_2O + 0.015SO_4^{2-} + 0.03H^+} \quad (4)$$

The molecular formula of HAOPs was thus determined to be:

$$\mathbf{Al(OH)_{2.43}(SO_4)_{0.285} \cdot (0.45)H_2O}$$

Table 4.1 Determination of Al mass ratio in HAOPs

	Exp. #1	Exp. #2
Volume of HAOPs stock filtered (ml)	20	10
Mass of filter paper (g)	1.32	2.62
Mass of filter paper plus HAOPs after desiccation (g)	2.13	2.98
Mass of HAOPs solids (g)	0.81	0.36
Al mass fraction (%)	24.7	27.8

4.3. NOM removal by HAOPs and other adsorbents

4.3.1. Batch adsorption test with HAOPs, alum and commercial PACs

Batch adsorption tests of 50% LP water were conducted with HAOPs or alum as the adsorbent. Very similar NOM removals from the feed water were achieved by HAOPs or alum, as illustrated in Figure 4.4. NOM removal efficiency was very sensitive to the adsorbent dose at low doses (~20% DOC and ~40% UV_{254} removal at a dose of 8 mg/L or 2 mg/L as Al), and reached a plateau at high doses (~70% and 80% DOC and UV_{254} removal, respectively). The removal efficiency plateau at high adsorbent doses suggests that there is a certain portion of NOM in LP water not collectable by HAOPs or alum, no matter how high the dose was. Also, removal of UV_{254} is higher than TOC, implying that HAOPs and alum selectively remove the hydrophobic fraction of NOM, since the hydrophobic NOM tends to have higher aromacity and have higher absorbance at 254 nm.

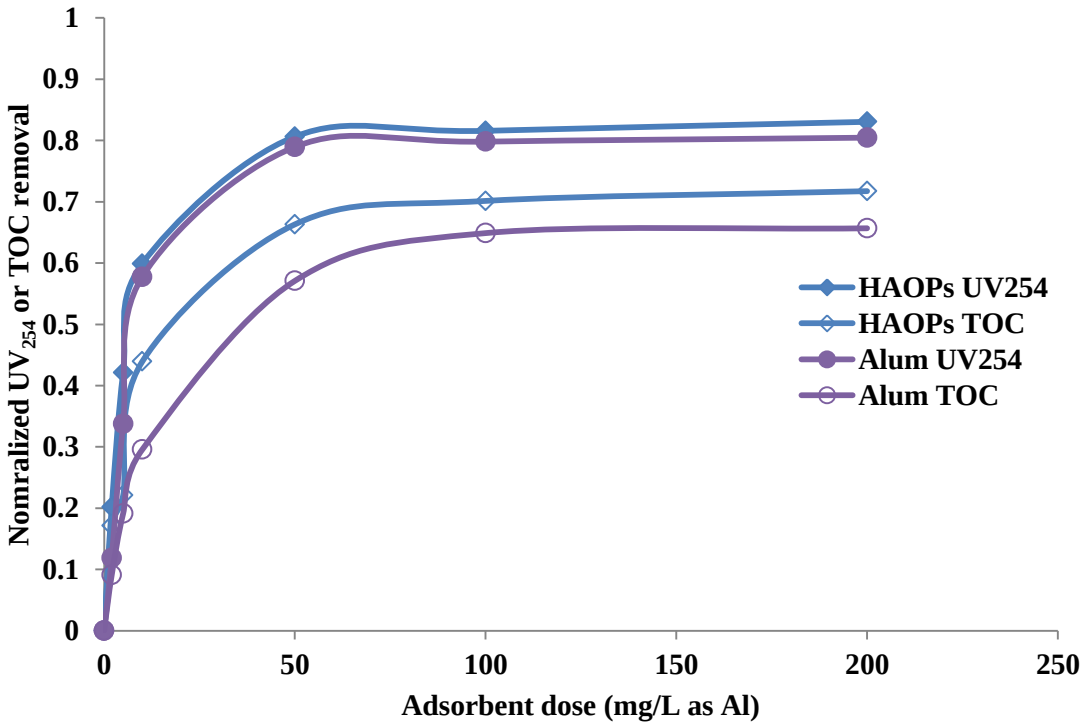

Figure 4.4 NOM removals from 50% LP water by HAOPs or alum adsorption. Batch adsorption tests were conducted at pH = 7.0

Two commercially available PACs, SA super and WPH, were applied in batch adsorption tests, as shown in Figure 4.5. Unlike HAOPs, no NOM removal efficiency plateau was observed for either PAC. Both NOM removal indicators (DOC and UV_{254}) increased with increasing adsorbent dose, achieving almost complete NOM removal from LP water (> 95%) at very high doses.

Before comparing the NOM removal efficiencies between HAOPs and the PACs, we need to consider the fact that the mass fraction of aluminum in HAOPs is close to one-fourth, based on the experimental result stated in Section 4.2. For instance, a dose of 10 mg/L as Al is equivalent to roughly a dose 40 mg/L adsorbent. Taking this factor into account, both PACs had lower NOM removal efficiencies than HAOPs did at low adsorbent doses (< 40 mg/L), that about 40% and 20% UV_{254} removal by SA super and WPH PAC, respectively, while about HAOPs achieved about 60% of UV_{254} removal. Therefore, HAOPs outperforms both PACs within the common adsorbent

dose range used in water treatment.

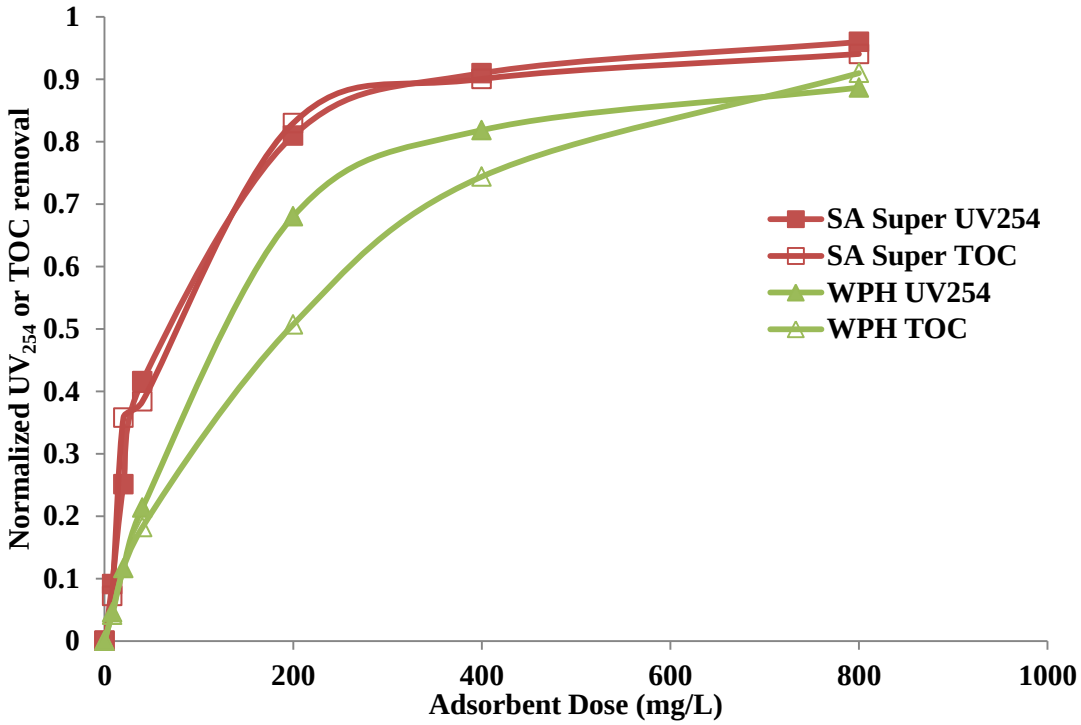

Figure 4.5 NOM removals from 50% LP water by two commercial available PACs adsorption. Batch adsorption tests were conducted at pH = 7.0

4.4. µGAF as pretreatment process

In practical membrane treatment applications, hollow fibers are widely used because they provide a lot of effective surface area per unit system volume. Applying HAOPs directly to such membranes is not very attractive, because the adsorbent solids could clog the fibers, and it could be difficult to wash away the pre-deposited adsorbent.

As mentioned in Section 2.5.3, with proper choice of adsorbent, the µGAF process has great potential as a pretreatment process to achieve satisfactory NOM removal, substantial membrane fouling reduction, if the adsorbent layer can be easily washed off at the end of a filtration cycle. To test this, µGAF cartridge tests were conducted using nylon mesh as the HAOPs support, 50% LP water as the feed, an adsorbent loading of 10 g Al/m^2, and a flux of 100 LMH for both µGAF and membrane units. The nominal pore size of the nylon mesh was 5 µm. Visually and based on the particle size distribution analysis, the nylon mesh was able to capture the vast majority of the adsorbent mass injected into the cartridge.

A mesh control run (feed water pumped through bare mesh, without HAOPs pre-deposition) was first conducted to identify whether the mesh itself can achieve some level of foulant or NOM removal. As a result, negligible resistance increase was observed in mesh control run, that the TMP increase was less than 0.01 psi up to V_{sp} (V_{sp}, defined as cumulative permeate volume per unit area) of 1600 L/m^2. Permeate samples were collected during the filtration cycle and the quality (in terms of UV_{254} removal efficiency) was analyzed, as illustrated in Figure 4.6, showing that no NOM was removed from the feed by a bare mesh. This result ensures that when the nylon mesh is used in the µGAF process to support the HAOPs, it has no effect on system performance.

Next, sequential µGAF-membrane filtration tests were conducted in cartridges;

and the experimental results are illustrated in Figure 4.7 and Figure 4.8. The bare membrane fouled rapidly and rejected very little NOM, while the μGAF pretreatment effectively removed NOM from the feed and significantly reduced membrane fouling. These results confirm once again that in a μGAF system, it is the adsorbent layer plays the major role of collecting foulants. With proper supporting media, μGAF serves as a good pretreatment for reducing membrane fouling.

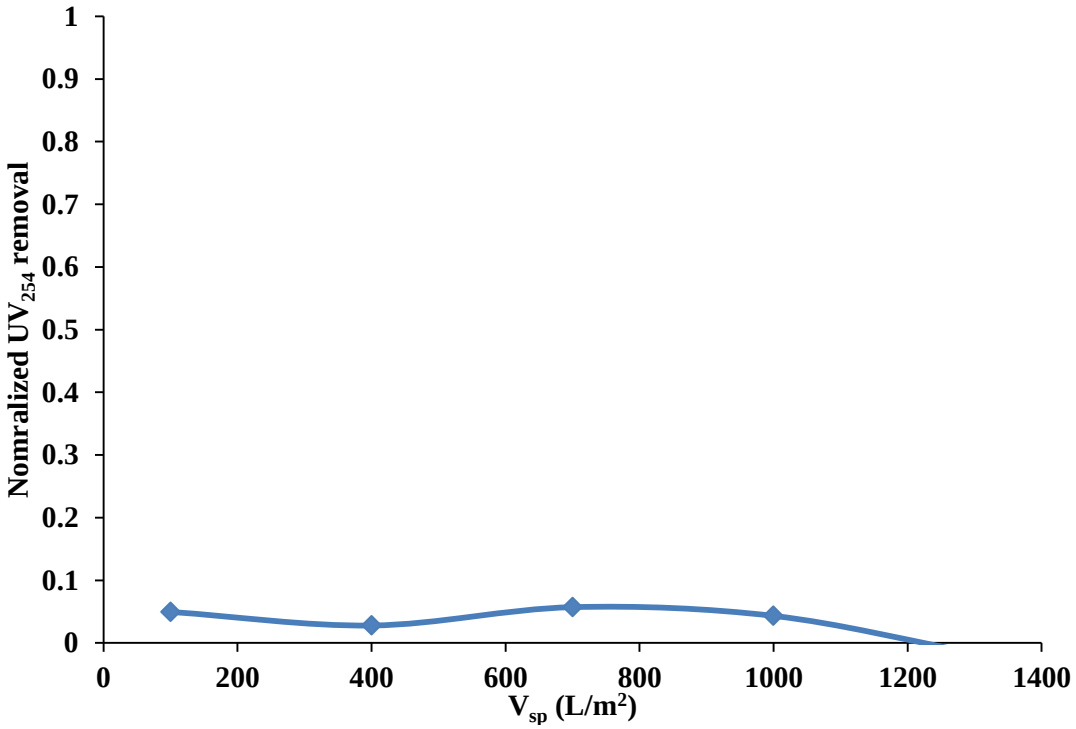

Figure 4.6 Normalized NOM removal (presented in UV_{254}) of 50% LP water when filtered with bare SEFAR nylon mesh

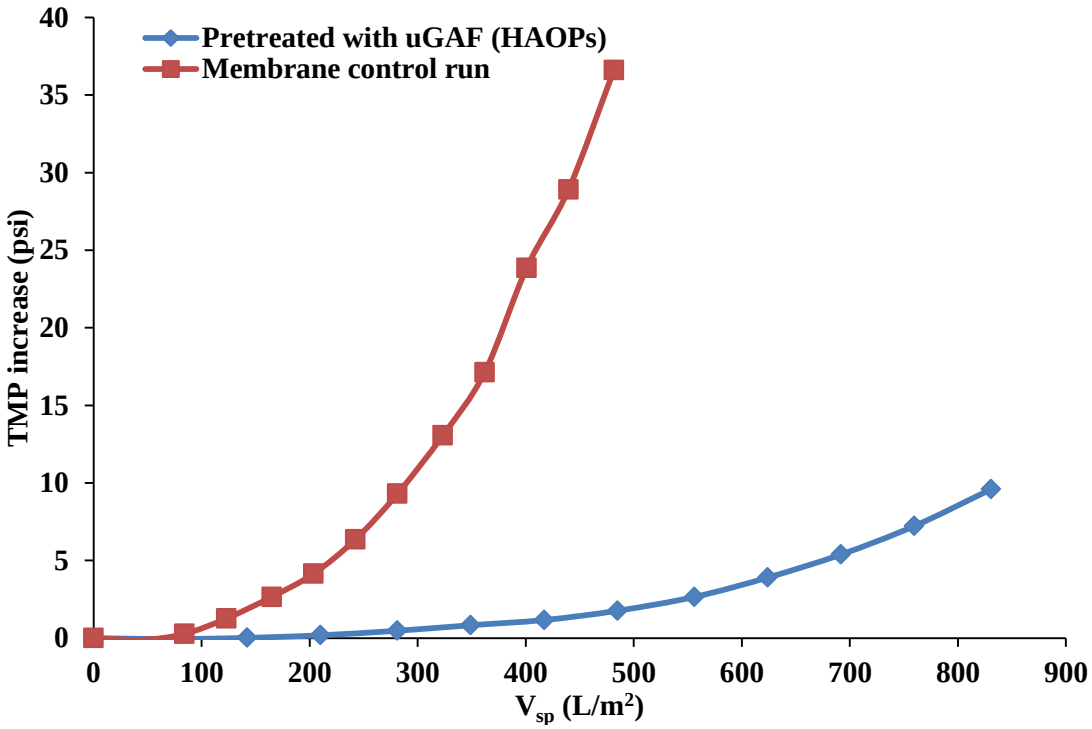

Figure 4.7 Pressure increase profile of PES membrane (0.05 µm) with or without µGAF pretreatment

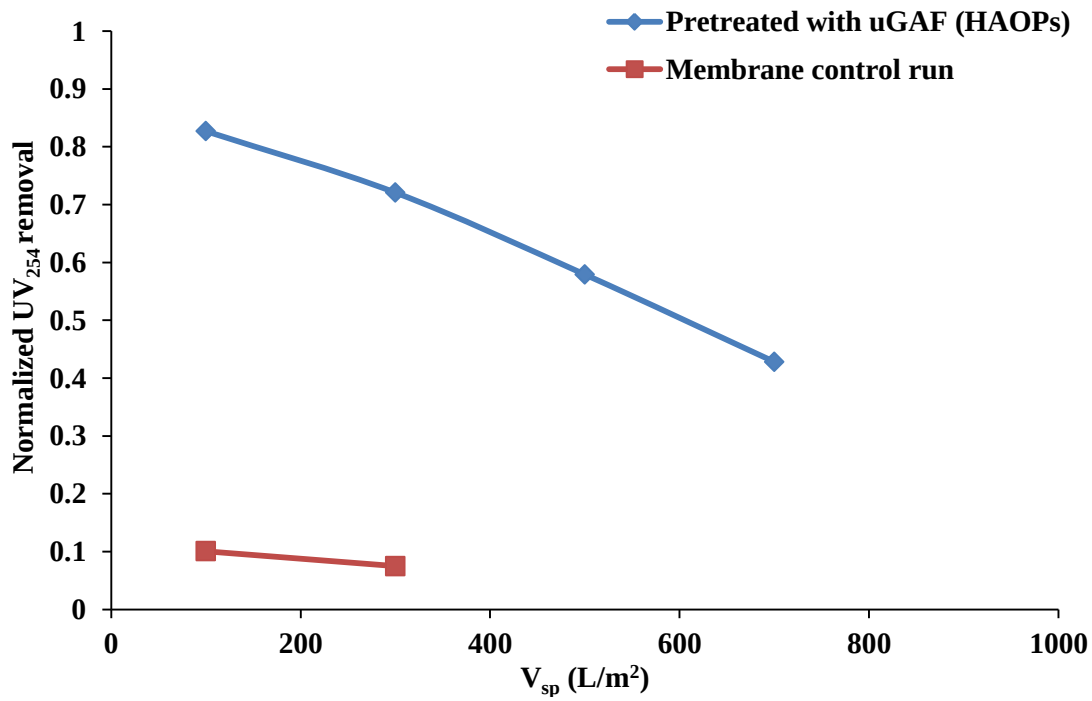

Figure 4.8 NOM removal (presented in UV_{254}) from 50% LP water with or without µGAF pretreatment

4.5. Effect of flux on μGAF process performance

As described in Section 2.5.1, operation flux can have a critical impact on membrane fouling. It has been observed and reported by many researchers, that higher permeation rate leads to more rapid membrane fouling [54,86–89]. To investigate the impact of flux on μGAF process, sequential μGAF-membrane filtration experiments were employed in cartridge systems. The experimental results are described in the following sections.

4.5.1. Fouling in sequential μGAF-membrane filtration with different applied flux to the upstream μGAF unit

In these experiments, 50% LP water was used as feed, the adsorbent surface loading was 10 g/L as Al, and three different fluxes (400, 250 and 100 LMH) were applied to the upstream μGAF unit. The duration of each experiment was adjusted so that the total permeate volume was the same in all tests.

Figure 4.9 (a) illustrates the increase of resistance across the μGAF units at different applied fluxes. Resistance was calculated by dividing monitored pressure loss across the μGAF unit with applied flux. As shown in the figure, significant differences in the resistance across the μGAF unit were observed. When the feed was directed to the upstream μGAF unit at 400, 250 and 100 LMH, the increase in resistance across the adsorbent layer was 3.9, 2.4 and 1.4 10^{11} m^{-1}, respectively, at V_{sp} around 1000 L/m^2. The result is consistent with previous research reports that higher flux induces more rapid foulant deposition and more compressed foulant layer, resulting in higher pressure increase.

The composite permeate from the upstream μGAF unit was collected in a temporary reservoir and then pumped to the downstream membrane unit at a fixed flux of 100 LMH. The TMP profiles are illustrated in Figure 4.9 (b). At a V_{sp} of about

800 L/m^2, the membrane fed with the composite permeate from the μGAF systems operated with 400, 250 and 100 LMH had TMP increases of 7.4, 10.6 and 13.8 psi, respectively, implying that more foulant was collected by the HAOPs layer when the μGAF unit was fed with a higher flux.

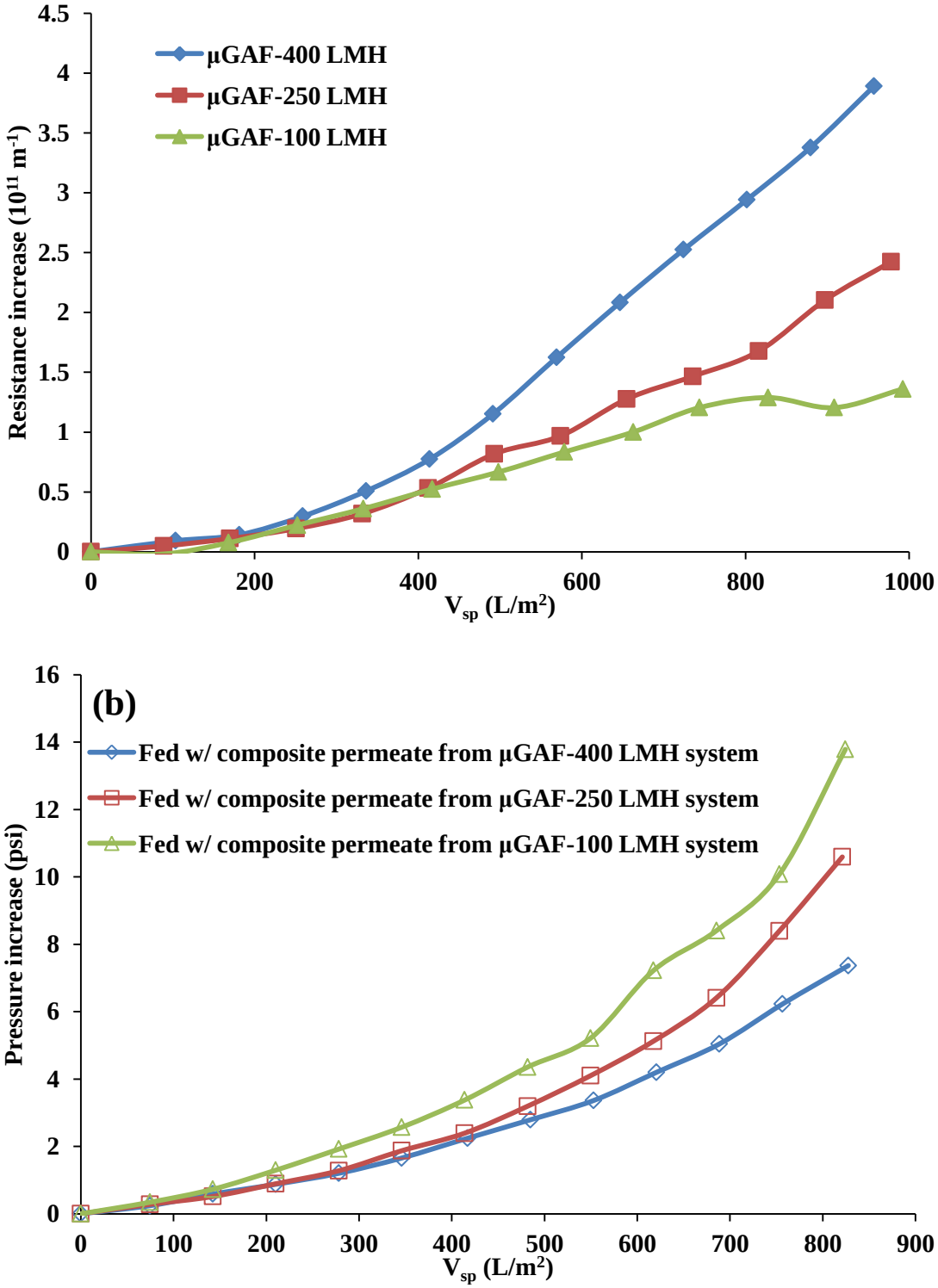

Figure 4.9 (a) the resistance increase profiles of the upstream μGAF units when fed with different flux and (b) the pressure increase profiles of downstream membrane units when fed with composite permeate collected from corresponding upstream μGAF units

4.5.2. The effect of flux on μGAF permeate quality

To confirm the previous interpretation, μGAF permeate qualities, including UV_{254} absorbance and TEP concentration, were analyzed. As shown in Figure 4.10 (a) and Figure 4.10 (b), the UV_{254} removal efficiencies for the composite permeate from 400-, 250- and 100-LMH systems were 54, 62 and 70%, respectively. Furthermore, 7, 12 and 24% of the TEP remained in the composite permeates collected from the 400-, 250- and 100-LMH system, respectively. Thus when feeding the μGAF unit with higher flux, more foulant is retained by the pre-deposited HAOPs layer, causing a higher fouling rate in the upstream μGAF unit. With less foulant exiting the μGAF unit and reaching the downstream membrane, better fouling control can be achieved.

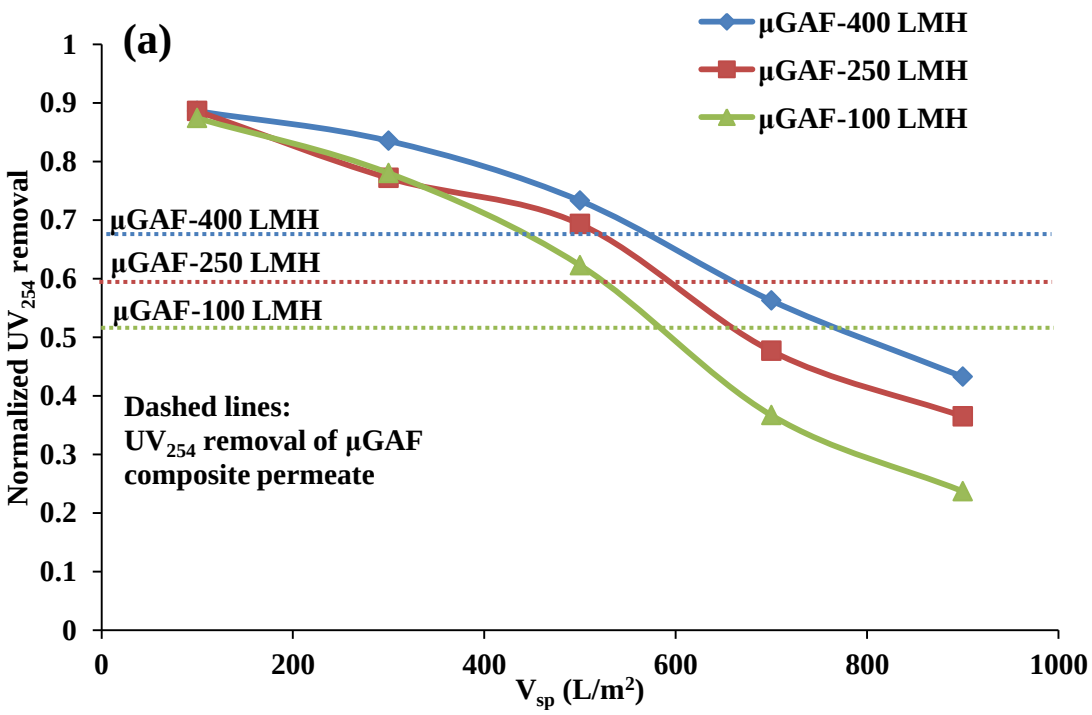

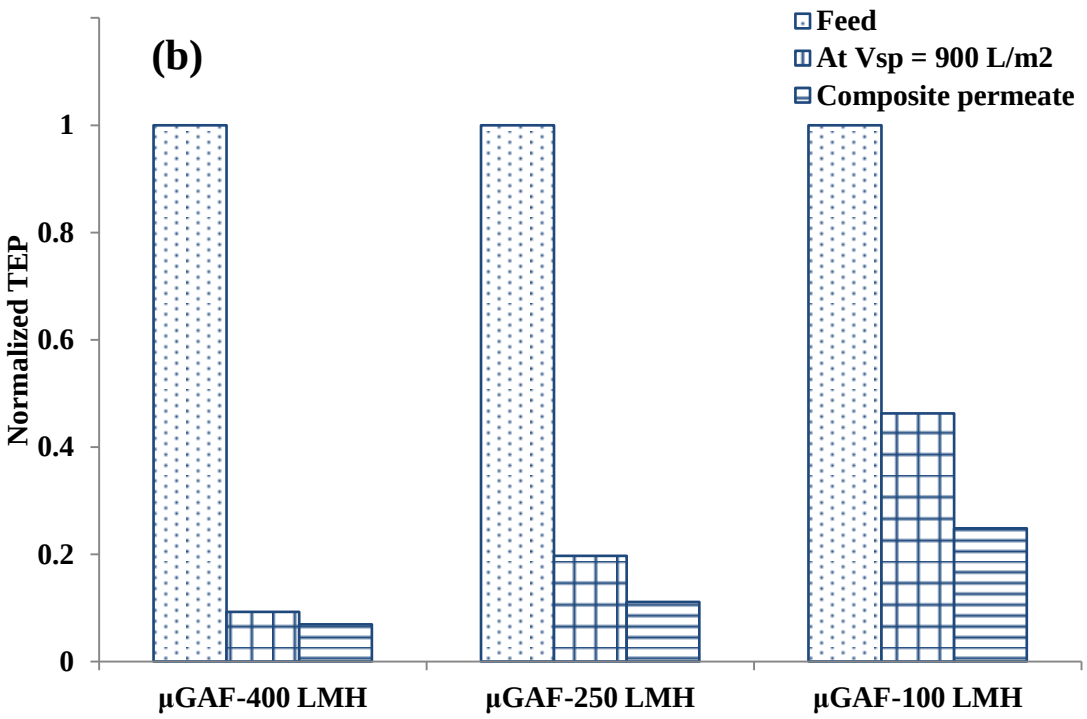

Figure 4.10 µGAF unit permeate quality when fed with different applied flux (a) UV_{254} absorbance and (b) TEP concentration

As noted previously, high membrane permeation rate result in higher TMP and can promote foulant layer compression and foulant deposition. A similar trend was observed in the µGAF system. To further explore the effect of pressure on fouling in the µGAF process, experiments were conducted as described in the following section.

4.6. Effect of pressure on μGAF process performance

This section describes an investigation of how pressure affects μGAF performance. The compressibility of the adsorbent layer with or without accumulated NOM was first investigated, followed by an examination of the effect of applied flux on μGAF performance in terms of both permeate quality and membrane fouling control. All experiments were conducted using the cartridge system described in Section 3.2.2, but in some experiments adjustments in experimental design were made to achieve the experimental goal..

4.6.1. Compressibility of fresh HAOPs layer

The compressibility of the adsorbent layer in the μGAF unit was examined using two approaches. The first approach was to monitor the head loss across the layer while altering the applied pressure to the system. The adsorbent was pre-deposited on a nylon mesh and installed in a cartridge, and pressure transducers were installed at both the entrance and the exit of the cartridge. DI water was pumped through the μGAF unit at a fixed flux for at least one hour as a pre-conditioning step. Once the head loss across the μGAF unit stabilized, the permeate line was connected to a closed chamber and DI water was pumped through the system. As the run proceeded the air in the chamber became compressed, and the pressure applied to the μGAF unit increased to keep the flux fixed. This design allowed the head loss across the adsorbent layer to be monitored as the applied pressure increased. The schematic setup is illustrated in Figure 4.11. If the adsorbent layer is compressible, the resistance across the adsorbent will increase as the applied pressure increases. On the other hand, if the HAOPs layer is incompressible, the head loss across the adsorbent layer should stay steady regardless of the applied pressure.

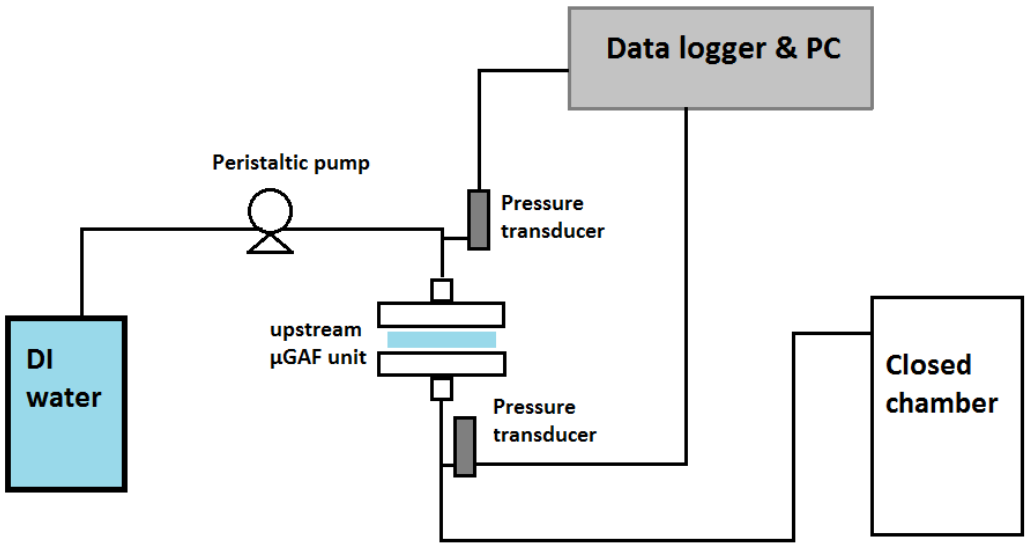

Figure 4.11 Schematic setup used in the experiments investigating the effect of applied pressure to µGAF process

This experiment was carried out with the flux fixed at 100 LMH and the HAOPs surface loading at 10 g/m^2 as Al, and the result is illustrated in Figure 4.12. The applied pressure to HAOPs layer increased from 0.6 psi to roughly 30 psi as filtration proceeded, but the head loss across the µGAF unit underwent negligible change. In fact, the head loss across the layer actually decreased slightly during the experiment, but the decrease is trivial compared to the overall increase of applied pressure.

The second approach tested was to monitor the head loss across the layer while altering the flux to the system. If the layer is incompressible, the specific resistance should remain constant at all fluxes applied. That is, the relationship between the head loss across the layer and the applied flux should be linear. When this experiment was conducted, a good linear relationship was observed between the two parameters, as shown in Figure 4.13. It can therefore be concluded that a fresh HAOPs layer is incompressible.

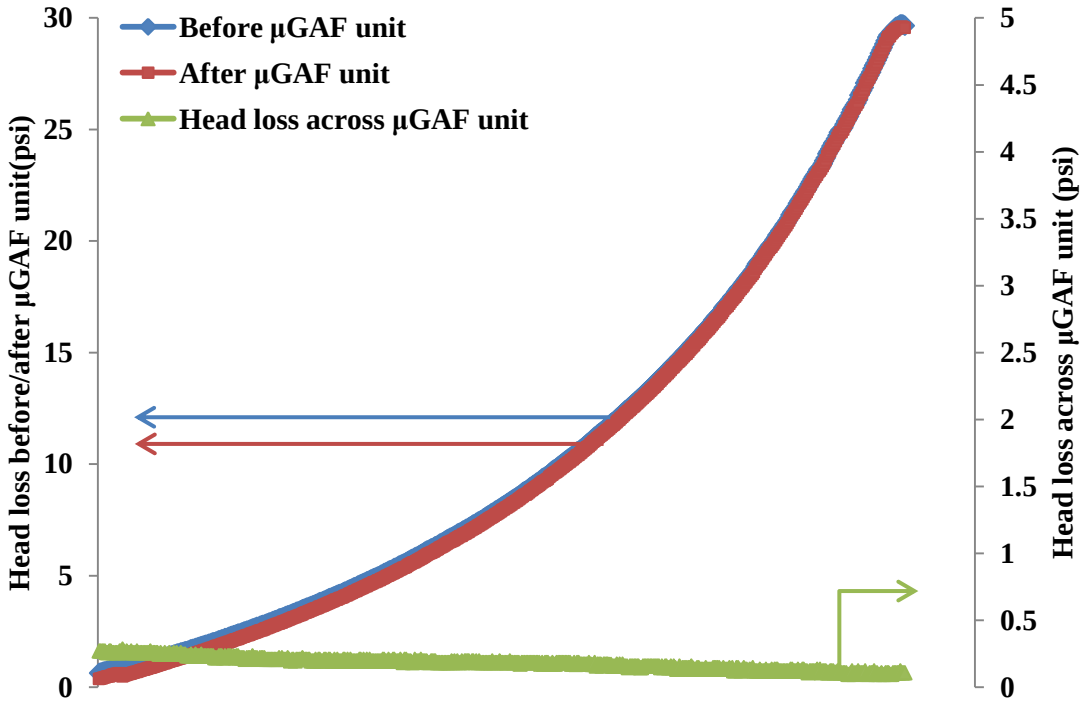

Figure 4.12 Head loss across fresh HAOPs layer with changing applied pressure

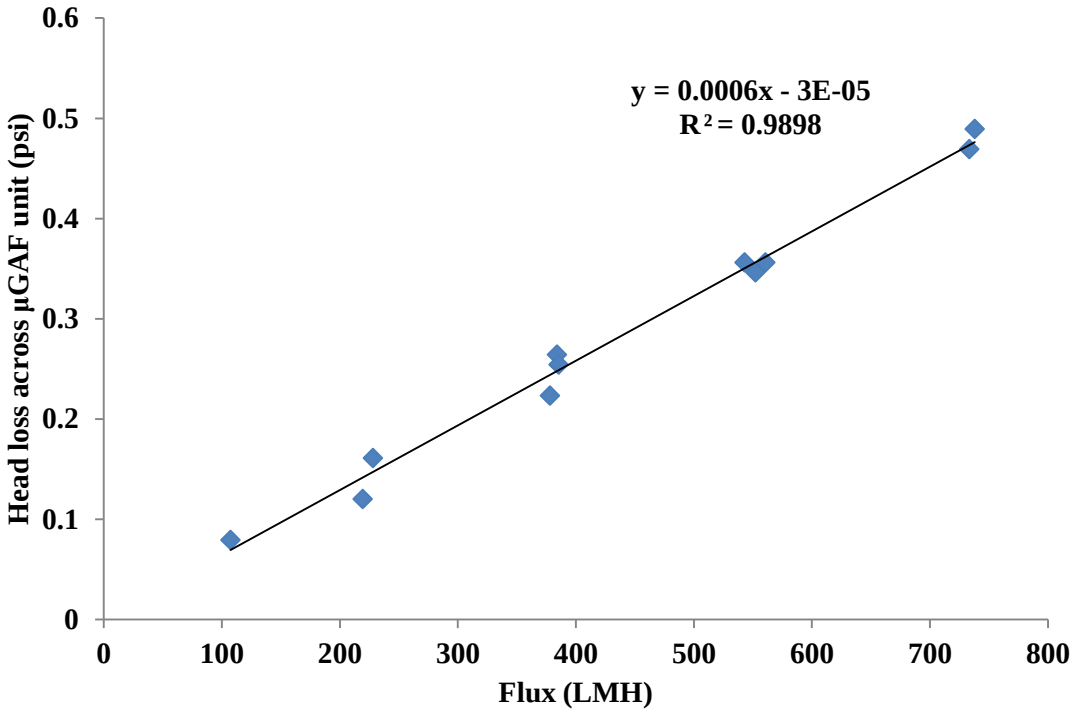

Figure 4.13 Relationship between fresh HAOPs layer head loss and applied flux

4.6.2. Compressibility of NOM accumulated on or in a HAOPs layer

As mentioned in the literature review, it has been reported in previous studies that foulant layers, especially when contain NOM, are often compressible [86–88]. A membrane control run was performed to investigate the compressibility of the NOM layer that accumulated on the membrane surface during filtration. 50% LP water was applied directly to the PES membrane at a flux of 250 LMH. The linear compressibility model reported by Chellam and Xu [78] was used to examine the compressibility of the foulant cake layer. In this model, the specific resistance is assumed to increase linearly with increasing pressure.

The pressure buildup profile during the run and the compressibility analysis are illustrated in Figure 4.14 (a) and (b), respectively. A good fit is observed in the foulant layer compressibility analysis (with $R^2 \geq 0.95$), suggesting that the foulant layer collected from 50% LP water is compressible.

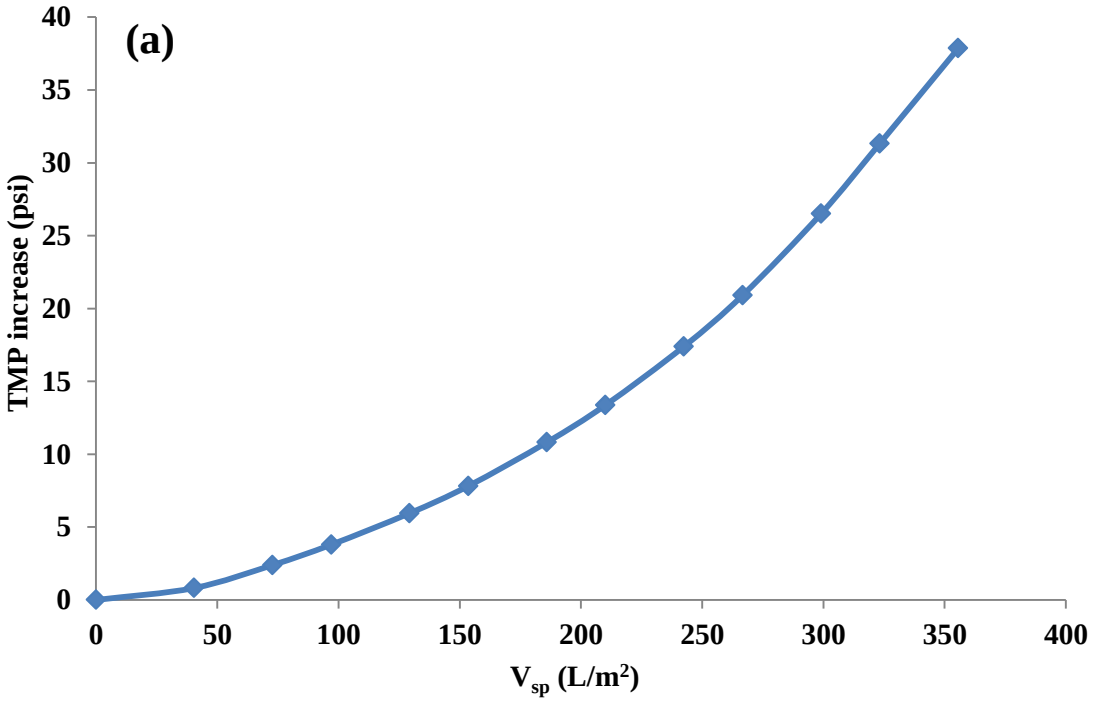

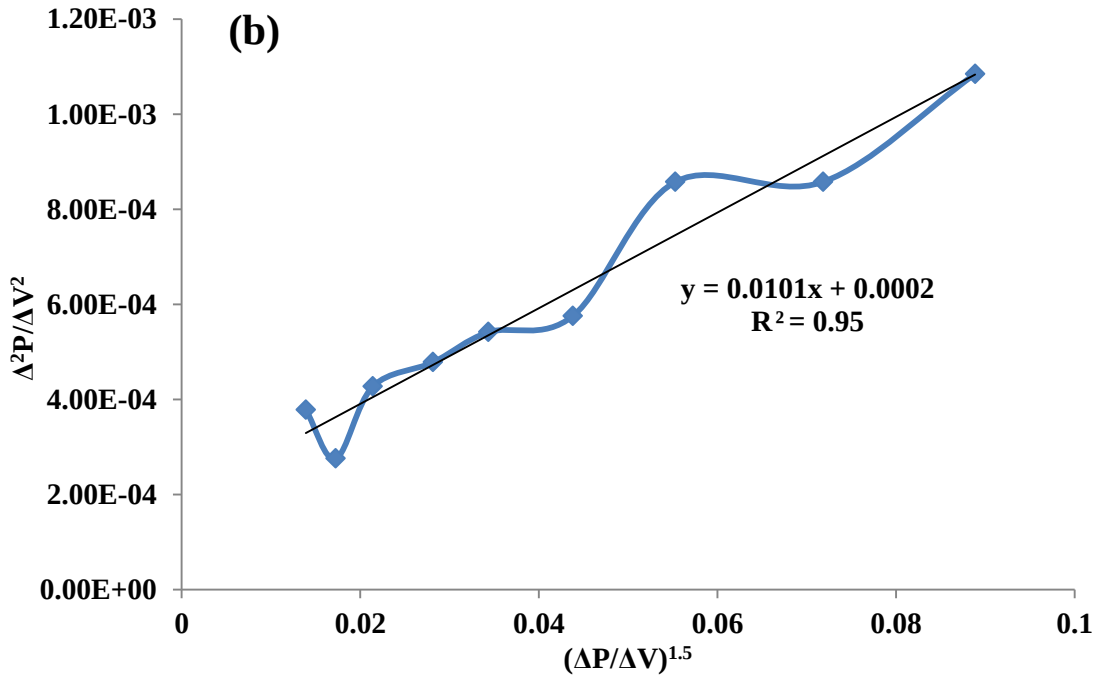

Figure 4.14 (a) Pressure profile and (b) linear compressibility analysis of the foulant layer in a membrane control run. 50% LP used as feed water, operated at a flux of 250 LMH

Next, the compressibility of the NOM accumulated on or in a HAOPs layer was examined. To start the test, 50% LP water was applied to a HAOPs layer (surface loading at 10 g/m^2 as Al) at a flux of 250 LMH. The specific volume filtered was about 1000 L/m^2. Right after the NOM buildup step, DI water was fed to the μGAF unit at a flux of 100 LMH for at least one hour. The compressibility tests were then performed, with the same setup as used in the prior compressibility tests with fresh HAOPs.

In the first experiment, the compressibility of the NOM/HAOPs layer was examined by applying different pressures to the system; the result is illustrated in Figure 4.15. The initial head loss across the layer was ~2.3 psi. As the applied pressure increased from 2.5 to 25 psi, the head loss had a small decrease from 2.3 psi to ~1.9 psi, consistent with the result from the test with a fresh HAOPs layer. The

relationship between operation flux and the head loss across the layer is illustrated in Figure 4.16; again, a strong linear relationship was observed. The results indicate that the HAOPs layer is incompressible, even when it contains NOM.

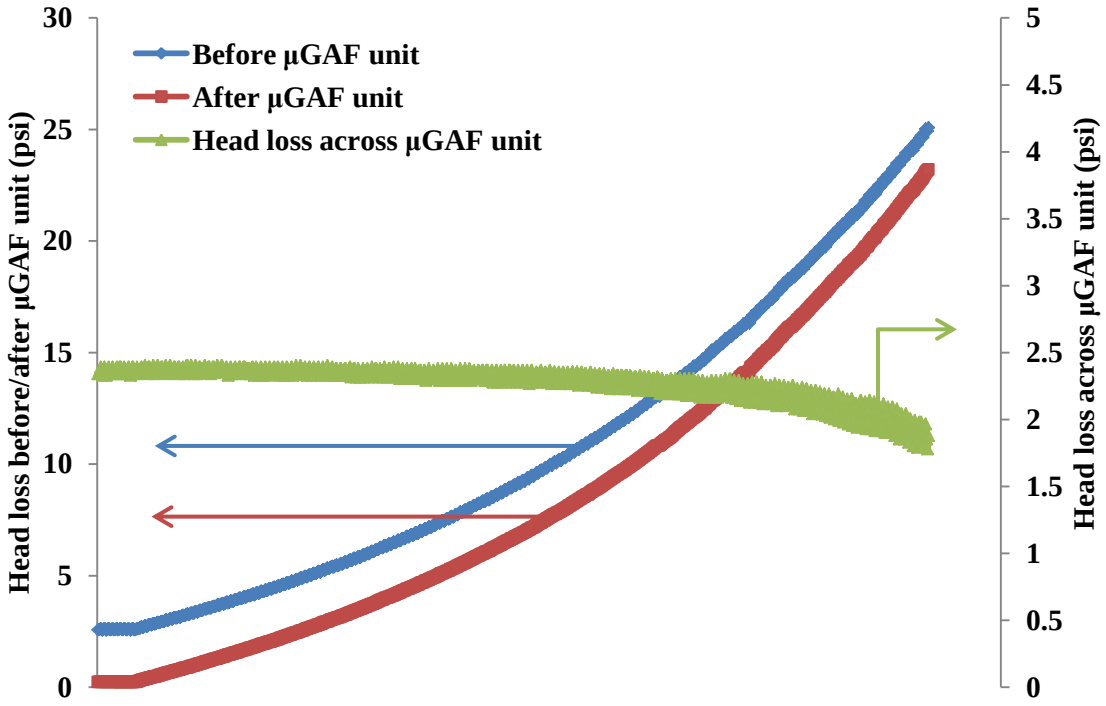

Figure 4.15 The change of NOM accumulated HAOPs layer during the compressibility test

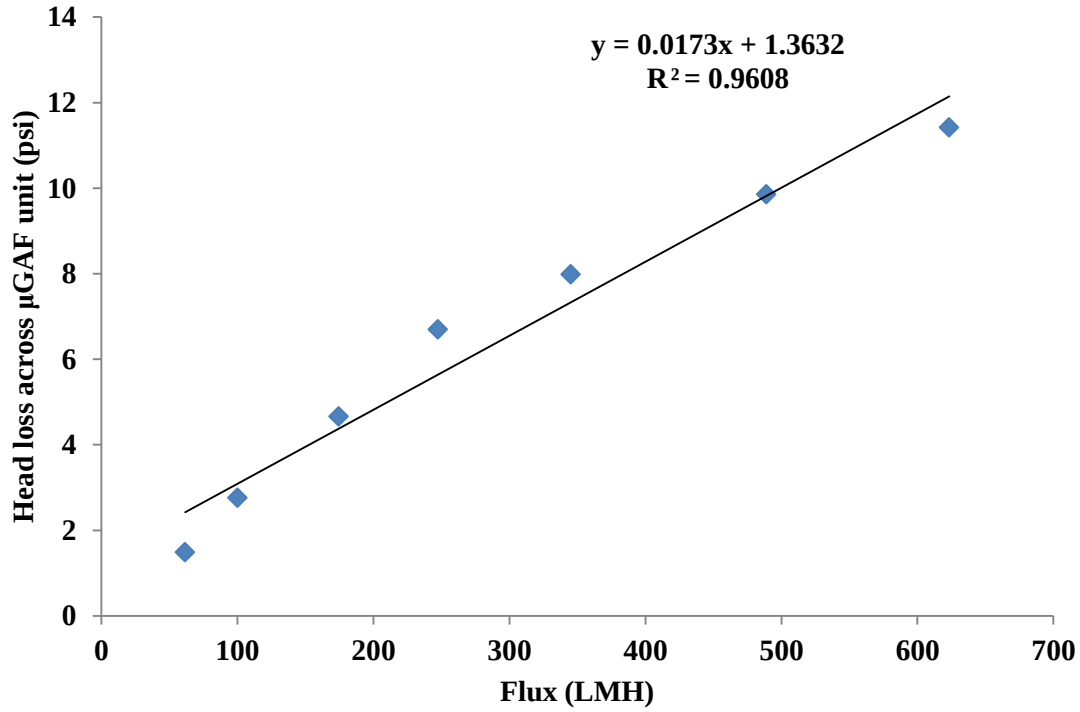

Figure 4.16 Relationship between NOM accumulated HAOPs layer head loss and applied flux

The experiments shed light on how NOM molecules accumulate onto the adsorbent layer in a μGAF process. Figure 4.17 (a) and (b) illustrates two possible scenarios of NOM foulant accumulation on HAOPs layer. One possibility, illustrated in Figure 4.17 (a), is that a uniform NOM foulant layer forms on top of the adsorbent layer during the run. Based on previous studies it has been suggested that the NOM foulant layer is compressible [54,87,88]. In that case, the hydraulic resistance would increase as the layer became more compressed. However, the experimental results suggest that the layer resistance stayed constant during the compressibility test. A reasonable explanation is that the NOM molecules adsorbed on the surface of adsorbent particles throughout the layer, as shown in Figure 4.17 (b). Since the adsorbent particles are orders of magnitude larger than NOM molecules, the adsorbed NOM molecules are not able to fill the gaps between the adsorbent particles, causing the resistance of the fouled layer to be independent of the applied pressure.

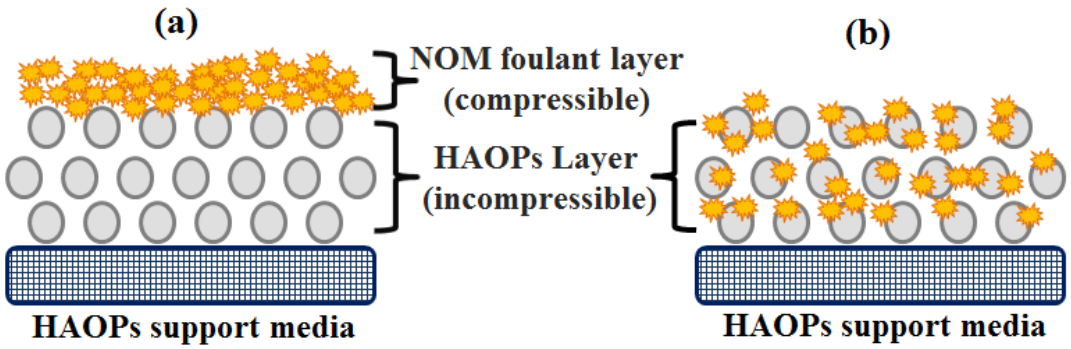

Figure 4.17 NOM accumulation on HAOPs layer by (a) forming a continuous NOM layer on top of adsorbent layer and (b) by adsorbing on the surface of adsorbent particles

4.6.3. Effect of applied pressure on μGAF process performance

The effect of applied pressure on μGAF process performance was then examined in sequential μGAF-membrane filtration systems. To apply additional pressure to the μGAF unit while keeping flux constant, a needle valve was installed at the exit of the μGAF unit cartridge. By altering the opening of the needle valve, pressure in and upstream of the adsorbent layer can be adjusted.

The performance of μGAF with no additional pressure was compared to μGAF with additional applied pressure of 5 or 15 psi induced by partial closure of the needle valve in two experiments. Figure 4.18 (a) and (c) illustrates the pressure buildup across the adsorbent layers in μGAF units. Regardless of the applied pressure, identical increases in head loss across the μGAF units were observed in both experiments. Also, as shown in Figure 4.18 (b) and (d), the downstream membranes had identical fouling extents and patterns — the TMP increased about 4.5 psi at a V_{sp} about 800 L/m^2. Thus, a hypothesis can be proposed, that the same amount of foulant broke through μGAF regardless of the applied pressure to the μGAF units, causing similar fouling of the membranes downstream. As illustrated in Figure 4.19, the NOM removal efficiencies throughout the filtration cycle were the same for all applied pressures tested, supporting this hypothesis.

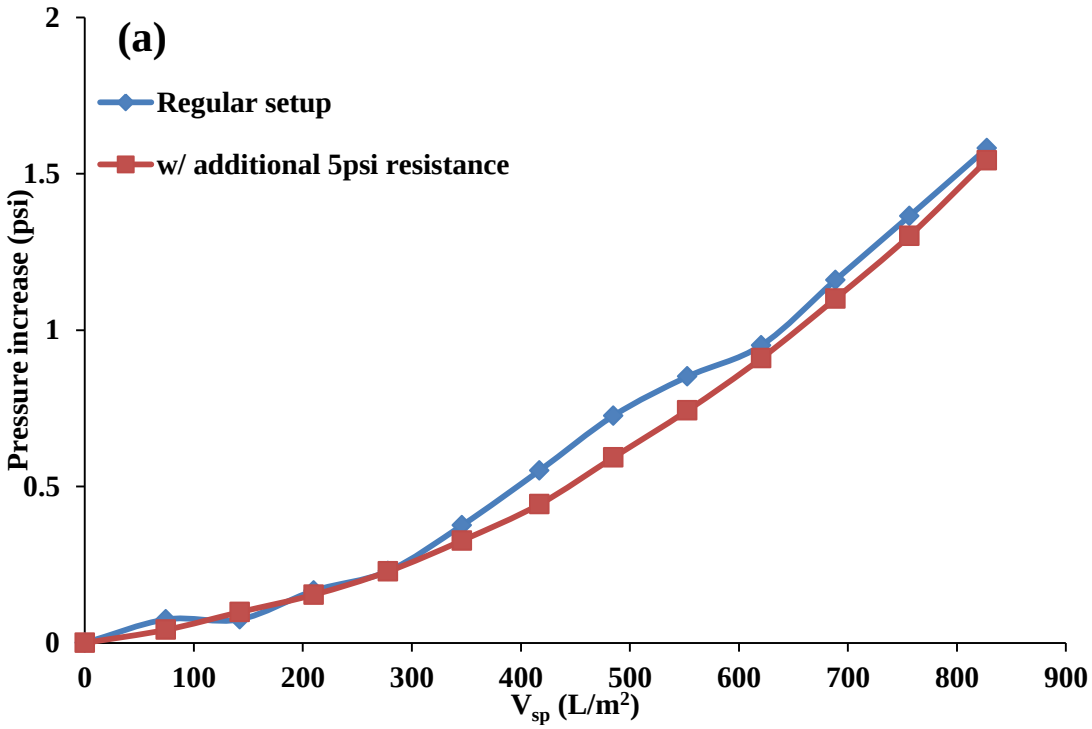

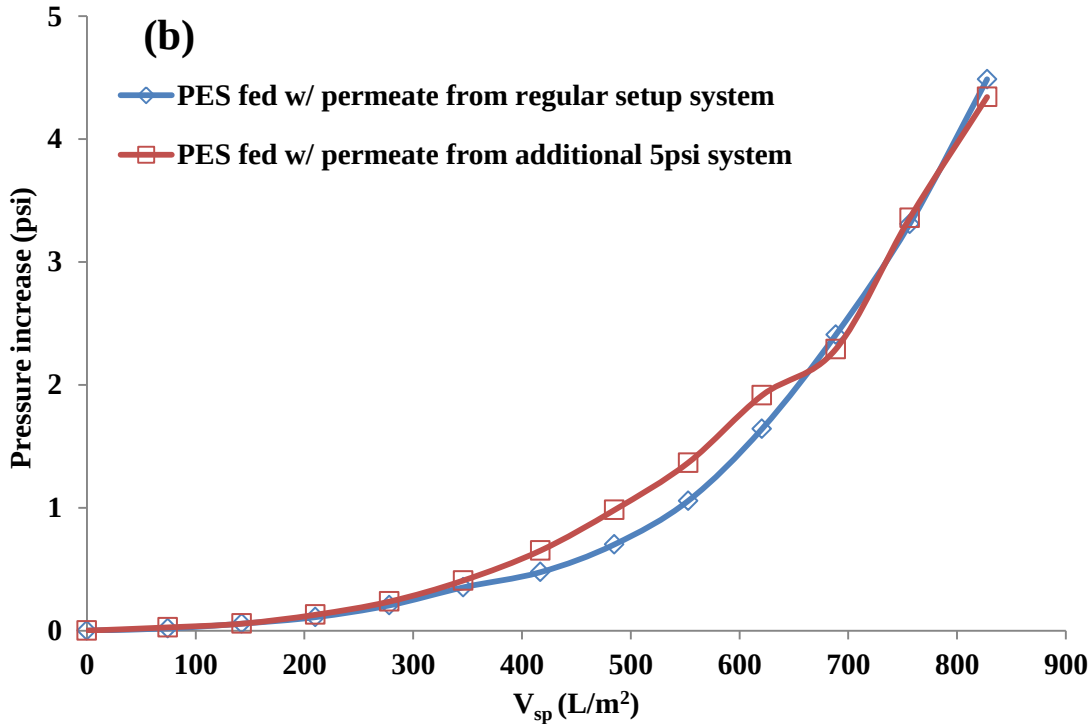

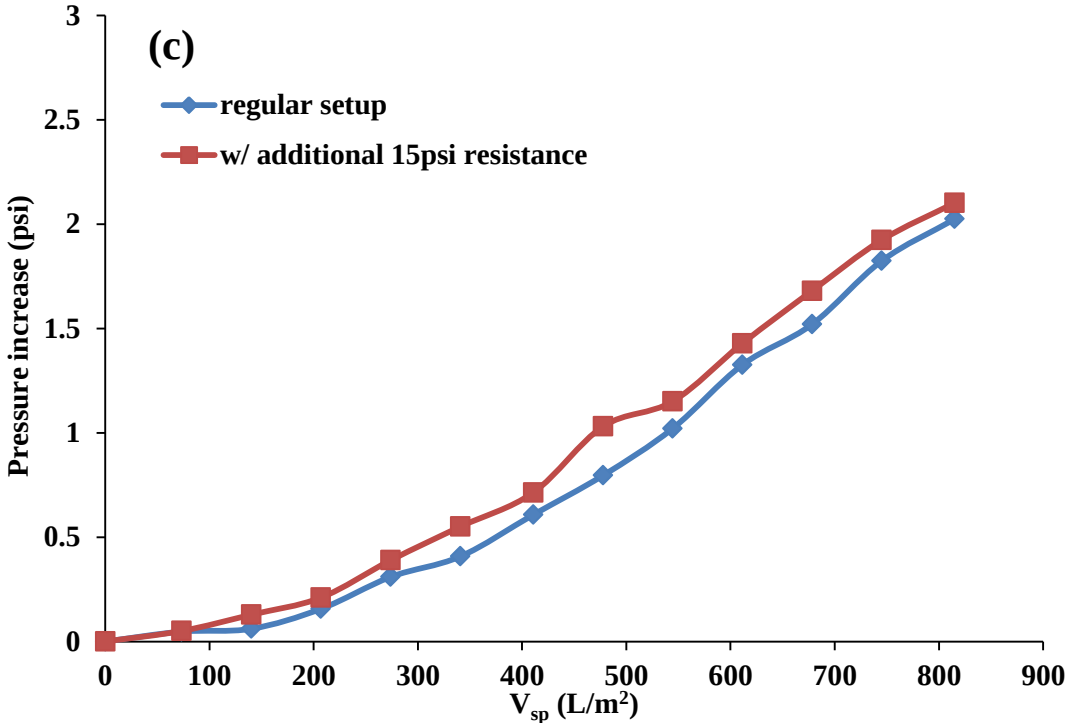

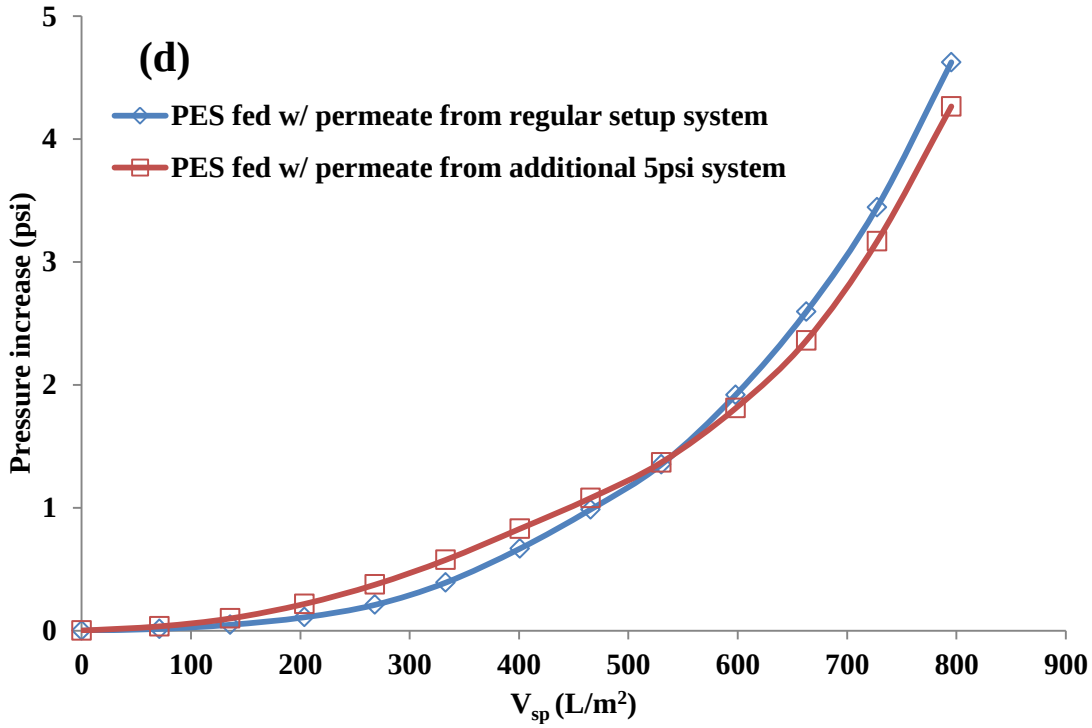

Figure 4.18 Pressure increase profiles of sequential µGAF-memrbane filtration under different applied pressure (a) the upstream µGAF unit with additional 5 psi resistance and (b) the downstream membrane, and (c) the upstream µGAF unit with additional 15 psi resistance and (d) the downstream membrane

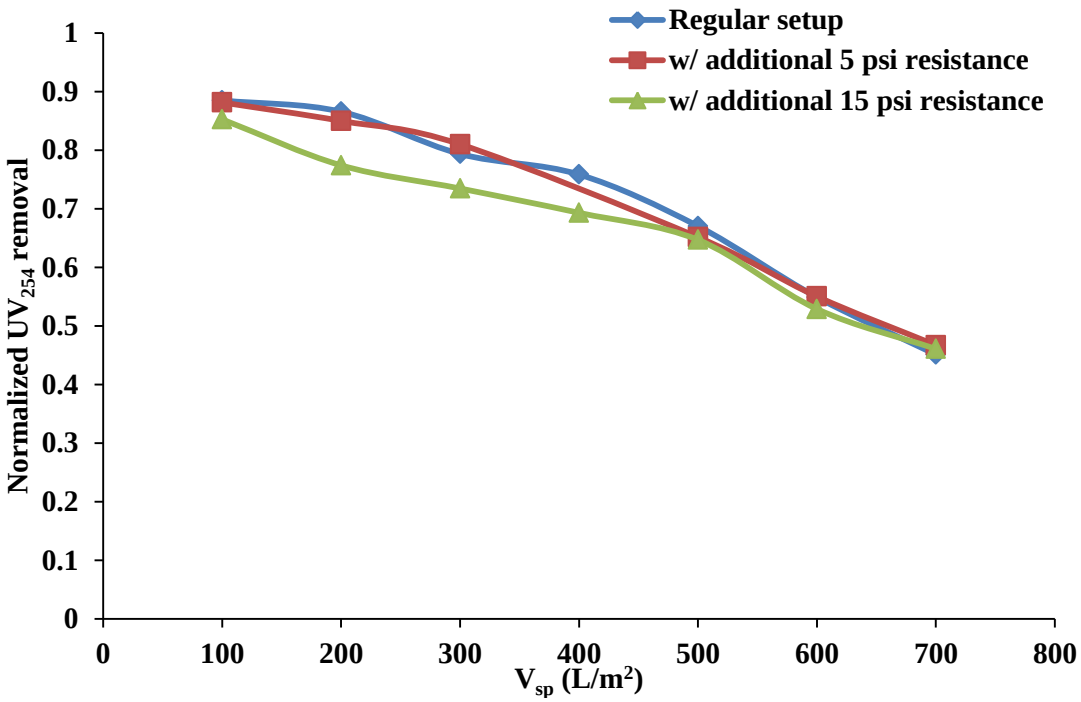

Figure 4.19 µGAF unit permeate quality when operated under different applied pressure

4.7. Effect of feed solution chemistry

Feed solution chemistry is a crucial factor affecting fouling behavior. The feed solution chemistry parameters studied in this research included pH, ionic strength and the concentration of divalent cations. Sequential μGAF-membrane filtration was used in the experiments.

4.7.1. Effect of pH

Feed solution (50% LP water) pH was adjusted to 3, 5, 7 or 9 by titrating with 1 M HCl or NaOH. A set of control runs was conducted first at a flux of 100 LMH to examine the effect of feed solution pH on bare membrane fouling. The experimental results are illustrated in Figure 4.20. The pH had a limited effect on bare membrane fouling, with the TMP increasing by 15 psi within V_{sp} of 600 L/m^2 at every pH tested.

Many researchers have reported that low pH enhances membrane fouling by humic acids because low pH lowers the negative charge on the molecules. The lower charge decreases repulsion between the humic macromolecules and the membrane and among themselves, resulting in more rapid membrane fouling [7,31,54]. In this study, however, lowering the solution pH had almost no effect on fouling. One possible explanation is that humic substances in the feed solution (50% LP water) were not the major foulant. Although deposition of humic acids can be enhanced at low pH, it did not affect the TMP increase during filtration.

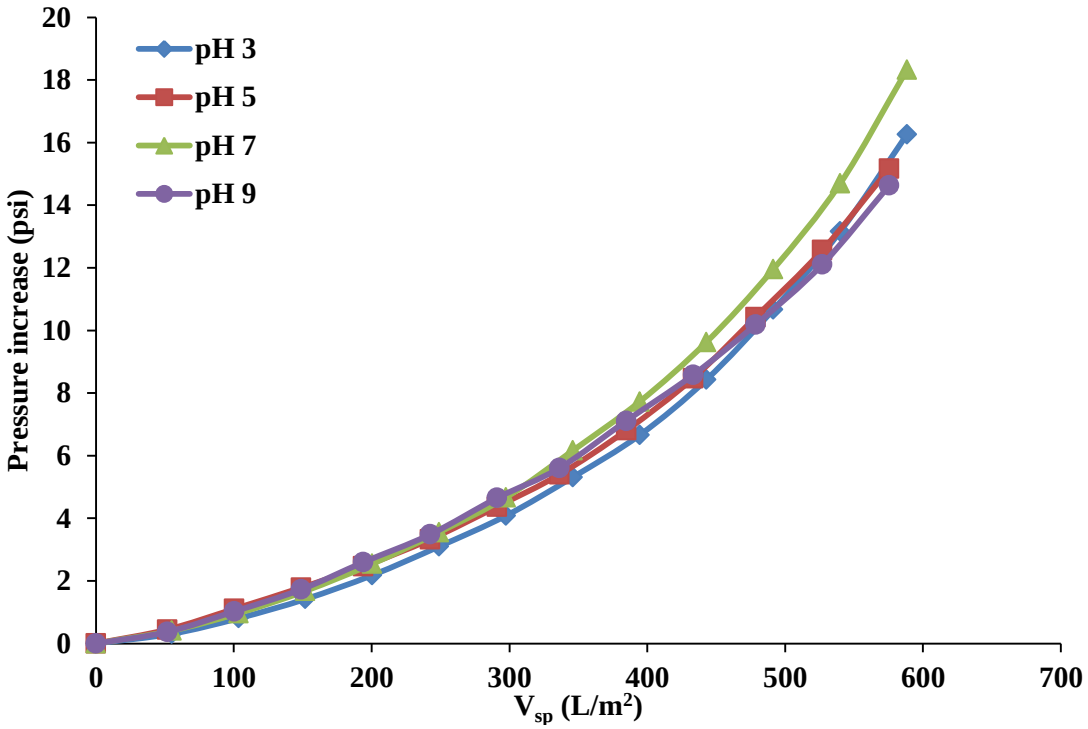

Figure 4.20 Bare membrane fouling when fed with 50% LP water at different pH values

On the other hand, the pH had a significant impact on fouling in sequential μGAF-membrane systems. In these experiments, the flux to the upstream μGAF unit was 250 LMH, with HAOPs loading at 10 g Al/m^2. The pressure increase across the upstream μGAF unit at different pH's is shown in Figure 4.21 (a). More fouling occurred in the μGAF unit as the feed solution pH decreased from 9 to 5, and especially when the pH was lowered to 3. The composite permeate from the upstream μGAF units was then fed to the membranes at a flux of 100 LMH. Figure 4.21 (b) illustrates that the membrane TMP increased 0.5, 2.2, 4.8 and 7.3 psi in the pH 3, 5, 7, and 9 systems, respectively, during runs to V_{sp} of 800 L/m^2. Combined with the pressure increase profiles in the upstream μGAF units, these results suggest that HAOPs collect more foulant at low pH. Thus, low pH promotes foulant removal by the μGAF and leads to better downstream membrane protection.

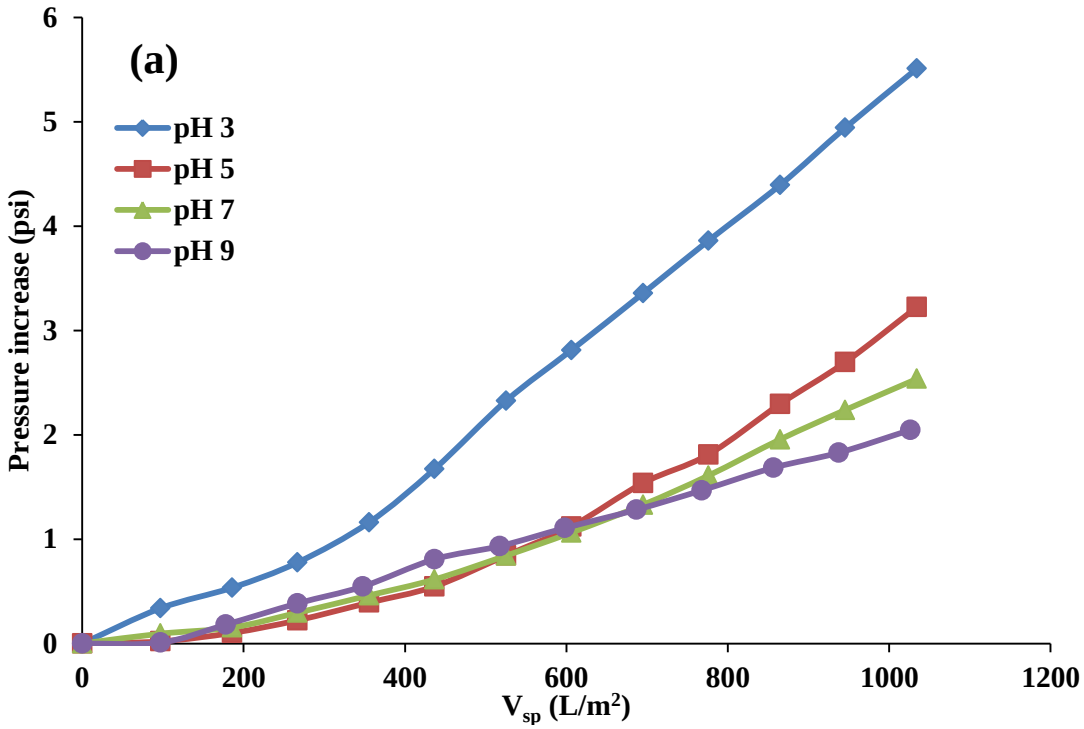

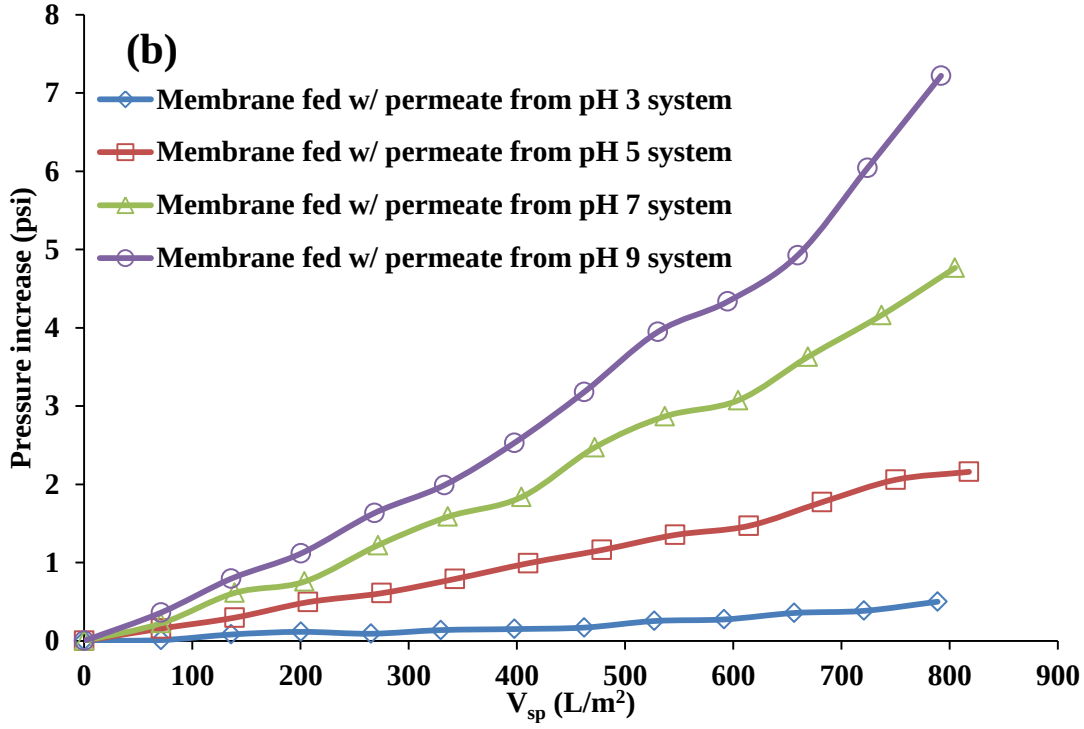

Figure 4.21 Pressure increase profiles of (a) the upstream µGAF units fed with 50% LP water of different pH and (b) the downstream membrane units fed with composite permeate collected from corresponding upstream µGAF units

Figure 4.22 (a) and (b) illustrate the removal efficiencies of UV_{254} and TEP achieved by the μGAF units at different pH's, respectively. Higher UV_{254} removal was achieved with decreasing pH. For instance, at pH 3 the μGAF unit achieved about 15% higher UV_{254} removal than at pH 9 throughout the run on average. The same pattern was observed for TEP removal — at pH 3, the μGAF unit removed more than 95% of the TEP from the feed, while at pH 9 the removal efficiency dropped to about 70%. The results are consistent with the hypothesis presented above. The composite permeate collected from the downstream membrane unit was also analyzed and contained much less TEP than the composite permeate collected from the upstream μGAF unit, suggesting that the polysaccharide molecules were retained by the membrane. Recalling that the bare membrane achieves negligible UV_{254} removal (see Figure 4.8), this result suggests that polysaccharide is a more important membrane foulant than humic substances.

Schlautman and Morgan [128] reported that humic acids and fulvic acids showed higher adsorption on colloidal sized aluminum oxide particles at low pH than high pH conditions. Low pH promotes protonation of mineral surface hydroxyl groups and makes them more exchangeable. As a result, carboxyl groups of humic substances can complex with the protonated metal ions more easily, leading to enhanced ligand exchange (which is one of the major mechanisms for humic substance adsorption onto mineral surfaces [129,130]) and adsorption of humic substances onto the surface. Humic substances can also adsorb onto minerals through anion exchange, in which a humic carboxyl group replaces an anion previously bound to the surface. The experimental results support the inferred mechanism, as higher UV_{254} removal efficiencies were observed at low pH conditions.

The effect of pH on polysaccharide adsorption to mineral oxides has been studied intensely; however, the effect of pH is not yet clarified. Iwasaki and Lai [131]

found much higher adsorption of corn starch on hematite at pH 6.8 than pH 11.3. Perry and Aplan [132] reported several polysaccharides had maximum adsorption to pyrite at around pH 7 and suggested that polysaccharides may have maximum adsorption to minerals when the pH is close to the isoelectric point (IEP) of the minerals. However, the maximum adsorption of polysaccharides does not always occur at the IEP of minerals, as reported by researchers in subsequent studies [133,134]. Studies showing little dependence of polysaccharide adsorption on pH have also been reported [135–138]. The IEP of HAOPs is at pH 7.63 (see Figure 4.2), so in this study, maximum TEP removal occurred at pH lower than the IEP. Overall, it is clear that TEP removal was enhanced at low pH in the μGAF process, leading to better membrane fouling control.

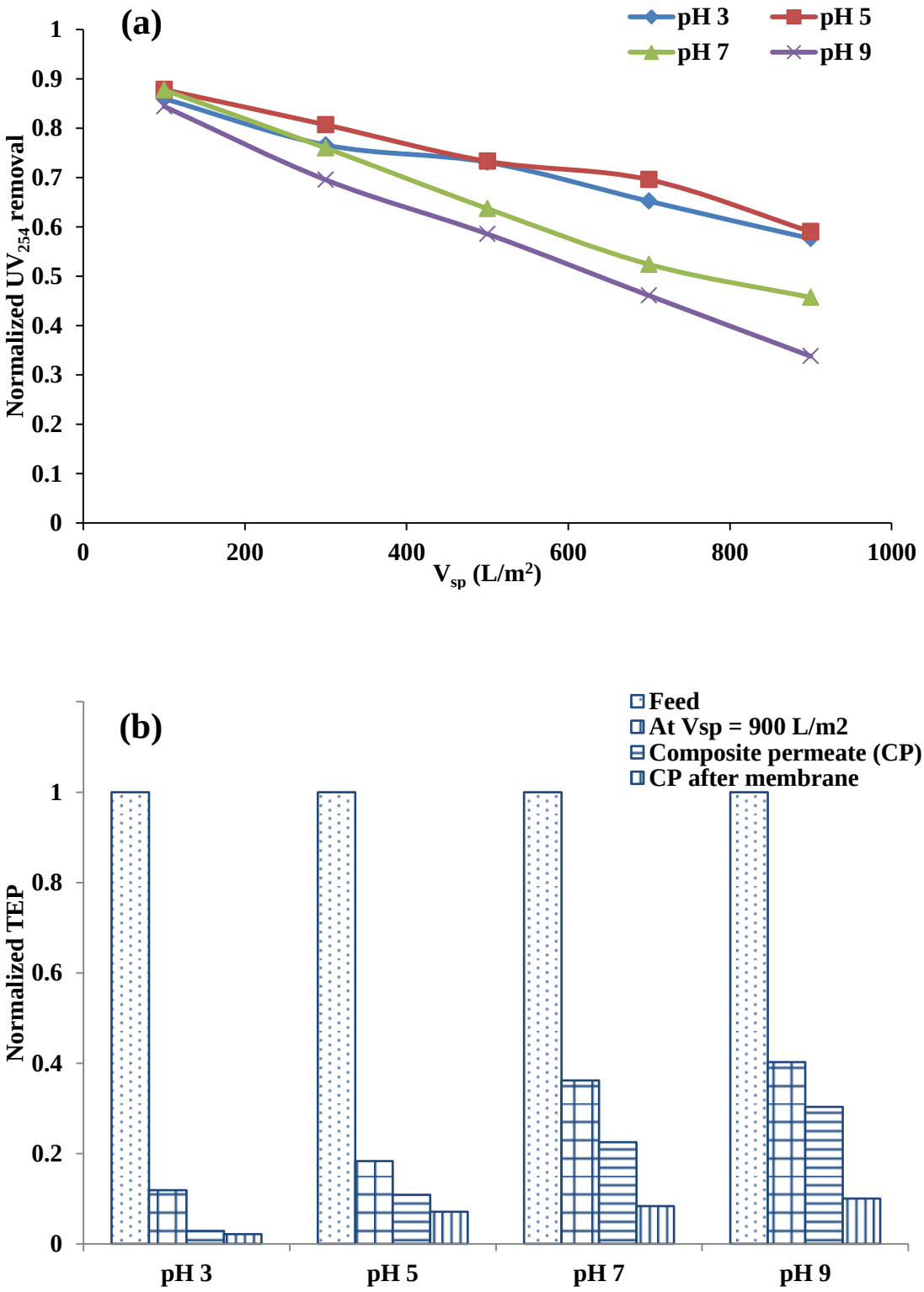

Figure 4.22 Sequential µGAF-membrane filtration permeate quality at different pH conditions (a) UV_{254} absorbance and (b) TEP concentration

4.7.2. Effect of ionic strength

Sequential μGAF-membrane filtration was used to investigate the effect of ionic strength on process performance. Feed solution (50% LP water) ionic strength was adjusted by adding NaCl. The original feed has a background ionic strength of about 2 mM (determined by applying Russell's factor [139] to the conductivity of the solution) and a total of four ionic strengths (background plus 0, 10 mM, 100 mM or 700 mM NaCl) were investigated. The highest ionic strength approximated the ionic strength of sea water.

Before carrying out the sequential μGAF-membrane filtration tests, control tests were conducted to examine the effect of ionic strength on membrane fouling. The flux was 100 LMH, and as illustrated in Figure 4.23, membrane fouling increased with increasing feed solution ionic strength. Similar patterns have been observed and reported in many previous studies, as described in the Literature Review section. High ionic strength causes double layer compression and charge screening of the NOM molecules, leading to decreased electrostatic repulsion between the membrane surface and NOM and more severe NOM deposition. High ionic strength can also depress inter-chain repulsion within NOM macromolecules, so the macromolecules become more coiled, resulting in a more compact foulant layer [140].

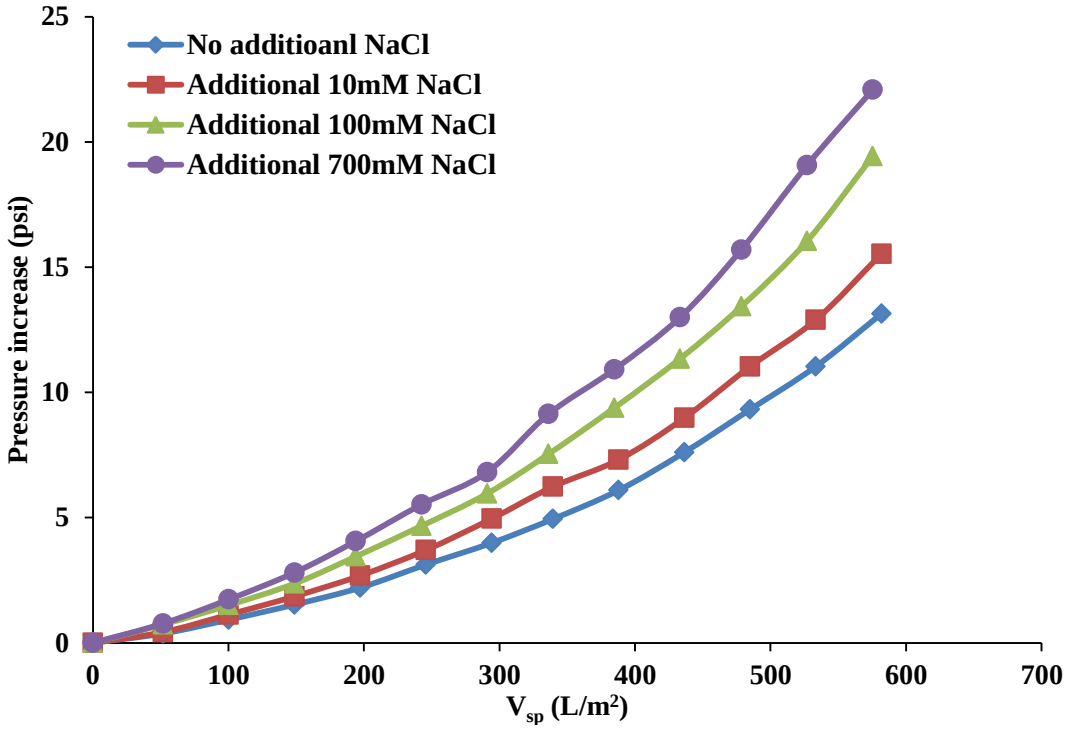

Figure 4.23 Bare membrane fouling when fed with 50% LP water of different ionic strengths. 50% LP water has a background ionic strength ~ 2mM.

Figure 4.24 (a) illustrates the pressure increase profiles of upstream μGAF units fed solutions with different ionic strengths. Similar fouling extents and patterns were observed regardless of the feed solution ionic strength, implying that feed solution ionic strength has only a small effect on the capability of the μGAF unit to collect foulant. The TMP increases of the downstream membranes were all around 5 psi (Figure 4.24 (b)), suggesting that a similar amount of foulant broke through the μGAF unit in all these experiments. The filtration permeate quality is also consistent with this interpretation, in that almost identical NOM removal efficiencies were achieved regardless of the amount of NaCl added to the feed. The system permeate qualities are illustrated in Figure 4.25 (a) and (b), demonstrating UV_{254} and TEP removal, respectively.

Comparing the fouling of membrane units with or without μGAF pretreatment, ionic strength has a noticeable impact on membrane fouling without pre-treatment,

but almost no effect on membrane fouling if the water is pretreated with HAOPs. The logical explanation is that most major foulants such as NOM macromolecules are collected in the upstream μGAF unit, and ionic strength has limited effect on the foulant's ability to pass through the HAOPs layer and reach the membrane surface.

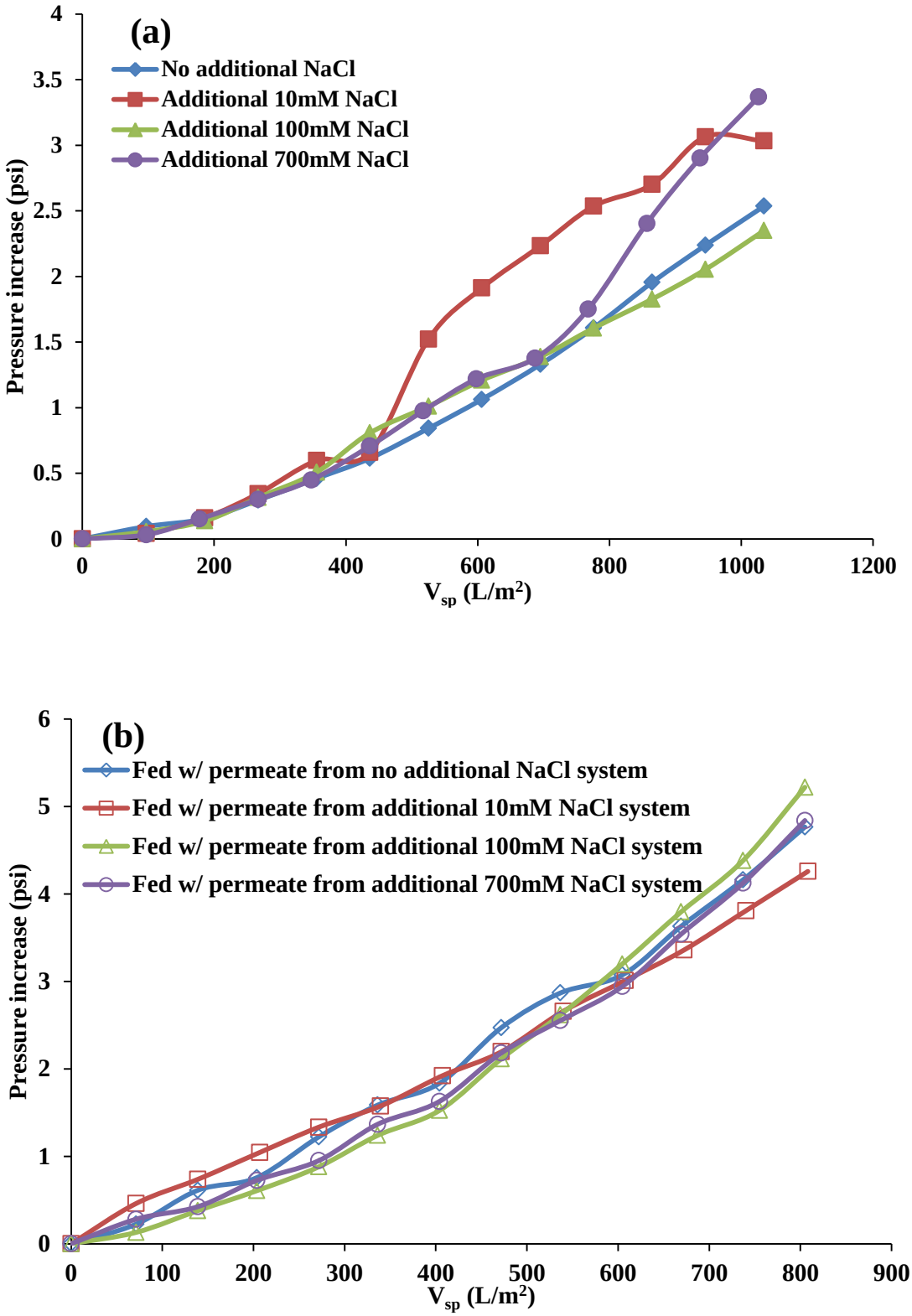

Figure 4.24 Pressure increase profiles of (a) the upstream μGAF units fed with 50% LP water of different ionic strengths and (b) the downstream membrane units fed with composite permeate collected from corresponding upstream μGAF units

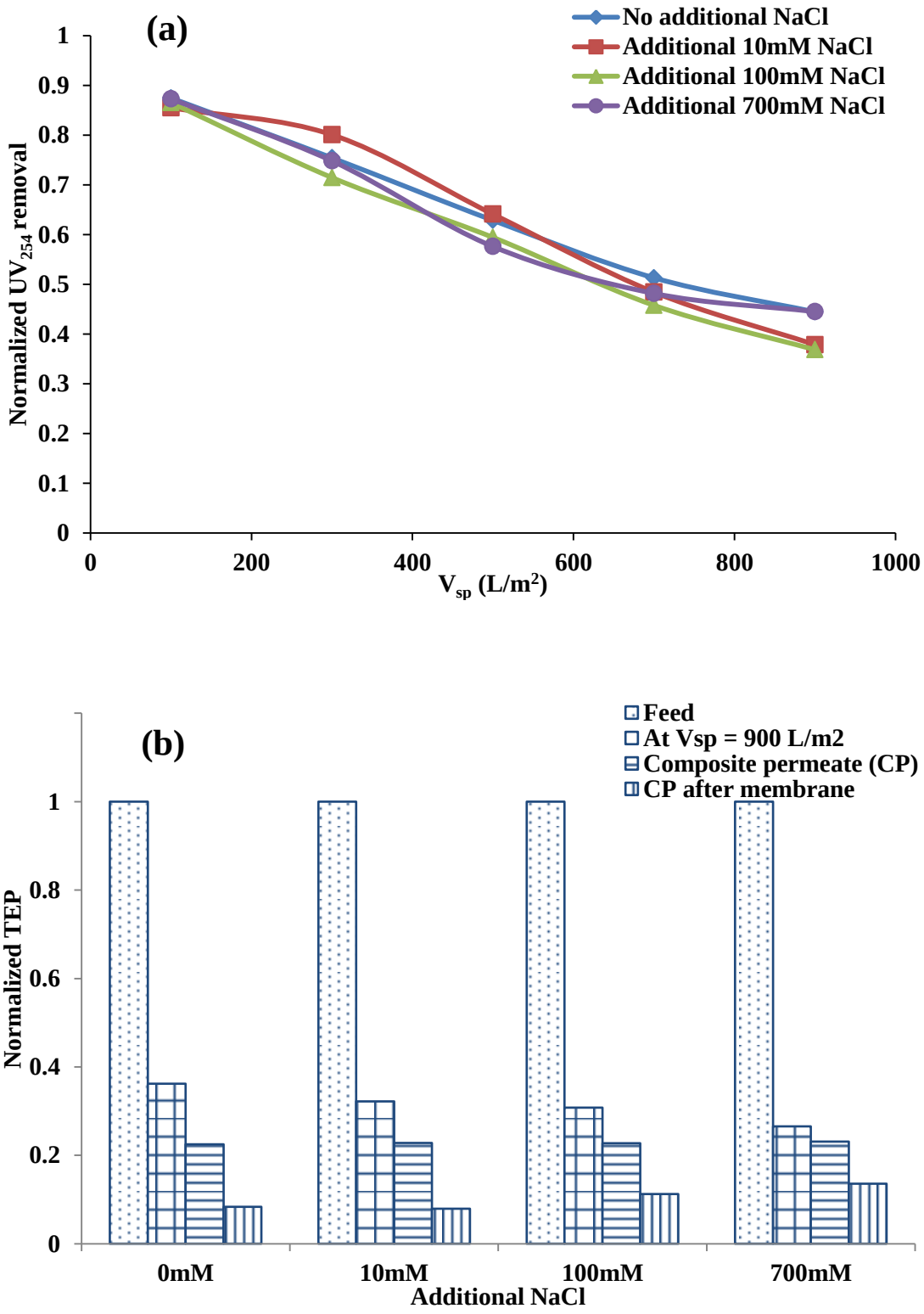

Figure 4.25 Sequential μGAF-membrane filtration permeate quality at different ionic strengths (a) UV_{254} absorbance and (b) TEP concentration

4.7.3. Effect of the concentration of divalent cations

The effects of the concentration of divalent cations were investigated with sequential μGAF-membrane filtration in cartridge setups. Calcium chloride ($CaCl_2$) and magnesium chloride ($MgCl_2$) were added to the feed solution (50% LP water), maintaining the total ionic strength at 100 mM by adding NaCl. Fluxes applied to the upstream μGAF and downstream membrane units were 250 and 100 LMH, respectively, and the HAOPs surface loading in the μGAF unit was 10 g/m^2 as Al.

The experimental results are illustrated in Figure 4.26 through Figure 4.28. In control runs (without μGAF pretreatment step), the divalent cations slightly reduced membrane fouling, as shown in Figure 4.26. The cations had no significant effect on either pressure drop across the μGAF units (Figure 4.27 (a)) or removal of UV_{254} absorbance or TEP (Figure 4.28 (a) and (b)), implying that the presence of divalent cations has negligible effect on the ability of HAOPs to collect NOM. However, a slight decrease in fouling was observed on the downstream membrane with the presence divalent cations, as illustrated in Figure 4.27 (b).

The effects of divalent cations on membrane fouling have been investigated in many previous studies, and it seems that the effects depend on the NOM source fed to the membrane. Some researchers used commercially available humic acids (SRHA or AHA) and reported that Ca^{2+} causes more rapid membrane fouling by promoting aggregation of humic acid macromolecules and increasing the NOM deposition rate [7,54–56,141]. In contrast, researchers using natural water as the NOM source have reported that calcium ion has a very limited effect on membrane fouling [142–144]. Further, when polysaccharides are the main NOM source and in MBR systems, it has been reported Ca^{2+} has almost no effect on or even reduces membrane fouling, because it promotes agglomeration of polysaccharide macromolecules, leading to a looser and more permeable foulant layer [58,145,146].

50% LP water was used as feed in this study, and the experimental results presented earlier suggest that polysaccharides are probably the key membrane foulants in the water. The results obtained here support this interpretation, in that the divalent cations do not cause more rapid fouling but instead slightly mitigate membrane fouling by forming a looser and more permeable foulant layer.

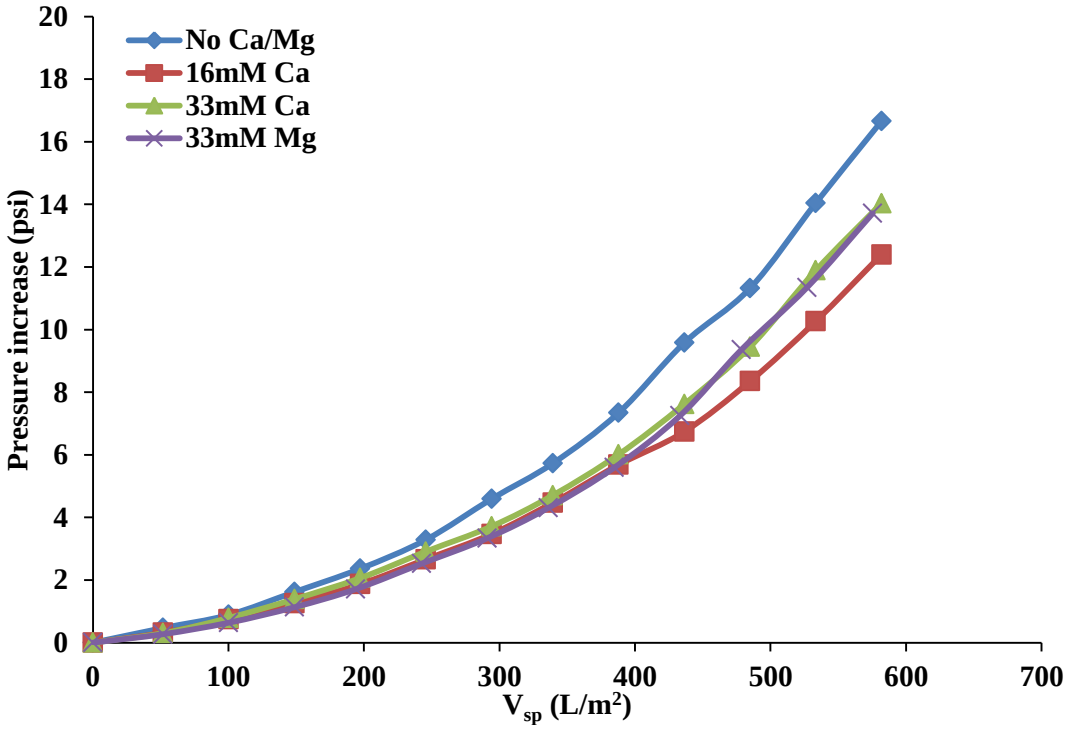

Figure 4.26 Bare membrane fouling when fed with 50% LP water of different Ca^{2+}/Mg^{2+}concentration. Total ionic strength fixed at 100mM.

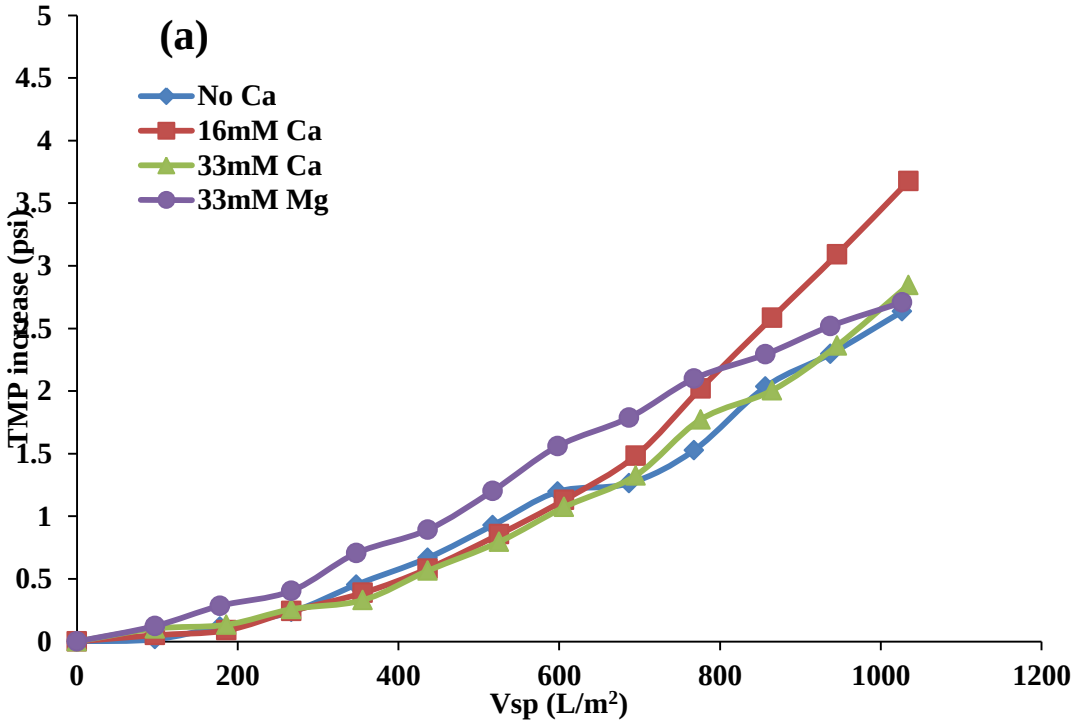

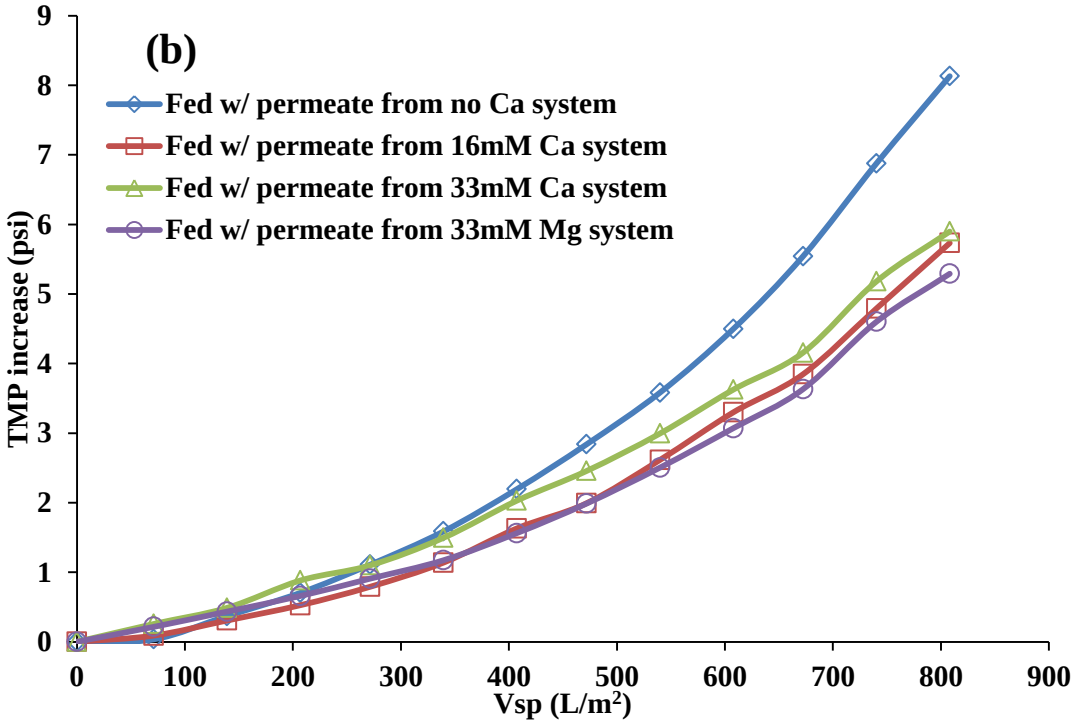

Figure 4.27 Pressure increase profiles of (a) the upstream μGAF units fed with 50% LP water of different Ca^{2+}/Mg^{2+} concentration and (b) the downstream membrane units fed with composite permeate collected from corresponding upstream μGAF units

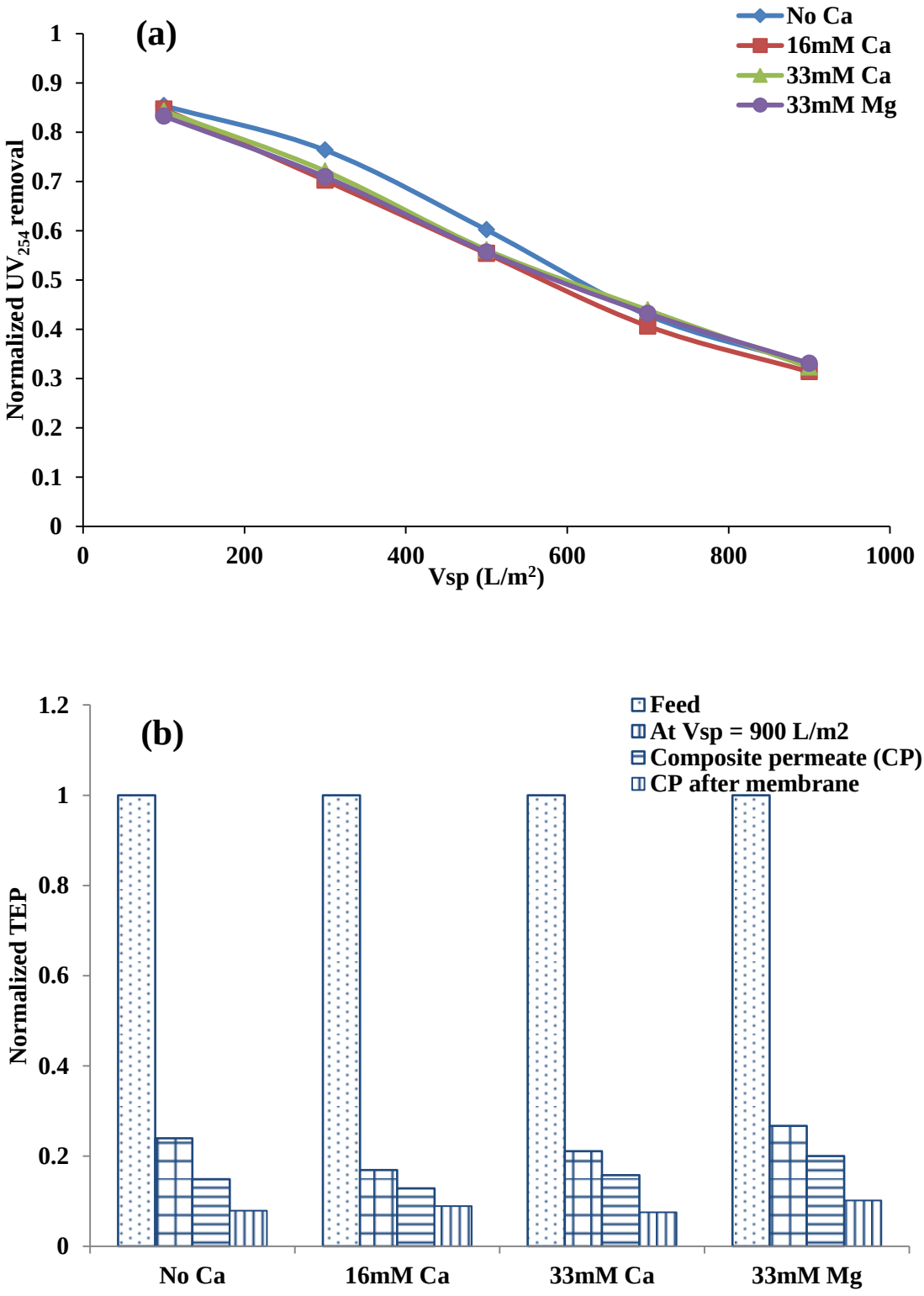

Figure 4.28 Sequential µGAF-membrane filtration permeate quality at different Ca^{2+}/Mg^{2+} concentration (a) UV_{254} absorbance and (b) TEP concentration

4.8. Key foulants in the HAOPs layer and membrane in μGAF applications

4.8.1. The effect of pre-filtration on fouling in pre-deposited HAOPs layer

As shown in previous sections, when raw water was fed to a bare membrane, the membrane fouled rapidly with negligible NOM removal. When μGAF pretreatment was applied, membrane fouling was reduced substantially, significant NOM removal was achieved, and the pressure drop across the μGAF unit increased. A straightforward conclusion is that fouling shifts from the membrane to the upstream μGAF unit because the μGAF unit captures most of the foulant in the adsorbent layer. The foulant in raw natural water is a complex mixture of different materials with different sizes. To investigate the effect of foulant size on fouling, 50% LP water was pre-filtered with filters of different nominal pore sizes and was fed to the μGAF unit. In this experiment, the flux applied to the μGAF unit was fixed at 250 LMH, and the HAOPs loading was 10 g/m^2 as Al.

As shown in Figure 4.29, pre-filtration mitigated μGAF fouling immensely. When no pre-filtration was applied, the pressure across the μGAF unit increased nearly 22 psi at a V_{sp} of 900 L/m^2. When 1-μm or 0.35-μm pre-filtration was applied, the pressure increased about 11 psi and 1.6 psi at V_{sp} around 1050 L/m^2, respectively. The UV_{254} absorbance and DOC concentrations were identical before and after pre-filtration, suggesting that only particulates or colloids were removed by pre-filtration, and the soluble foulant (i.e., NOM) was not altered in the feed. Therefore, the result suggests that particulate and colloidal fouling are the dominant fouling mechanism within the adsorbent layer.

Experiments investigating the capability of the HAOPs layer to collect colloids were then carried out by feeding clean water with fluorescence polystyrene beads to the sequential μGAF-membrane system. The flux was 100 LMH for both the μGAF and membrane units in this experiment, and the HAOPs loading was 10 g/m^2 as Al.

Three different sizes of beads (1-µm, 0.31-µm and 0.1-µm) were tested. At the end of the filtration cycle, the downstream membrane was retrieved and examined under microscope to count the retained fluorescence beads. The results are shown in Table 4.2. The HAOPs layer was most effective at collecting 1-um particles, and the collection efficiency decreased with decreasing particle size.

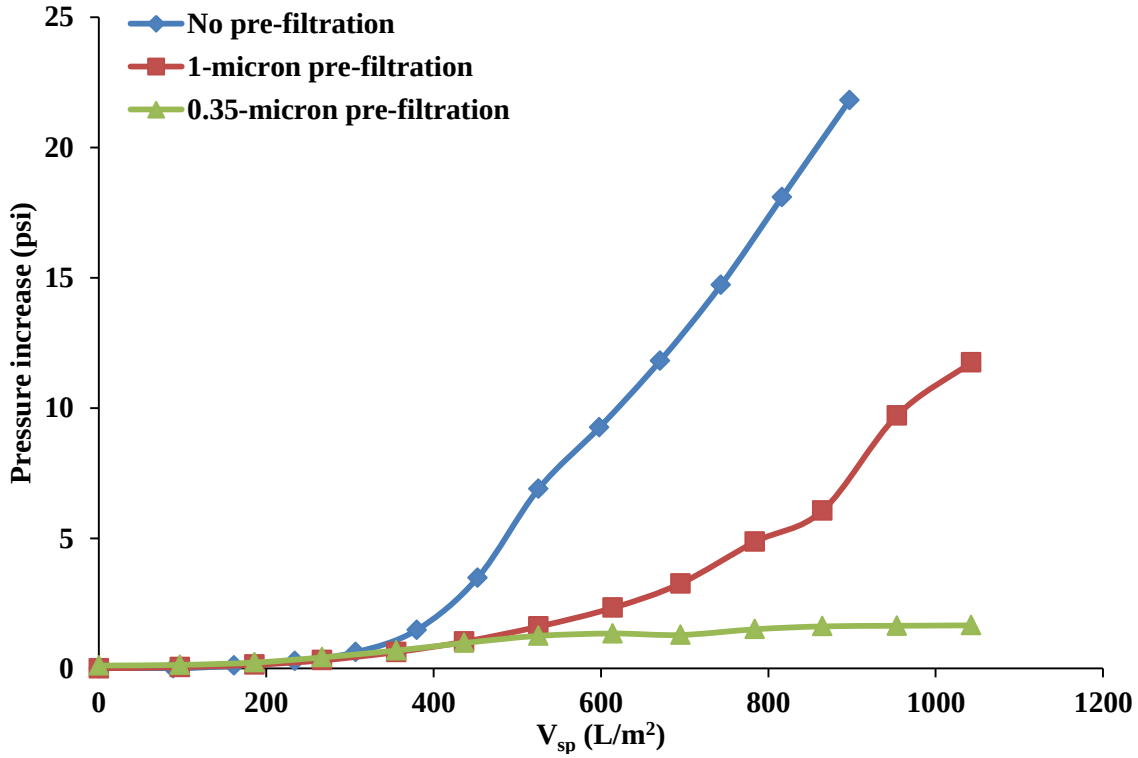

Figure 4.29 Pressure profiles of µGAF units fed with 50% LP water with or without pre-filtration. Operation flux = 250 LMH, HAOPs loading = 10 g/m^2 as Al

Table 4.2 Removal efficiencies of various sizes of particles by µGAF

Particle size (µm)	Removal (%) at V_{sp} = 100 L/m^2	Removal (%) at V_{sp} = 400 L/m^2	Removal (%) at V_{sp} = 800 L/m^2
1	99.85	99.46	98.26
0.31	95.43	91.09	81.38
0.1	97.05	77.61	79.11

4.8.2. The effect of pre-filtration on process performance in a sequential μGAF-membrane filtration system

Further experiments were carried out in sequential μGAF-membrane filtration systems to investigate the effect of pre-filtration when the membrane was fed with water that had been pre-treated with HAOPs in a μGAF unit. 0.35-μm cartridge filters were used for pre-filtration. The fluxes applied to the upstream μGAF and downstream membrane units were 250 and 100 LMH, respectively. The HAOPs surface loading was 10 g/m^2 as Al for all tests.

The results are illustrated in Figure 4.30. Once again, a dramatic difference in the pressure increase at the upstream μGAF unit was observed. Pre-filtration significantly reduced the pressure increase across the HAOPs layer. However, pre-filtration did not have a significant impact on fouling of the downstream membranes. Since pre-filtration removes only particles or colloids and does not alter soluble foulants, the results suggest that the dominant foulants for the downstream membrane were not colloids or particulates but the soluble materials in the feed such as soluble NOM. The slightly higher pressure increase on the downstream membrane unit in the system without pre-filtration was probably due to the escaped particles having some synergistic effect with soluble foulant on membrane fouling, but the difference was not remarkable compared to the different pressure increases across the upstream μGAF units.

The effect of pre-filtration on membrane performance in control runs (feed being pumped directly to the membrane without HAOPs pre-treatment) was also investigated. The same membrane fouling pattern occurred as was observed at the downstream membrane in the sequential μGAF-membrane filtration system, suggesting pre-filtration had no effect on membrane fouling. The result agrees with the previous interpretation, that the membrane fouling was dominated by the presence

of soluble foulant in the water but not particulates or colloids.

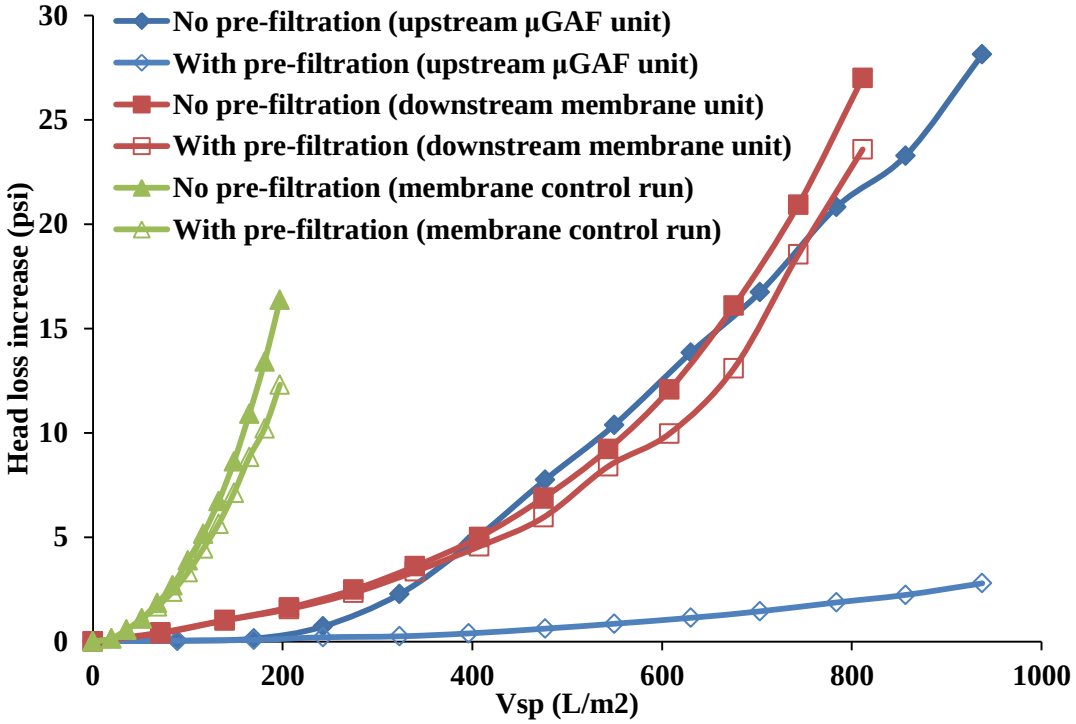

Figure 4.30 Pressure profiles of sequential µGAF-membrane filtration systems with or without pre-filtration. Pressure profiles of membrane control runs with or without pre-filtration were included as reference, with operational flux of 100 LMH

4.8.3. Modeling µGAF fouling

In 1982, Hermia [75] developed a series of equations to predict particulate fouling behavior on membranes. This classic model series include four scenarios, which were described in the literature review. The equations developed by Hermia [75] were exclusively for dead end, constant pressure filtration and particulate contaminants. In 1993, Hlavacek and Bouchet [77] extended the model that they modified Hermia's equations for constant flowrate condition, as listed in Table 4.3.

Table 4.3 Hlavacek and Bouchet's membrane fouling model for constant flowrate condition [77]

Law	Linearized form
Complete blocking	$\frac{1}{\Delta P} = a + bV$
Standard blocking	$\frac{1}{\sqrt{\Delta P}} = a' + b'V$
Intermediate blocking	$\ln \Delta P = a'' + b''V$

An attempt was made to model the μGAF process by considering the μGAF unit as a membrane and fitting experimental data to the established models. In this study, filtration experiments were operated under constant flowrate, dead end filtration, so Hlavacek and Bouchet's models were chosen for experimental data fitting. From the previous section, it was observed that in a μGAF process, particulates are the primary cause of fouling in the μGAF unit.

Pressure increase data for μGAF systems operated with three different fluxes (100, 250 and 400 LMH) were used in blocking law analysis. The model fitting results for complete blocking, standard blocking and intermediate blocking are illustrated in Figure 4.31 (a), (b) and (c), respectively. In all experiments, 50% LP water was used as feed and the HAOPs surface loading in μGAF unit was 10 g/m^2 as Al. In the analysis for all three fluxes, the complete blocking law had the poorest fit, with linear regression coefficients R^2 of 0.74-0.82; the standard blocking gave the R^2 between 0.86 and 0.91; and the intermediate blocking law had the best fits, with R^2 greater than 0.95. The consistent good fits over the flux range investigated suggest that the intermediate blocking law can be helpful for predicting fouling in the μGAF unit.

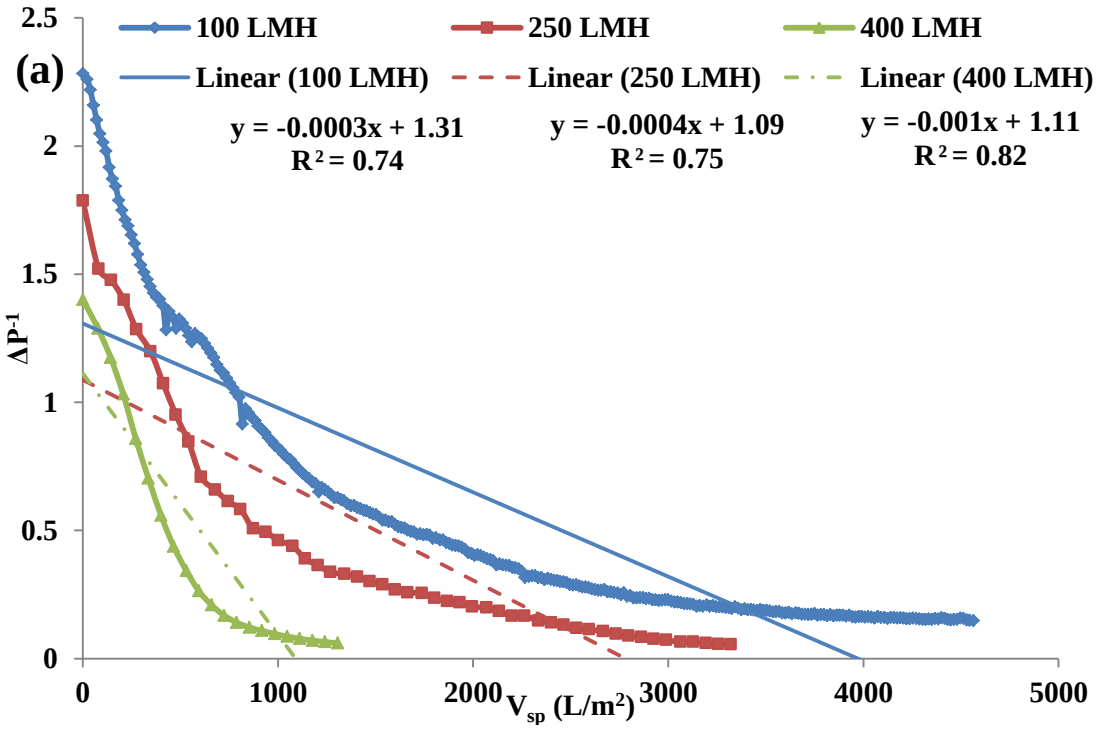

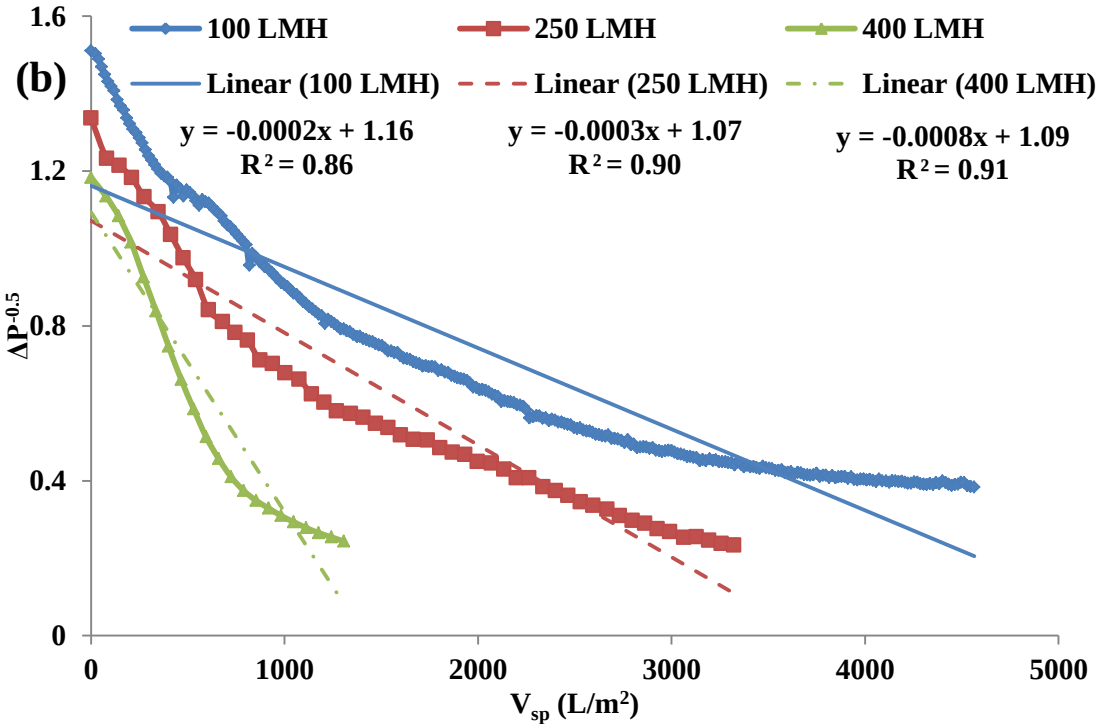

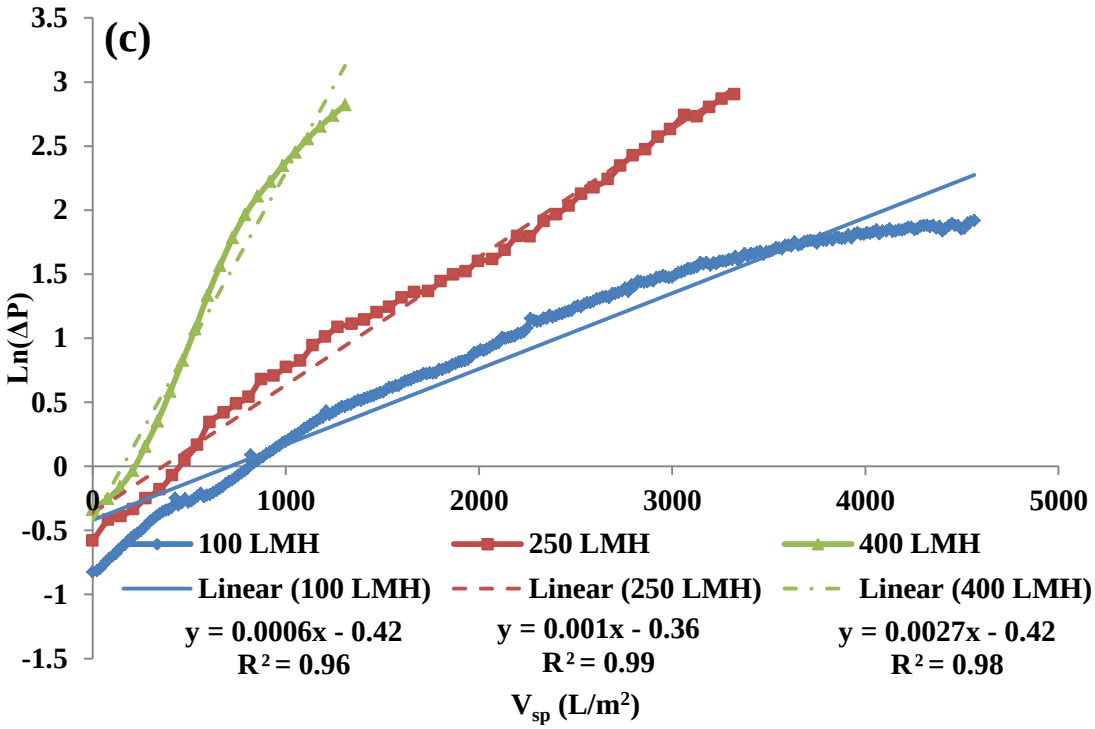

Figure 4.31 (a) Complete blocking law analysis, (b) standard blocking law analysis and (c) intermediate blocking law analysis of µGAF

4.9. Large bench scale experiments of μGAF process application

In this section, experimental results of large bench scale experiments of the μGAF process are reported. All experiments were operated using tubular filtration setup with LU water as feed.

4.9.1. Comparison of membrane fouling control and NOM removal efficiency between μGAF and conventional coagulation

Four approaches for treating the feed water were compared with respect to membrane fouling control and NOM removal. The first approach was a control experiment in which the feed water was passed directly through a bare ceramic membrane, and the membrane was hydraulically cleaned every two hours by introducing a total of four short pulses of backflow accompanied with cross-flow and air scouring, with each pulse lasting 10 seconds and a 10 second pause between each pulse. The second experiment simulated a conventional coagulation treatment process. The desired dose of alum was added into the feed water, the pH was adjusted to 7.0, and the solution was mixed 30 minutes. Then, the flocs settled for two hours and the supernatant was fed to a bare ceramic membrane. The third experiment was identical to the second, but HAOPs were used instead of alum. In both cases, the doses were 5.6 mg/L as Al. The membranes in the second and third experiment were also hydraulically backwashed every two hours as in the control experiment. In all experiments, filtration processes were operated at a flux of 75 LMH.

In the fourth experiment, the μGAF process was used. HAOPs were pre-deposited onto the ceramic membrane surface and LU water was fed at a flux of 75 LMH for 22 hours at a HAOPs surface loading of 10 g Al/m^2. The duration of the treatment cycle and the adsorbent surface loading were chosen so that the effective

dose of Al (mg of Al used to treat per liter of water) were the same as in the two preceding experiments.

Experimental results for system pressure build up and UV_{254} removal are shown in Figure 4.32 (a) and (b), respectively. In the control run without any Al addition, the membrane fouled rapidly, with the pressure reaching 22 psi at a V_{sp} of 2300 L/m^2. Conventional coagulation with alum or HAOPs reduced fouling, generating pressures of the systems about 6 to 8 psi at a V_{sp} around 6000 L/m^2, with HAOPs having slightly better performance than alum. In these three systems, the membranes were hydraulically backwashed every two hours, but the TMP built steadily throughout the cycles, suggesting that a portion of the fouling was not hydraulically reversible and a more aggressive cleaning approach would be required to remove the residual foulants. By comparison, in the μGAF system, the fouling was substantially reduced, with the TMP increasing to at most 4 psi in each cycle of 1700 L/m^2. Also, the backwash after each run brought the TMP back to the initial level, suggesting minimum foulant residual was left in the system. The μGAF system also had better NOM removal efficiency, achieving more than 70% UV_{254} removal throughout a Vsp of 1700 L/m^2, compared to only 40-55% and less than 10% removals were achieved by conventional coagulation and bare membrane filtration, respectively. In conclusion, μGAF with HAOPs outperformed all other approaches both on fouling control and NOM removal efficiency.

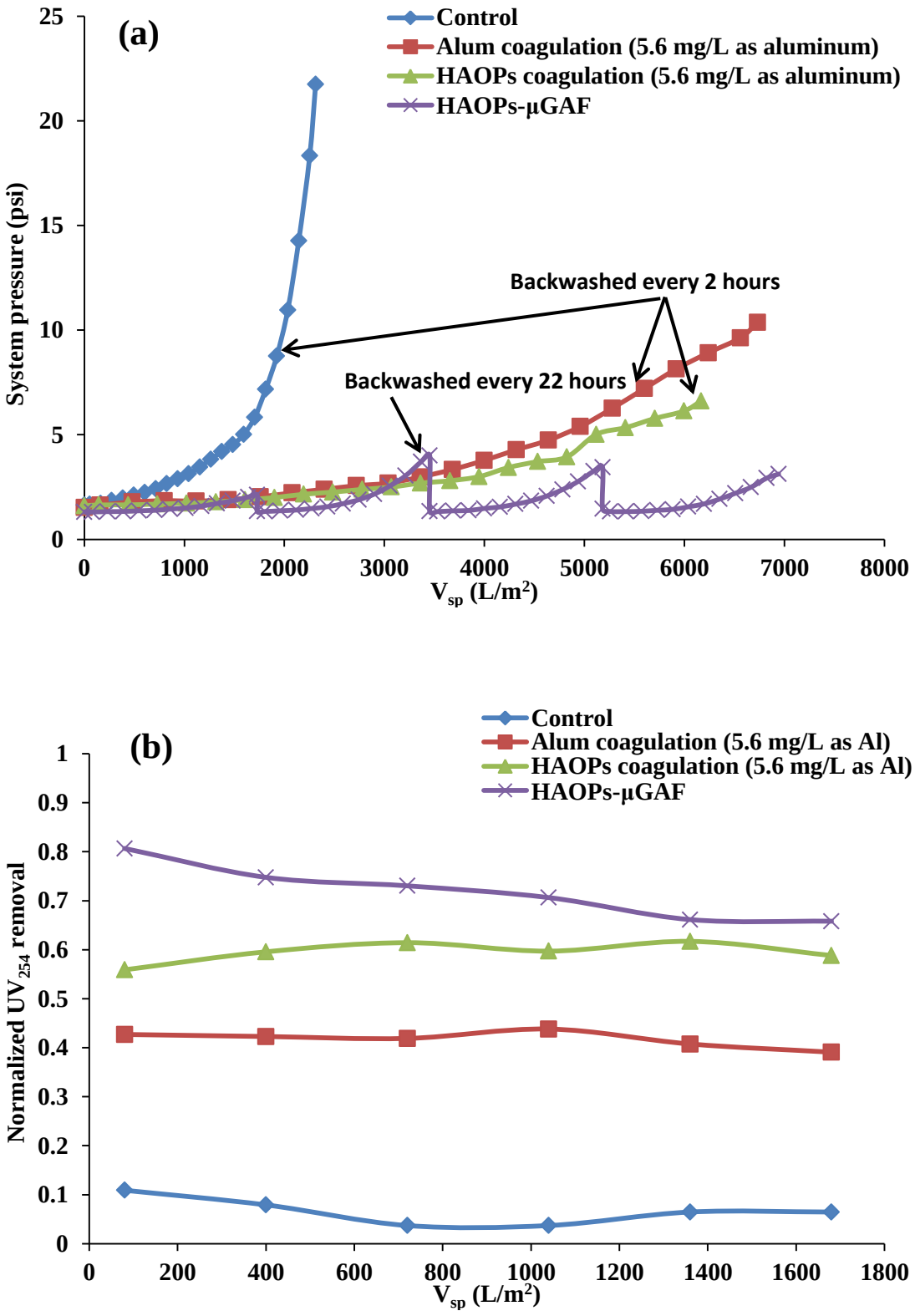

Figure 4.32 (a) Pressure increase profiles of four different approaches and (b) fractional removal of NOM (presented in UV_{254}) of four different approaches for treating LU water

Further exploration of the μGAF process was then conducted in a long-term test using the same experimental conditions as described previously, except that the HAOPs surface loading was increased to 15 g Al/m^2 in this particular test. Thirty filtration cycles were conducted, and the results are shown in Figure 4.33 (a) and (b). The μGAF system achieved substantial NOM removal efficiency during all 30 cycles and maintained long-term stable operation with a much lower backwash frequency than conventional membrane processes.

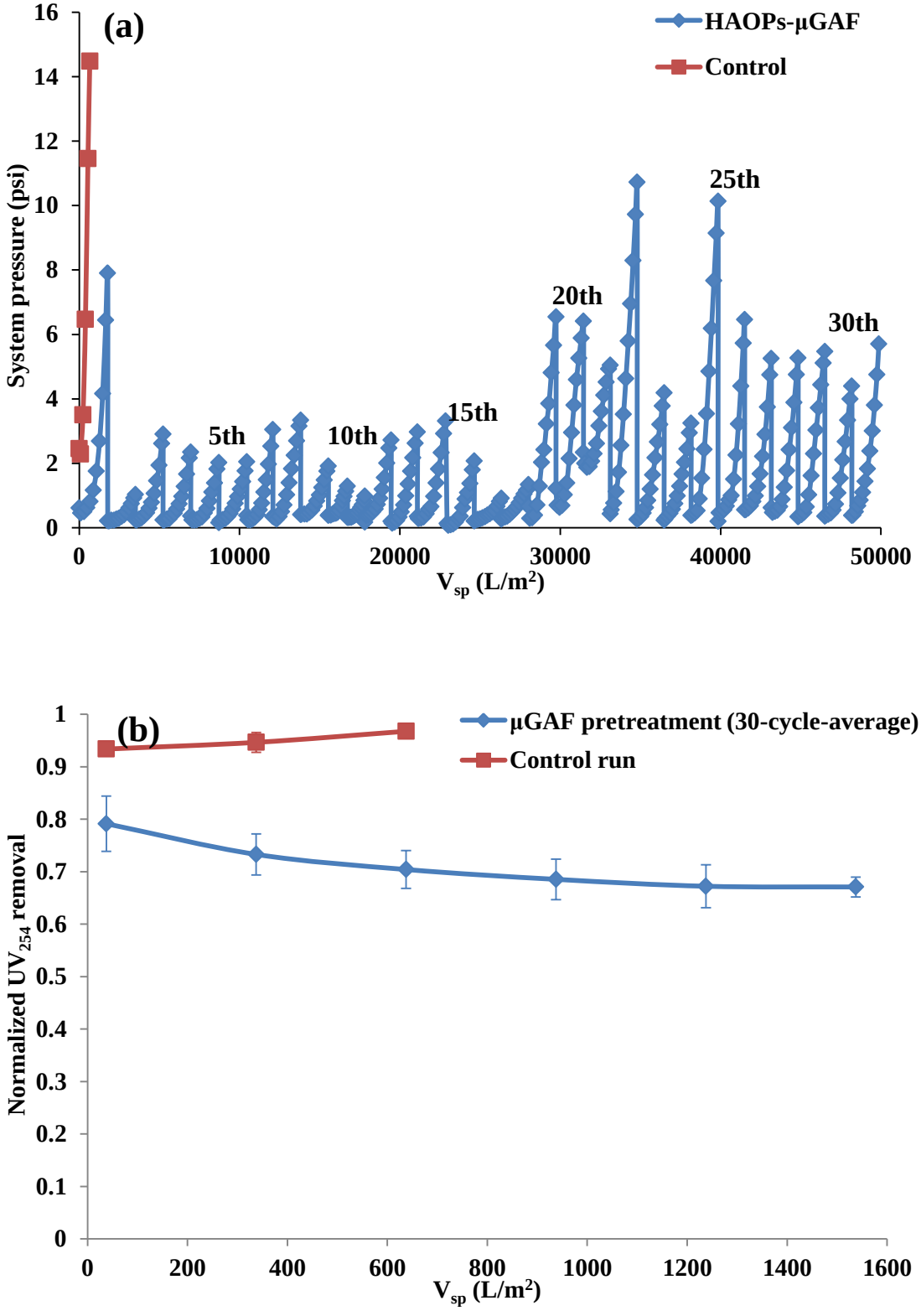

Figure 4.33 (a) Pressure increase profiles of the μGAF system during 30 sequential, 22-h filtration cycles and (b) average NOM removal (presented in UV_{254}) of permeate from μGAF system in each filtration cycle. A control run is presented as reference

4.9.2. μGAF as pretreatment for membrane filtration

Experiments described in the previous section demonstrated that membrane fouling can be greatly reduced by pre-depositing adsorbent (HAOPs) onto a membrane surface. However, this operational mode is not likely to be applied in real practice. Hollow fiber membranes are widely used in water treatment applications, and it is difficult to pre-deposit the adsorbent directly onto the membrane surface in such systems, since the adsorbent particles could clog these narrow membrane fibers. To avoid this issue, the μGAF and membrane units were separated. A mesh tube was pre-deposited with HAOPs serving as the μGAF unit upstream in series with a membrane unit downstream.

In the first experiment, nylon mesh was used in the μGAF unit upstream and a ceramic membrane was used downstream. HAOPs were deposited on the nylon mesh at a surface loading of 10 g/L as Al. LU water was passed through the μGAF unit at a flux of 100 LMH, and the permeate from the μGAF unit was fed to the downstream ceramic membrane at a flux of 70 LMH. The μGAF unit was operated for 15 days or a total of 19, 18-h filtration cycles, with hydraulic cleaning at the end of each cycle. No cleaning was applied to the downstream ceramic membrane throughout the entire experiment.

The pressure profiles of both treatment units and the NOM removal efficiencies are illustrated in Figure 4.34 (a) and (b), respectively. A consistent pressure increase (~3 psi) occurred in the μGAF unit each cycle, and hydraulic cleaning was able to bring the TMP back down fully. Approximately 70% UV_{254} removal was also achieved consistently. Throughout the run, the downstream ceramic membrane experienced negligible TMP increase, even though the membrane was not cleaned in any way during the entire experiment. The results suggest that although a portion of NOM (which contains ~30% of UV_{254}) passed through the HAOPs layer and reached

the downstream membrane, this NOM did not contribute to membrane fouling; i.e., that the μGAF unit collected almost all of the foulant from the feed.

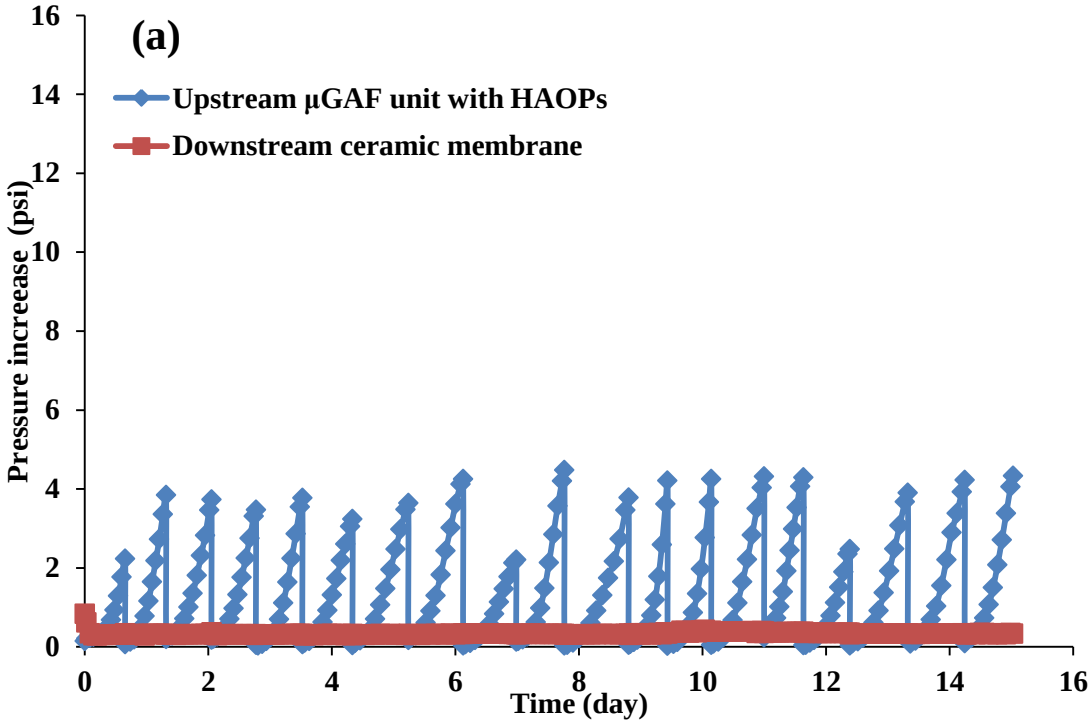

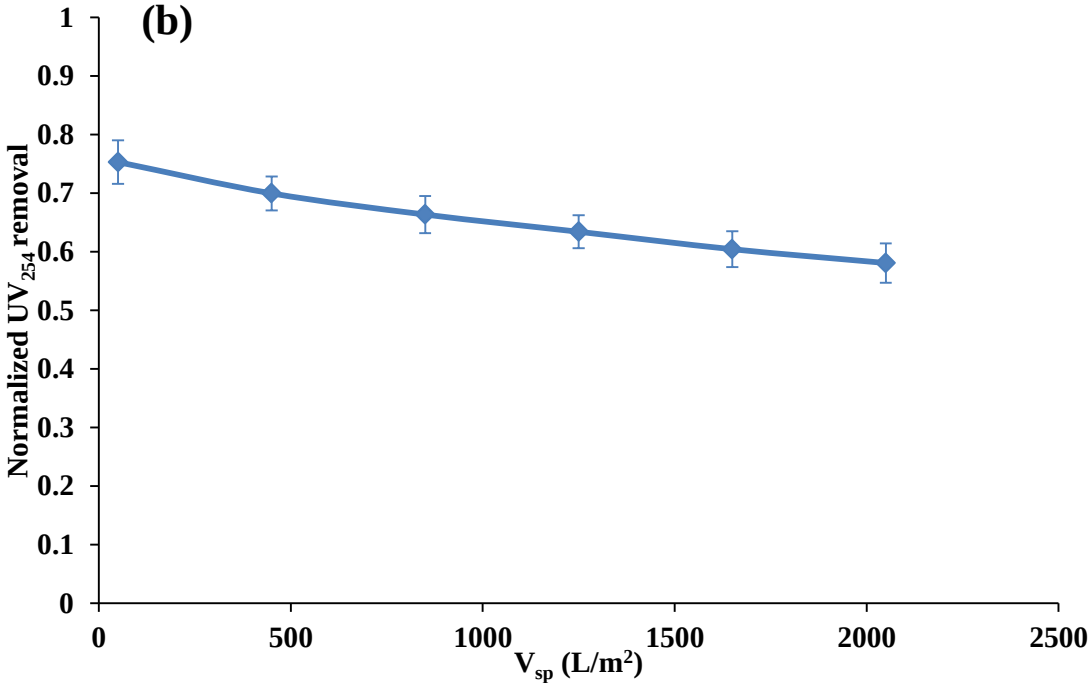

Figure 4.34 (a) Pressure increase profiles of upstream µGAF unit and downstream ceramic membrane. The µGAF unit was hydraulically backwashed at the end of each cycle and no cleaning attempt was applied to ceramic membrane, and (b) average fractional NOM removal of the µGAF unit permeate in each filtration cycle during the 15-days experiment

The experiment was repeated with a PES hollow fiber UF module to determine whether similar fouling mitigation would occur with a different membrane. In this experiment, the HAOPs loading and the feed water flux to the upstream μGAF unit were 15 g/m^2 and 150 LMH, respectively. The duration of each filtration cycle was set at 22 h. Permeate from the upstream μGAF unit was fed to the downstream UF membrane module at 60 or 90 LMH.

Once again, significant membrane fouling reduction was achieved, as shown in Figure 4.35 (a). When the UF module was fed with μGAF-pretreated water and operated at 60 LMH, negligible TMP increase was observed over 14000 L/m^2 of V_{sp}. In comparison, in the control run, the TMP of the UF module increased 1.7 psi within a V_{sp} of only 1300 L/m^2. When the UF module was fed with μGAF-pretreated water and operated at 90 LMH, the TMP increased by about 4 psi over 24000 L/m^2 of V_{sp}. When the membrane was chemically cleaned with diluted bleach (by soaking in 0.5% NaOCl for 1 h), the fouling was fully reversed. After the cleaning process, the filtration cycle for UF module was repeated and the fouling pattern was almost identical to the first run. The UV_{254} removal was consistent at ~70% each run, as shown in Figure 4.35 (b). The results suggested that foulants were collected in the upstream μGAF pretreatment unit. In contrast, in the control run, a much higher fouling rate was observed, that the TMP increase of the membrane reached about 4 psi over a V_{sp} only of 1400 L/m^2.

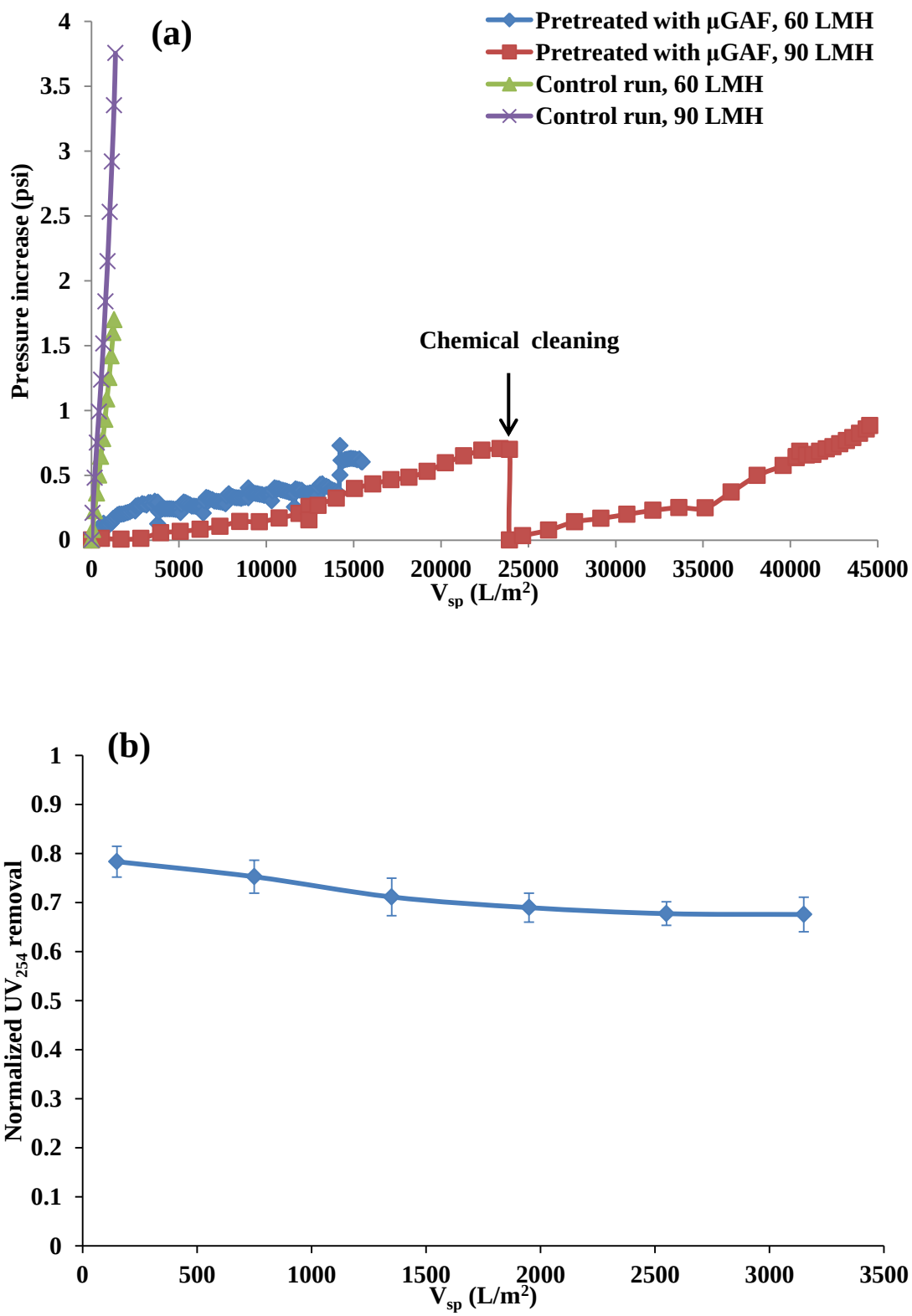

Figure 4.35 (a) Pressure increase profiles of PES hollow fiber UF membrane module under different operational conditions and (b) average fractional breakthrough of NOM (presented in UV_{254}) of the µGAF unit permeate in each filtration cycle

4.9.3. μGAF pretreatment for water containing high humic substances and turbidity

Experiments described in the previous section demonstrated that μGAF is a satisfactory pretreatment process for LU water. However, LU water is of high quality, so the membrane fouling rate was low even in control runs. To further explore the potential of μGAF pretreatment, raw LU was amended with either humic substances and/or particulates to investigate the μGAF process under more challenging circumstances. In these experiments, #316 stainless steel mesh was used to make the HAOPs support tube for the μGAF unit. The mesh had nominal 10-μm openings.

In the first experiment, the feed water was prepared by blending LU water with 10 mg/L of Aldrich humic acid (AHA). After blending, the UV_{254} of the feed increased from 0.07 cm^{-1} to 0.40 cm^{-1}. The μGAF unit was operated at a flux of 150 LMH and with a HAOPs surface loading of 7.5 g/m^2 as Al. Five filtration cycles were carried out. Hydraulic backwash was applied to the μGAF unit whenever the pressure reached 6 psi.

The pressure drop across the mesh tube increased more rapidly in this experiment than in the experiment with raw LU water as feed. In each run, the pressure reached 6 psi after about 10 hours of filtration (or at V_{sp} ~1500 L/m^2). Once again, μGAF pretreatment was efficient at removing NOM, achieving UV_{254} removal of around 80-90% throughout each filtration cycle. The percentage removal was even higher than when the system was fed with raw LU water, indicating that HAOPs are more effective at removing humic substances than a complex mixture of NOM in the raw LU water.

In the second experiment, identical operational conditions were applied except that the feed water was prepared by mixing Arizona road dust into raw LU water to increase the turbidity of the feed to 50±10 NTU. Twenty-one filtration cycles were

conducted, and as would be expected, the μGAF unit showed more rapid fouling than when fed with untreated raw LU water. The TMP reached 6 psi within 10-17 hours (13 hours on average) of filtration time. Excellent turbidity removal was achieved by the μGAF process – the turbidity of the permeate was consistently about 0.8 NTU without significant breakthrough throughout the run. The high turbidity of the feed had no effect on UV_{254} removal, which was consistently close to 60% throughout the experiment.

Results of the two experiments are illustrated in Figure 4.36 and Figure 4.37, representing the pressure increase profiles and permeate quality, respectively. The μGAF process showed once again its ability to collect contaminants in the feed water. Also, in both cases, the TMP buildup in the μGAF units was reversed by the backwashing step, suggesting that the fouling was hydraulically reversible.

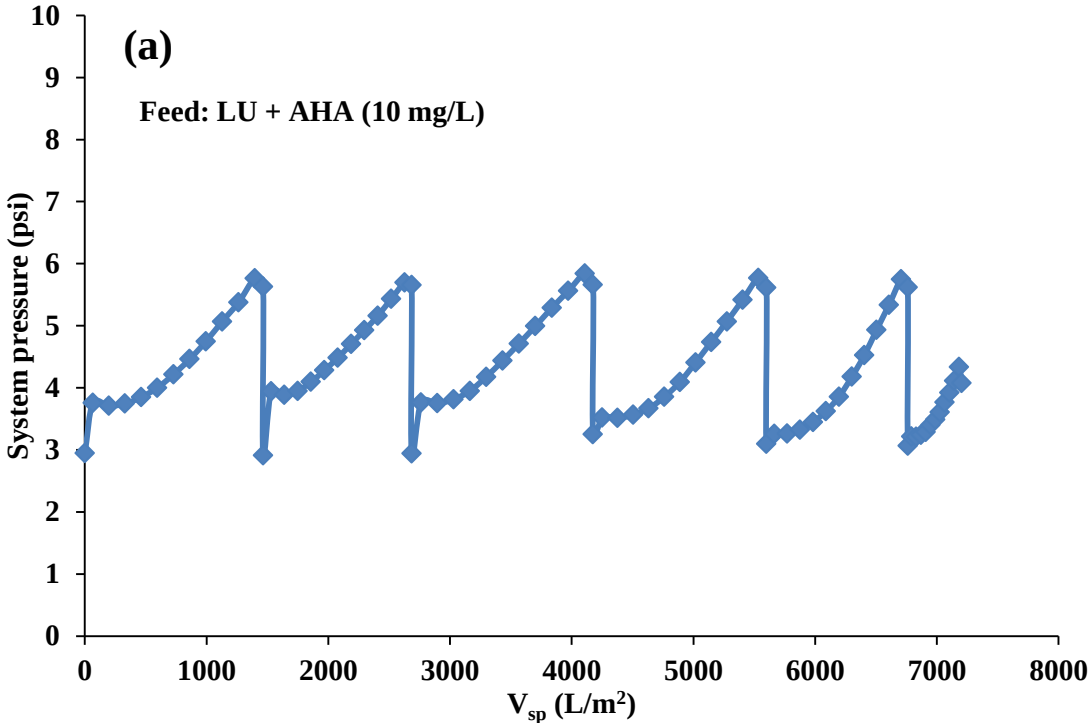

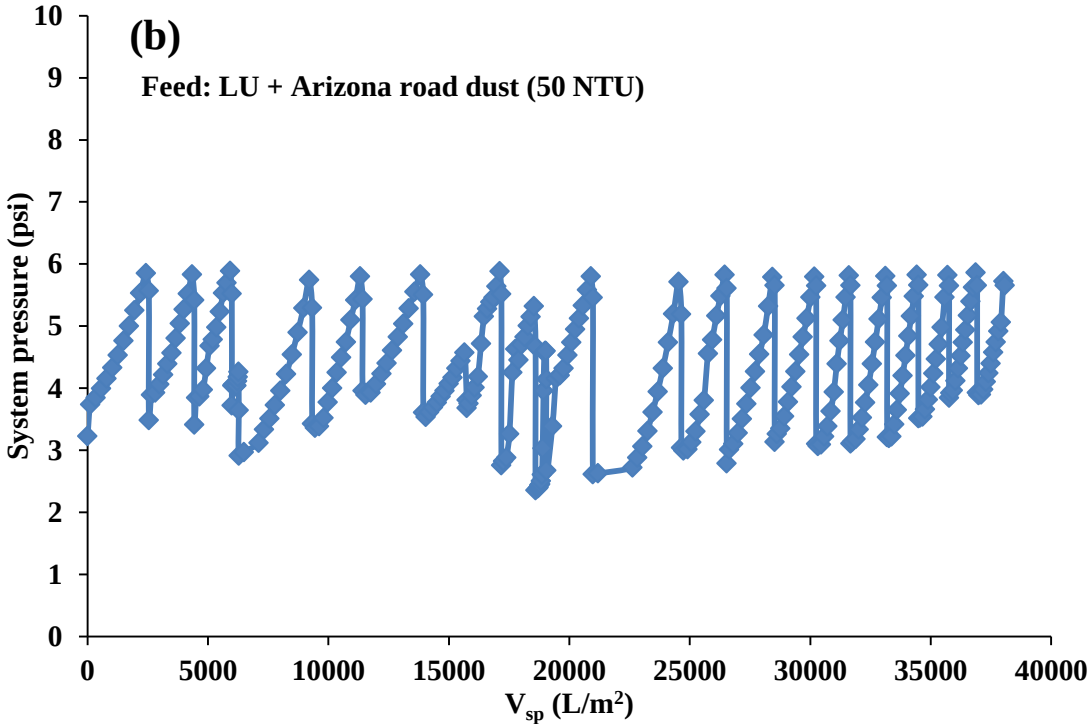

Figure 4.36 Pressure increase profiles of µGAF unit when fed with different challenging feed water: (a) fed with LU water + AHA (10 mg/L) mixture and (b) fed with LU water + Arizona road dust mixture (50 NTU)

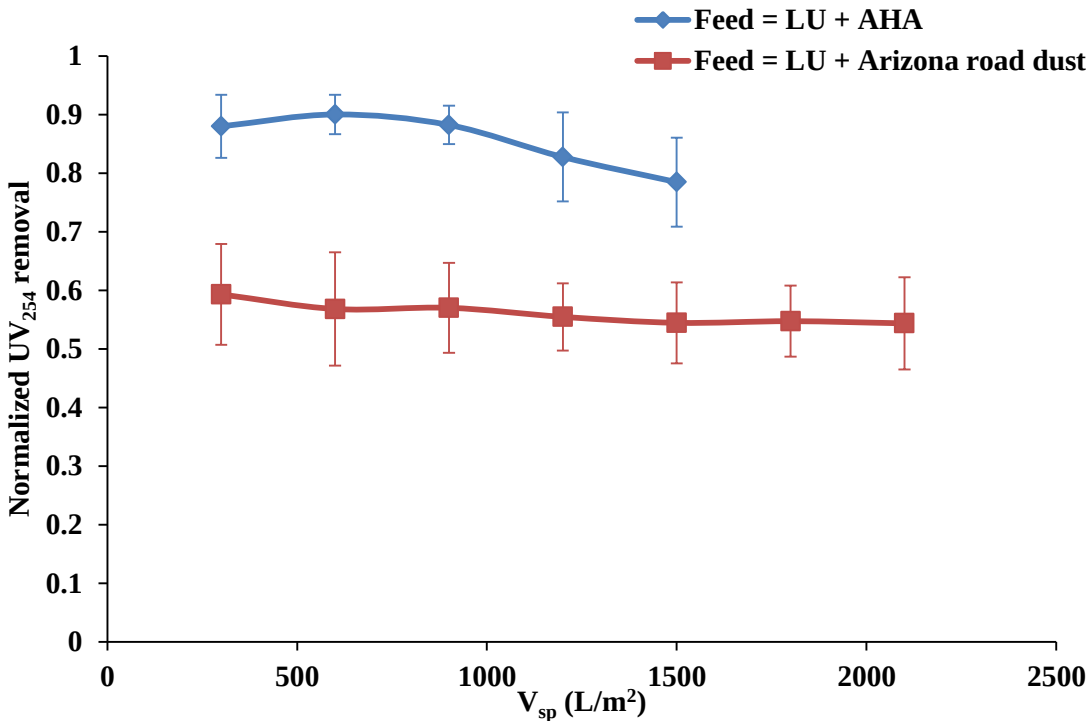

Figure 4.37 Average fractional NOM removal (presented in UV_{254}) when applying μGAF pretreatment to LU water with additional Aldrich humic acid or Arizona road dust

5. Conclusions

This study investigated microgranular adsorptive filtration (μGAF), a process that integrates granular media filtration and packed bed adsorption by passing water through a layer of adsorbent pre-deposited on a support layer. In this research, the goal was NOM removal from water, and effects of operational parameters on μGAF process performance were investigated. The factors investigated included the applied flux and pressure to the μGAF treatment unit, and the pH, ionic strength and concentration of divalent cations in the feed. The key foulants in the adsorbent layer and a downstream UF membrane were explored, and the fouling patterns were compared with model predictions. Lastly, larger bench-scale μGAF systems were tested for treating natural water to explore the potential application of μGAF in practice.

Heated aluminum oxide particles (HAOPs) were used as the main adsorbent. HAOPs collect NOM effectively from natural waters, and they have especially high affinity for humic substances. HAOPs collect NOM efficiently at low adsorbent doses, but the efficiency plateaus at high doses, suggesting that the adsorbent is not capable of collecting some NOM fractions. HAOPs outperformed two commercially available PACs at low/practical adsorbent doses, but the PACs performed better at high doses.

The potential of μGAF as a pretreatment prior to membrane filtration was examined. A coarse nylon mesh was used in the μGAF unit to support the pre-deposited HAOPs layer. The upstream μGAF unit collected NOM effectively and substantially reduced fouling of the downstream membrane.

The effect of flux on μGAF process performance was investigated using sequential μGAF-membrane filtration systems. In conventional membrane filtration, higher permeation rates lead to higher TMP and can promote foulant deposition. A

similar trend was observed in μGAF systems. That is, when different fluxes were applied to the μGAF unit, higher fluxes led to increased resistance across the HAOPs layer. The μGAF units fed at higher fluxes had higher NOM removal efficiencies, and the permeate collected from the higher flux pre-treatment steps led to better fouling reduction at the downstream membrane.

The HAOPs layer was found to be incompressible, even when some NOM had accumulated on or in the adsorbent layer. By contrast, when raw water was fed to a bare membrane, the NOM layer was compressible. A reasonable interpretation of this outcome is that during μGAF, the NOM molecules adsorb on the surface of HAOPs particles throughout the layer. HAOPs particles are orders of magnitude larger than NOM molecules so the adsorbed NOM is not able to fill the gaps between adsorbent particles and form a continuous layer. This result causes the resistance of the fouled layer to be independent of the applied pressure. Finally, experiments showed that the applied pressure had no effect on μGAF performance — either on fouling of the μGAF unit or the efficiency of fouling control at the downstream membrane unit.

Effects of feed solution chemistry on μGAF performance were investigated in experiments with sequential μGAF and membrane filtration units. Low pH of the feed enhanced NOM removal by HAOPs, leading to better downstream membrane fouling control.

Previous studies had found that high solution ionic strength usually leads to more severe fouling in conventional membrane processes. In this study, however, solution ionic strength had no significant effect on process performance, suggesting that the ionic strength has a limited effect on the ability of HAOPs to collect NOM macromolecules. Effects of the concentration of divalent cations were also investigated. Addition of Ca^{2+} or Mg^{2+} had almost no effect on NOM removal by the μGAF units, but a slight fouling reduction was observed in systems with higher

concentrations of divalent cations in the feed. A possible explanation is that divalent cations can promote agglomeration pf polysaccharide macromolecules, leading to a looser foulant layer structure.

Particulate and colloidal matter was found to be the dominant foulant in μGAF units, whereas soluble materials such as NOM were the key foulants in the downstream membrane units. Fouling of the μGAF unit could be modeled reasonably well by Hermia's intermediate fouling scenario ($R^2 \geqq 0.95$).

Lastly, larger bench scale experiments of the μGAF/membrane process were carried out with tubular μGAF units with different meshes, membrane materials and feed water quality. All the systems tested achieved satisfactory NOM removal and membrane fouling mitigation, showing significant potential for the process in real water treatment applications.

Reference

[1] A.S. Al-Amoudi, Factors affecting natural organic matter (NOM) and scaling fouling in NF membranes: A review, Desalination. 259 (2010) 1–10.

[2] G. Amy, J. Cho, Interactions between natural organic matter (NOM) and membranes: Rejection and fouling, Water Sci. Technol. 40 (1999) 131–139. doi:10.1016/S0273-1223(99)00649-6.

[3] D. Jermann, W. Pronk, S. Meylan, M. Boller, Interplay of different NOM fouling mechanisms during ultrafiltration for drinking water production, Water Res. 41 (2007) 1713–1722.

[4] W. Yuan, A. Kocic, A.L. Zydney, Analysis of humic acid fouling during microfiltration using a pore blockage–cake filtration model, J. Membr. Sci. 198 (2002) 51–62.

[5] S. Lee, J. Cho, M. Elimelech, Combined influence of natural organic matter (NOM) and colloidal particles on nanofiltration membrane fouling, J. Membr. Sci. 262 (2005) 27–41.

[6] W. Yuan, A.L. Zydney, Humic acid fouling during microfiltration, J. Membr. Sci. 157 (1999) 1–12.

[7] W. Yuan, A.L. Zydney, Humic acid fouling during ultrafiltration, Environ. Sci. Technol. 34 (2000) 5043–5050.

[8] D. Jermann, W. Pronk, R. Kägi, M. Halbeisen, M. Boller, Influence of interactions between NOM and particles on UF fouling mechanisms, Water Res. 42 (2008) 3870–3878.

[9] L. Fan, J.L. Harris, F.A. Roddick, N.A. Booker, Influence of the characteristics of natural organic matter on the fouling of microfiltration membranes, Water Res. 35 (2001) 4455–4463.

[10] S. Lee, M. Elimelech, Relating organic fouling of reverse osmosis membranes to intermolecular adhesion forces, Environ. Sci. Technol. 40 (2006) 980–987.

[11] H. Huang, K. Schwab, J.G. Jacangelo, Pretreatment for low pressure membranes in water treatment: a review, Environ. Sci. Technol. 43 (2009) 3011–3019.

[12] Y. Chang, M.M. Benjamin, Iron Oxide Adsorption and UF to Remove NOM and Control Fouling, J. Am. Water Works Assoc. 88 (1996) 74–88.

[13] Y.-J. Chang, K.-H. Choo, M.M. Benjamin, S. Reiber, Combined adsorption-UF process increases TOC removal, J. Am. Water Works Assoc. 90 (1998) 90–102.

[14] Z. Cai, J. Kim, M.M. Benjamin, NOM Removal by Adsorption and Membrane Filtration Using Heated Aluminum Oxide Particles, Environ. Sci. Technol. 42 (2008) 619–623. doi:10.1021/es7021285.

[15] J. Kim, Z. Cai, M.M. Benjamin, Effects of adsorbents on membrane fouling by natural organic matter, J. Membr. Sci. 310 (2008) 356–364.

[16] J. Kim, Z. Cai, M.M. Benjamin, NOM fouling mechanisms in a hybrid adsorption/membrane system, J. Membr. Sci. 349 (2010) 35–43.

[17] Z. Cai, Investigation of microgranular adsorptive filtratino system, University of Washington, 2011.

[18] A. Matilainen, E.T. Gjessing, T. Lahtinen, L. Hed, A. Bhatnagar, M. Sillanpää, An overview of the methods used in the characterisation of natural organic matter (NOM) in relation to drinking water treatment, Chemosphere. 83 (2011) 1431–1442.

[19] I.H. Suffet, P. MacCarthy, Aquatic humic substances. Influence of fate and treatment of pollutants., The American Chemical Society, 1989. http://www.cabdirect.org/abstracts/19921965461.html (accessed August 4, 2013).

[20] J. Cho, G. Amy, J. Pellegrino, Y. Yoon, Characterization of clean and natural organic matter (NOM) fouled NF and UF membranes, and foulants characterization, Desalination. 118 (1998) 101–108. doi:10.1016/S0011-9164(98)00100-3.

[21] H. Ma, H.E. Allen, Y. Yin, Characterization of isolated fractions of dissolved organic matter from natural waters and a wastewater effluent, Water Res. 35 (2001) 985–996.

[22] F.H. Frimmel, Characterization of natural organic matter as major constituents in aquatic systems, J. Contam. Hydrol. 35 (1998) 201–216.

[23] C. Pelekani, G. Newcombe, V.L. Snoeyink, C. Hepplewhite, S. Assemi, R. Beckett, Characterization of Natural Organic Matter Using High Performance Size Exclusion Chromatography, Environ. Sci. Technol. 33 (1999) 2807–2813. doi:10.1021/es9901314.

[24] P.C. Singer, Humic substances as precursors for potentially harmful disinfection by-products, Water Sci. Technol. 40 (1999) 25–30.

[25] N. Lee, G. Amy, J.-P. Croue, H. Buisson, Identification and understanding of fouling in low-pressure membrane (MF/UF) filtration by natural organic matter (NOM), Water Res. 38 (2004) 4511–4523.

[26] J.P. Croue, J.F. Debroux, G.L. Amy, G.R. Aiken, J.A. Leenheer, Natural organic matter: structural characteristics and reactive properties, Form. Control Disinfect. -Prod. Drink. Water. (1999) 65–93.

[27] G.V. Korshin, C.-W. Li, M.M. Benjamin, Monitoring the properties of natural organic matter through UV spectroscopy: a consistent theory, Water Res. 31 (1997) 1787–1795.

[28] J.A. Leenheer, J.-P. Croué, Peer reviewed: characterizing aquatic dissolved organic matter, Environ. Sci. Technol. 37 (2003) 18A–26A.

[29] W. Chen, P. Westerhoff, J.A. Leenheer, K. Booksh, Fluorescence excitation-emission matrix regional integration to quantify spectra for dissolved organic matter, Environ. Sci. Technol. 37 (2003) 5701–5710.

[30] Y.-P. Chin, G. Aiken, E. O'Loughlin, Molecular Weight, Polydispersity, and Spectroscopic Properties of Aquatic Humic Substances, Environ. Sci. Technol. 28 (1994) 1853–1858. doi:10.1021/es00060a015.

[31] C. Jucker, M.M. Clark, Adsorption of aquatic humic substances on hydrophobic ultrafiltration membranes, J. Membr. Sci. 97 (1994) 37–52. doi:10.1016/0376-7388(94)00146-P.

[32] C.-F. Lin, T.-Y. Lin, O.J. Hao, Effects of humic substance characteristics on UF performance, Water Res. 34 (2000) 1097–1106.

[33] C.-F. Lin, Y.-J. Huang, O.J. Hao, Ultrafiltration processes for removing humic substances: effect of molecular weight fractions and PAC treatment, Water Res. 33 (1999) 1252–1264.

[34] S. Nataraj, R. Schomäcker, M. Kraume, I.M. Mishra, A. Drews, Analyses of polysaccharide fouling mechanisms during crossflow membrane filtration, J. Membr. Sci. 308 (2008) 152–161. doi:10.1016/j.memsci.2007.09.060.

[35] T. Berman, M. Holenberg, Don't fall foul of biofilm through high TEP levels, Filtr. Sep. 42 (2005) 30–32.

[36] T. Berman, R. Mizrahi, C.G. Dosoretz, Transparent exopolymer particles (TEP): A critical factor in aquatic biofilm initiation and fouling on filtration membranes, Desalination. 276 (2011) 184–190.

[37] T. de la Torre, V. Iversen, J. Stüber, A. Drews, B. Lesjean, M. Kraume, Searching for a universal fouling indicator for membrane bioreactors, Desalination Water Treat. 18 (2010) 264–269. doi:10.5004/dwt.2010.1783.

[38] T. de la Torre, The quest for a universal indicator for MBR fouling, Technischen Universität Berlin, 2013.

[39] T. De la Torre, B. Lesjean, A. Drews, M. Kraume, Monitoring of transparent exopolymer particles (TEP) in a membrane bioreactor (MBR) and correlation with other fouling indicators, Water Sci Technol. 58 (2008) 1903–1909.

[40] L.O. Villacorte, M.D. Kennedy, G.L. Amy, J.C. Schippers, The fate of Transparent Exopolymer Particles (TEP) in integrated membrane systems: Removal through pre-treatment processes and deposition on reverse osmosis membranes, Water Res. 43 (2009) 5039–5052. doi:10.1016/j.watres.2009.08.030.

[41] M.D. Kennedy, F.P. Muñoz Tobar, G. Amy, J.C. Schippers, Transparent exopolymer particle (TEP) fouling of ultrafiltration membrane systems,

Desalination Water Treat. 6 (2009) 169–176.

[42] E. Bar-Zeev, I. Berman-Frank, B. Liberman, E. Rahav, U. Passow, T. Berman, Transparent exopolymer particles: Potential agents for organic fouling and biofilm formation in desalination and water treatment plants, Desalination Water Treat. 3 (2009) 136–142. doi:10.5004/dwt.2009.444.

[43] S. Van Nevel, T. Hennebel, K. De Beuf, G. Du Laing, W. Verstraete, N. Boon, Transparent exopolymer particle removal in different drinking water production centers, Water Res. 46 (2012) 3603–3611.

[44] U. Passow, Transparent exopolymer particles (TEP) in aquatic environments, Prog. Oceanogr. 55 (2002) 287–333.

[45] E. Bar-Zeev, U. Passow, S. Romero-Vargas Castrillón, M. Elimelech, Transparent Exopolymer Particles: From Aquatic Environments and Engineered Systems to Membrane Biofouling, Environ. Sci. Technol. 49 (2014) 691–707. doi:10.1021/es5041738.

[46] B. Wu, T. Kitade, T.H. Chong, T. Uemura, A.G. Fane, Role of initially formed cake layers on limiting membrane fouling in membrane bioreactors, Bioresour. Technol. 118 (2012) 589–593.

[47] R. Dreywood, Qualitative Test for Carbohydrate Material, Ind. Eng. Chem. Anal. Ed. 18 (1946) 499–499. doi:10.1021/i560156a015.

[48] L.H. Koehler, Differentiation of Carbohydrates by Anthrone Reaction Rate and Color Intensity, Anal. Chem. 24 (1952) 1576–1579. doi:10.1021/ac60070a014.

[49] M. Dubois, K.A. Gilles, J.K. Hamilton, Pa. Rebers, F. Smith, Colorimetric method for determination of sugars and related substances, Anal. Chem. 28 (1956) 350–356.

[50] K. Raunkj\a er, T. Hvitved-Jacobsen, P.H. er Nielsen, Measurement of pools of protein, carbohydrate and lipid in domestic wastewater, Water Res. 28 (1994) 251–262.

[51] U. Passow, A.L. Alldredge, A dye-binding assay for the spectrophotometric measurement of transparent exopolymer particles (TEP), Limnol. Oceanogr. 40 (1995) 1326–1335.

[52] S.H. Arruda Fatibello, A.A. Henriques Vieira, O. Fatibello-Filho, A rapid spectrophotometric method for the determination of transparent exopolymer particles (TEP) in freshwater, Talanta. 62 (2004) 81–85.

[53] T. Carroll, S. King, S.R. Gray, B.A. Bolto, N.A. Booker, The fouling of microfiltration membranes by NOM after coagulation treatment, Water Res. 34 (2000) 2861–2868.

[54] S. Hong, M. Elimelech, Chemical and physical aspects of natural organic matter (NOM) fouling of nanofiltration membranes, J. Membr. Sci. 132 (1997) 159–

181. doi:10.1016/S0376-7388(97)00060-4.

[55] A. Seidel, M. Elimelech, Coupling between chemical and physical interactions in natural organic matter (NOM) fouling of nanofiltration membranes: implications for fouling control, J. Membr. Sci. 203 (2002) 245–255.

[56] W.-Y. Ahn, A.G. Kalinichev, M.M. Clark, Effects of background cations on the fouling of polyethersulfone membranes by natural organic matter: experimental and molecular modeling study, J. Membr. Sci. 309 (2008) 128–140.

[57] H.-C. Kim, B.A. Dempsey, Membrane fouling due to alginate, SMP, EfOM, humic acid, and NOM, J. Membr. Sci. 428 (2013) 190–197. doi:10.1016/j.memsci.2012.11.004.

[58] J. Tian, M. Ernst, F. Cui, M. Jekel, Effect of different cations on UF membrane fouling by NOM fractions, Chem. Eng. J. 223 (2013) 547–555. doi:10.1016/j.cej.2013.03.043.

[59] R.M. Mcdonogh, A.G. Fane, C.J. Fell, Charge effects in the cross-flow filtration of colloids and particulates, J. Membr. Sci. 43 (1989) 69–85.

[60] R.D. Cohen, R.F. Probstein, Colloidal fouling of reverse osmosis membranes, J. Colloid Interface Sci. 114 (1986) 194–207.

[61] K. Boussu, A. Belpaire, A. Volodin, C. Van Haesendonck, P. Van der Meeren, C. Vandecasteele, et al., Influence of membrane and colloid characteristics on fouling of nanofiltration membranes, J. Membr. Sci. 289 (2007) 220–230. doi:10.1016/j.memsci.2006.12.001.

[62] Ś.F.E. Boerlage, M.D. Kennedy, M.P. Aniye, E.M. Abogrean, G. Galjaard, J.C. Schippers, Monitoring particulate fouling in membrane systems, Desalination. 118 (1998) 131–142. doi:10.1016/S0011-9164(98)00107-6.

[63] P. Aimar, P. Bacchin, Slow colloidal aggregation and membrane fouling, J. Membr. Sci. 360 (2010) 70–76.

[64] S.G. Yiantsios, A.J. Karabelas, The effect of colloid stability on membrane fouling, Desalination. 118 (1998) 143–152. doi:10.1016/S0011-9164(98)00110-6.

[65] G. Belfort, R.H. Davis, A.L. Zydney, The behavior of suspensions and macromolecular solutions in crossflow microfiltration, J. Membr. Sci. 96 (1994) 1–58.

[66] W.-M. Lu, Y.-P. Huang, K.-J. Hwang, Methods to determine the relationship between cake properties and solid compressive pressure, Sep. Purif. Technol. 13 (1998) 9–23.

[67] V.V. Tarabara, I. Koyuncu, M.R. Wiesner, Effect of hydrodynamics and solution ionic strength on permeate flux in cross-flow filtration: direct experimental

observation of filter cake cross-sections, J. Membr. Sci. 241 (2004) 65–78.
[68] C.Y. Tang, T.H. Chong, A.G. Fane, Colloidal interactions and fouling of NF and RO membranes: a review, Adv. Colloid Interface Sci. 164 (2011) 126–143.
[69] P. Bacchin, P. Aimar, V. Sanchez, Model for colloidal fouling of membranes, AIChE J. 41 (1995) 368–376.
[70] R.W. Field, D. Wu, J.A. Howell, B.B. Gupta, Critical flux concept for microfiltration fouling, J. Membr. Sci. 100 (1995) 259–272.
[71] J.A. Howell, Sub-critical flux operation of microfiltration, J. Membr. Sci. 107 (1995) 165–171.
[72] S.S. Madaeni, The effect of operating conditions on critical flux in membrane filtration of latexes, Process Saf. Environ. Prot. 75 (1997) 266–269.
[73] C. Henry, J.-P. Minier, G. Lefèvre, Towards a description of particulate fouling: From single particle deposition to clogging, Adv. Colloid Interface Sci. 185–186 (2012) 34–76. doi:10.1016/j.cis.2012.10.001.
[74] Q. Li, M. Elimelech, Synergistic effects in combined fouling of a loose nanofiltration membrane by colloidal materials and natural organic matter, J. Membr. Sci. 278 (2006) 72–82. doi:10.1016/j.memsci.2005.10.045.
[75] J. Hermia, Constant pressure blocking filtration law application to powder-law non-Newtonian fluid, Trans Inst Chem Eng. 60 (1982) 183–187.
[76] W.R. Bowen, J.I. Calvo, A. Hernandez, Steps of membrane blocking in flux decline during protein microfiltration, J. Membr. Sci. 101 (1995) 153–165.
[77] M. Hlavacek, F. Bouchet, Constant flowrate blocking laws and an example of their application to dead-end microfiltration of protein solutions, J. Membr. Sci. 82 (1993) 285–295.
[78] S. Chellam, W. Xu, Blocking laws analysis of dead-end constant flux microfiltration of compressible cakes, J. Colloid Interface Sci. 301 (2006) 248–257.
[79] X.-M. Wang, T.D. Waite, Impact of gel layer formation on colloid retention in membrane filtration processes, J. Membr. Sci. 325 (2008) 486–494.
[80] K.-J. Hwang, Y.-T. Wang, E. Iritani, N. Katagiri, Effects of porous gel particle compression properties on microfiltration characteristics, J. Membr. Sci. 341 (2009) 286–293.
[81] J. Mendret, C. Guigui, P. Schmitz, C. Cabassud, In situ dynamic characterisation of fouling under different pressure conditions during dead-end filtration: compressibility properties of particle cakes, J. Membr. Sci. 333 (2009) 20–29.
[82] B.-K. Hwang, C.-H. Lee, I.-S. Chang, A. Drews, R. Field, Membrane bioreactor: TMP rise and characterization of bio-cake structure using CLSM-image analysis, J. Membr. Sci. 419 (2012) 33–41.

[83] Y.-J. Chang, M.M. Benjamin, Modeling formation of natural organic matter fouling layers on ultrafiltration membranes, J. Environ. Eng. 129 (2003) 25–32.

[84] T.V. Bugge, M.K. Jørgensen, M.L. Christensen, K. Keiding, Modeling cake buildup under TMP-step filtration in a membrane bioreactor: Cake compressibility is significant, Water Res. 46 (2012) 4330–4338.

[85] C. Sun, L. Fiksdal, A. Hanssen-Bauer, M.B. Rye, T. Leiknes, Characterization of membrane biofouling at different operating conditions (flux) in drinking water treatment using confocal laser scanning microscopy (CLSM) and image analysis, J. Membr. Sci. 382 (2011) 194–201.

[86] M.W. Chudacek, A.G. Fane, The dynamics of polarisation in unstirred and stirred ultrafiltration, J. Membr. Sci. 21 (1984) 145–160. doi:10.1016/S0376-7388(00)81551-3.

[87] W.S. Opong, A.L. Zydney, Hydraulic permeability of protein layers deposited during ultrafiltration, J. Colloid Interface Sci. 142 (1991) 41–60. doi:10.1016/0021-9797(91)90032-4.

[88] D.C. Sioutopoulos, A.J. Karabelas, The effect of permeation flux on the specific resistance of polysaccharide fouling layers developing during dead-end ultrafiltration, J. Membr. Sci. 473 (2015) 292–301. doi:10.1016/j.memsci.2014.09.030.

[89] L. Song, M. Elimelech, Particle Deposition onto a Permeable Surface in Laminar Flow, J. Colloid Interface Sci. 173 (1995) 165–180. doi:10.1006/jcis.1995.1310.

[90] V. Chen, A.G. Fane, S. Madaeni, I.G. Wenten, Particle deposition during membrane filtration of colloids: transition between concentration polarization and cake formation, J. Membr. Sci. 125 (1997) 109–122. doi:10.1016/S0376-7388(96)00187-1.

[91] L. Vera, R. Villarroel-López, S. Delgado, S. Elmaleh, Cross-flow microfiltration of biologically treated wastewater, Desalination. 114 (1997) 65–75. doi:10.1016/S0011-9164(97)00155-0.

[92] Z. Wang, Z. Wu, X. Yin, L. Tian, Membrane fouling in a submerged membrane bioreactor (MBR) under sub-critical flux operation: membrane foulant and gel layer characterization, J. Membr. Sci. 325 (2008) 238–244.

[93] M. Mänttäri, M. Nyström, Critical flux in NF of high molar mass polysaccharides and effluents from the paper industry, J. Membr. Sci. 170 (2000) 257–273.

[94] P. van der Marel, A. Zwijnenburg, A. Kemperman, M. Wessling, H. Temmink, W. van der Meer, An improved flux-step method to determine the critical flux and the critical flux for irreversibility in a membrane bioreactor, J. Membr. Sci. 332 (2009) 24–29.

[95] J. Kim, F.A. DiGiano, Defining critical flux in submerged membranes: influence of length-distributed flux, J. Membr. Sci. 280 (2006) 752–761.

[96] D.Y. Kwon, S. Vigneswaran, A.G. Fane, R.B. Aim, Experimental determination of critical flux in cross-flow microfiltration, Sep. Purif. Technol. 19 (2000) 169–181.

[97] S. Ognier, C. Wisniewski, A. Grasmick, Membrane bioreactor fouling in sub-critical filtration conditions: a local critical flux concept, J. Membr. Sci. 229 (2004) 171–177.

[98] B. Bolto, J. Gregory, Organic polyelectrolytes in water treatment, Water Res. 41 (2007) 2301–2324.

[99] B. Bolto, D. Dixon, R. Eldridge, S. King, Cationic polymer and clay or metal oxide combinations for natural organic matter removal, Water Res. 35 (2001) 2669–2676. doi:10.1016/S0043-1354(00)00552-2.

[100] B. Bolto, G. Abbt-Braun, D. Dixon, R. Eldgridge, F. Frimmel, S. Hesse, et al., Experimental evaluation of cationic polyelectrolytes for removing natural organic matter from water, Water Sci. Technol. 40 (1999) 71.

[101] T. Kvinnesland, H. Ødegaard, The effects of polymer characteristics on nano particle separation in humic substances removal by cationic polymer coagulation, Water Sci. Technol. 50 (2004) 185–191.

[102] S.-K. Kam, J. Gregory, The interaction of humic substances with cationic polyelectrolytes, Water Res. 35 (2001) 3557–3566. doi:10.1016/S0043-1354(01)00092-6.

[103] A.M. Jack, M.M. Clark, Using PAC-UF to treat a low-quality surface water, J. Am. Water Works Assoc. 90 (1998) 83–95.

[104] S. Mozia, M. Tomaszewska, A.W. Morawski, Application of an ozonation–adsorption–ultrafiltration system for surface water treatment, Desalination. 190 (2006) 308–314.

[105] C.-W. Li, Y.-S. Chen, Fouling of UF membrane by humic substance: Effects of molecular weight and powder-activated carbon (PAC) pre-treatment, Desalination. 170 (2004) 59–67. doi:10.1016/j.desal.2004.03.015.

[106] A. Vilgé-Ritter, A. Masion, T. Boulangé, D. Rybacki, J.-Y. Bottero, Removal of Natural Organic Matter by Coagulation-Flocculation: A Pyrolysis-GC-MS Study, Environ. Sci. Technol. 33 (1999) 3027–3032. doi:10.1021/es981232p.

[107] D.A. Fearing, J. Banks, S. Guyetand, C. Monfort Eroles, B. Jefferson, D. Wilson, et al., Combination of ferric and MIEX® for the treatment of a humic rich water, Water Res. 38 (2004) 2551–2558. doi:10.1016/j.watres.2004.02.020.

[108] T.H. Boyer, P.C. Singer, Bench-scale testing of a magnetic ion exchange resin for removal of disinfection by-product precursors, Water Res. 39 (2005) 1265–

1276. doi:10.1016/j.watres.2005.01.002.

[109] T.H. Boyer, P.C. Singer, A pilot-scale evaluation of magnetic ion exchange treatment for removal of natural organic material and inorganic anions, Water Res. 40 (2006) 2865–2876.

[110] T.H. Boyer, P.C. Singer, Stoichiometry of Removal of Natural Organic Matter by Ion Exchange, Environ. Sci. Technol. 42 (2007) 608–613. doi:10.1021/es071940n.

[111] R. Fabris, E.K. Lee, C.W.K. Chow, V. Chen, M. Drikas, Pre-treatments to reduce fouling of low pressure micro-filtration (MF) membranes, J. Membr. Sci. 289 (2007) 231–240. doi:10.1016/j.memsci.2006.12.003.

[112] H. Huang, H.-H. Cho, K.J. Schwab, J.G. Jacangelo, Effects of magnetic ion exchange pretreatment on low pressure membrane filtration of natural surface water, Water Res. 46 (2012) 5483–5490.

[113] H. Humbert, H. Gallard, V. Jacquemet, J.-P. Croué, Combination of coagulation and ion exchange for the reduction of UF fouling properties of a high DOC content surface water, Water Res. 41 (2007) 3803–3811. doi:10.1016/j.watres.2007.06.009.

[114] B.P. Allpike, A. Heitz, C.A. Joll, R.I. Kagi, G. Abbt-Braun, F.H. Frimmel, et al., Size exclusion chromatography to characterize DOC removal in drinking water treatment, Environ. Sci. Technol. 39 (2005) 2334–2342.

[115] G. Vos, Y. Brekvoort, H.A. Oosterom, M.M. Nederlof, Treatment of canal water with ultrafiltration to produce industrial and household water, Desalination. 118 (1998) 297–303. doi:10.1016/S0011-9164(98)00151-9.

[116] A. Wilczak, E.W. Howe, E.M. Aieta, R.G. Lee, How preoxidation affects particle removal during clarification and filtration, J. Am. Water Works Assoc. (1992) 85–94.

[117] J. Plummer, J. Edzwald, Effects of chlorine and ozone on algal cell properties and removal of algae by coagulation., Aqua. 51 (2002) 307–318.

[118] X. Wang, L. Wang, Y. Liu, W. Duan, Ozonation pretreatment for ultrafiltration of the secondary effluent, J. Membr. Sci. 287 (2007) 187–191. doi:10.1016/j.memsci.2006.10.016.

[119] L. Heng, Y. Yanling, G. Weijia, L. Xing, L. Guibai, Effect of pretreatment by permanganate/chlorine on algae fouling control for ultrafiltration (UF) membrane system, Desalination. 222 (2008) 74–80. doi:10.1016/j.desal.2007.01.126.

[120] B. Schlichter, V. Mavrov, H. Chmiel, Study of a hybrid process combining ozonation and microfiltration/ultrafiltration for drinking water production from surface water, Desalination. 168 (2004) 307–317.

doi:10.1016/j.desal.2004.07.014.
[121] J. Kim, S.H.R. Davies, M.J. Baumann, V.V. Tarabara, S.J. Masten, Effect of ozone dosage and hydrodynamic conditions on the permeate flux in a hybrid ozonation–ceramic ultrafiltration system treating natural waters, J. Membr. Sci. 311 (2008) 165–172. doi:10.1016/j.memsci.2007.12.010.
[122] B. Schlichter, V. Mavrov, H. Chmiel, Study of a hybrid process combining ozonation and membrane filtration — filtration of model solutions, Desalination. 156 (2003) 257–265. doi:10.1016/S0011-9164(03)00348-5.
[123] S.-R. Chae, H. Yamamura, K. Ikeda, Y. Watanabe, Comparison of fouling characteristics of two different poly-vinylidene fluoride microfiltration membranes in a pilot-scale drinking water treatment system using pre-coagulation/sedimentation, sand filtration, and chlorination, Water Res. 42 (2008) 2029–2042. doi:10.1016/j.watres.2007.12.011.
[124] D. Sąkol, K. Konieczny, Application of coagulation and conventional filtration in raw water pretreatment before microfiltration membranes, Desalination. 162 (2004) 61–73. doi:10.1016/S0011-9164(04)00028-1.
[125] K. Lee, K. Choo, S. Choi, K. Yamamoto, Development of an integrated iron oxide adsorption/membrane separation system for water treatment, Water Supply. 2 (2002) 293–300.
[126] K. Choo, I. Park, S. Choi, Removal of natural organic matter using iron oxide-coated membrane systems, Water Supply. 4 (2005) 207–213.
[127] M. Zhang, C. Li, M.M. Benjamin, Y. Chang, Fouling and natural organic matter removal in adsorbent/membrane systems for drinking water treatment, Environ. Sci. Technol. 37 (2003) 1663–1669.
[128] M.A. Schlautman, J.J. Morgan, Adsorption of aquatic humic substances on colloidal-size aluminum oxide particles: influence of solution chemistry, Geochim. Cosmochim. Acta. 58 (1994) 4293–4303.
[129] G. Sposito, The surface chemistry of soils, Oxford University Press ; Oxford Oxfordshire, New York, 1984.
[130] G. Sposito, The chemistry of soils, Oxford University Press, New York, 1989.
[131] I. Iwasaki, R.W. Lai, Starches and starch products as depressants in soap flotation of activated silica from iron ores, Trans AIME. 232 (1965) 364–371.
[132] R.W. Perry, F.F. Aplan, Polysaccharides and xanthated polysaccharides as pyrite depressants during coal flotation, Coal Sci. Technol. 9 (1985) 215–238.
[133] Q. Liu, J.S. Laskowski, The role of metal hydroxides at mineral surfaces in dextrin adsorption, I. Studies on modified quartz samples, Int. J. Miner. Process. 26 (1989) 297–316.
[134] R.K. Rath, S. Subramanian, Adsorption, electrokinetic and differential flotation

studies on sphalerite and galena using dextrin, Int. J. Miner. Process. 57 (1999) 265–283.

[135] S. Subramanian, J.S. Laskowski, Adsorption of dextrin onto graphite, Langmuir. 9 (1993) 1330–1333.

[136] R.K. Rath, S. Subramanian, Studies on adsorption of guar gum onto biotite mica, Miner. Eng. 10 (1997) 1405–1420.

[137] R.K. Rath, S. Subramanian, J.S. Laskowski, Adsorption of dextrin and guar gum onto talc. A comparative study, Langmuir. 13 (1997) 6260–6266.

[138] J. Wang, P. Somasundaran, D.R. Nagaraj, Adsorption mechanism of guar gum at solid–liquid interfaces, Miner. Eng. 18 (2005) 77–81.

[139] L.L. Russell, Chemical aspects of ground water recharge with wastewaters, University of California, Berkeley, 1976.

[140] K. Ghosh, M. Schnitzer, Macromolecular structures of humic substances., Soil Sci. 129 (1980) 266–276.

[141] Q. Li, M. Elimelech, Organic fouling and chemical cleaning of nanofiltration membranes: measurements and mechanisms, Environ. Sci. Technol. 38 (2004) 4683–4693.

[142] J. Kim, W. Shi, Y. Yuan, M.M. Benjamin, A serial filtration investigation of membrane fouling by natural organic matter, J. Membr. Sci. 294 (2007) 115–126.

[143] Y. Gao, D. Chen, L.K. Weavers, H.W. Walker, Ultrasonic control of UF membrane fouling by natural waters: effects of calcium, pH, and fractionated natural organic matter, J. Membr. Sci. 401 (2012) 232–240.

[144] J. Cho, G. Amy, J. Pellegrino, Membrane filtration of natural organic matter: factors and mechanisms affecting rejection and flux decline with charged ultrafiltration (UF) membrane, J. Membr. Sci. 164 (2000) 89–110.

[145] W.J.C. Van de Ven, K. van't Sant, I.G.M. Pünt, A. Zwijnenburg, A.J.B. Kemperman, W.G.J. van der Meer, et al., Hollow fiber dead-end ultrafiltration: influence of ionic environment on filtration of alginates, J. Membr. Sci. 308 (2008) 218–229.

[146] S. Arabi, G. Nakhla, Impact of cation concentrations on fouling in membrane bioreactors, J. Membr. Sci. 343 (2009) 110–118.